

PERFORMANCE EVALUATION OF 3-PHASE 4-SWITCH INVERTER FED BRUSHLESS DC MOTOR DRIVE

A DISSERTATION

*Submitted in partial fulfillment of the
requirements for the award of the degree*

of

MASTER OF TECHNOLOGY

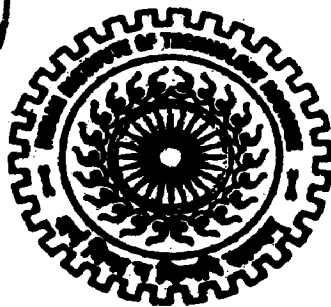
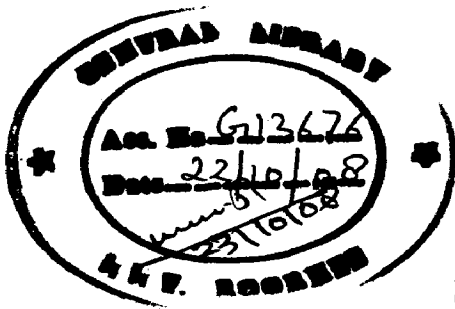
in

ELECTRICAL ENGINEERING

(With Specialization in Power Apparatus & Electric Drives)

By

KALLEM RAJENDER



**DEPARTMENT OF ELECTRICAL ENGINEERING
INDIAN INSTITUTE OF TECHNOLOGY ROORKEE
ROORKEE - 247 667 (INDIA)
JUNE, 2008**

CANDIDATE'S DECLARATION

I hereby declare that the work, which is presented in this dissertation report, entitled "PERFORMANCE EVALUATION OF 3-PHASE, 4-SWITCH INVERTER FED BRUSHLESS DC MOTOR DRIVE", being submitted in partial fulfillment of the requirements for the award of the degree of **MASTER OF TECHNOLOGY** with specialization in **POWER APPARATUS AND ELECTRIC DRIVES**, in the Department of Electrical Engineering, Indian Institute of Technology, Roorkee, is an authentic record of my own work carried out from July 2007 to June 2008, under the guidance and supervision of Dr. Pramod Agarwal, Professor and Dr. Mukesh kumar pathak, assistant professor, Department of Electrical Engineering, Indian Institute of Technology, Roorkee.

The results embodied in this dissertation have not submitted for the award of any other Degree or Diploma.

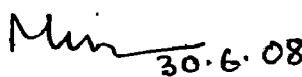
Date:

Place: Roorkee


KALLEM RAJENDER

CERTIFICATE

This is to certify that the statement made by the candidate is correct to the best of my knowledge and belief.


30.6.08
DR. MUKESH KUMAR PATHAK
Assistant Professor
Department of Electrical Engineering
Indian Institute of Technology Roorkee
Roorkee – 247667, (INDIA)


DR. PRAMOD AGARWAL
Professor
Department of Electrical Engineering
Indian Institute of Technology Roorkee
Roorkee – 247667, (INDIA)

ABSTRACT

Brushless Direct Current (BLDC) motor is a self synchronous motor, similar to PMSM in structure. Its many advantages like easy speed control than other AC machines, high efficiency, high power density, low noise, and low maintenance cost while having characteristics similar to DC motor makes it suitable for many applications. A three phase BLDC motor is fed by six switch inverter operating in 120° mode and only two phases are 'on' at any instant. Other 60° of operation in a half cycle, one phase current is zero and other two phases are 'on'. This concept led to development of four switch inverter (FSTPI) fed BLDC motor drive. Different PWM techniques used for BLDC motor drives are triangular carrier method, hysteresis band control techniques. These are briefly explained. A most popular direct current control PWM technique using hysteresis band for current controlled voltage source inverter feeding BLDC motor is presented. In this work, first a six switch inverter fed drive developed in MATLAB-Simulink using simulink and power system block set toolboxes and its performance is evaluated with different speed controllers like PI, Sliding mode, Fuzzy. Next, a FSTPI fed BLDC motor drive is developed. The dynamic response of FSTPI-BLDCM drive under various operating conditions such as starting, speed reversal, and load perturbation is simulated using different speed controllers mentioned above. Results of four switch operation are compared with the six operation of BLDC motor drive.

In four switch inverter fed drive, capacitors in one leg has its own affects on the performance of the drive and detailed analysis is done in all regions of operation. Drive performance is compared for different values of capacitances and initial rotor positions. Due to unbalanced voltage operation of FSTPI, at high speeds commutation torque ripple problem is severe and introduces more noise in the drive and sometimes it may affect speed response. Commutation torque ripple in FSTPI drive is analyzed and compared with its six switch counterpart at all speeds of operation with rated load. A new way to reduce commutation torque ripple is presented. This developed technique is applied to forward motoring operation of the FSTPI-BLDCM drive. This technique ensures the FSTPI fed drive can be much more practically applied for the industrial applications. Validity of the proposed scheme is verified by the simulation results.

ACKNOWLEDGEMENTS

First and foremost, I would like to express my sincere appreciation to my supervisor, Dr. Pramod Agarwal, for the patience and guidance throughout the entire duration of my thesis. Continuous monitoring and time management was an inspiring force for me to complete the work. Without his supervision, this thesis would never have been a success. Working under his guidance has been a great experience which has given me a deep insight in the area of technical research.

I would also like to express my sincere gratitude to my co-guide, Dr. Mukesh kumar pathak, for his continuous support and evaluating my progress from time to time in completion of this work.

I am also thankful to my Head of the Department, Dr. S. P. Gupta for providing all facilities in completion of this work.

Last, but not the least, I would also like to thank my friends and research scholars for their support during my work.

Date:


KALLEM RAJENDER

Place: Roorkee.

CONTENTS

ABSTRACT

ACKNOWLEDGEMENTS

CONTENTS

LIST OF FIGURES

LIST OF TABLES

CHAPTER 1 INTRODUCTION

1.0 General	1
1.1 Characteristics and applications of BLDC motor	2
1.2 Inverter topologies for three phase BLDC motor drive	4
1.3 Literature review	6
1.4 Authors contribution	7
1.5 Conclusion	8

CHAPTER 2 CURRENT CONTROL STRATEGIES OF VSI FOR BLDC MOTOR

2.0 Introduction	9
2.1 Advantages of pwm techniques	10
2.2 Triangular carrier method (TC)	10
2.3 Hysteresis band method (HB)	11
2.4 Conclusion	13

CHAPTER 3 MODELING OF FOUR SWITCH THREE PHASE (FSTP) INVERTER FED BLDC MOTOR DRIVE

3.0 Introduction	14
3.1 Direct current control PWM	14
3.2 Analysis of BLDC motor drive	18

3.2.1 Modeling of back emf based on rotor position	19
3.3 Mathematical modeling of pm BLDC motor	20
3.4 Modeling of speed controllers	23
3.4.1 Proportional Integral (PI) speed controller	23
3.4.2 Sliding Mode Speed Controller	24
3.4.3 Fuzzy logic speed controller	25
3.5 Conclusion	28
CHAPTER 4 MATLAB IMPLEMENTATION OF FOUR SWITCH THREE PHASE INVERTER FED BLDC MOTOR DRIVE	
4.0 Introduction	29
4.1 Four quadrant operation of FSTP inverter fed BLDCM drive	29
4.2 Proportional-Integral (PI) Speed controller based BLDCM drive	34
4.2.1 Analysis of starting response	35
4.2.2 Analysis of load perturbation	42
4.2.3 Analysis of speed reversal	44
4.2.4 Analysis of regeneration	45
4.2.5 Analysis of commutation torque ripple	47
4.2.6 Novel commutation torque ripple in FSTPI fed motor	57
4.3 Sliding mode speed controller based FSTPI-BLDC motor drive	61
4.4 Fuzzy Speed controller based FSTPI-BLDC motor drive	63
4.5 Conclusion	69
CHAPTER 5 RESULTS AND DISCUSSIONS	70
CHAPTER 6 CONCLUSION AND FUTURE SCOPE	82
REFERENCES	84
APPENDIX-A MOTOR PARAMETERS	88

LIST OF FIGURES

Figure.No	Name	Page.No
1.	Speed-torque characteristics of typical Brushless DC motor (Ref: [1])	2
2.	Basic circuit of six switch inverter fed BLDC motor	4
3.	Basic circuit of four switch inverter fed BLDC motor	5
4.	Triangular carrier (TC) PWM current control technique	10
5.	Decoder circuit for single quadrant BLDC motor	11
6.	Hysteresis band current control technique	12
7.	Hysteresis current controller and decoder circuit	12
8.	Four switch inverter for driving BLDC motor	15
9.	Hall signals, switching signals, back emf and currents of three phases	16
10.	Implementation of direct current controlled PWM (Ref:[9])	16
11.	Basic block diagram of PMBLDC motor drive system	18
12.	Block diagram of PI speed controller	24
12 (b)	Block diagram of sliding mode controller. (Ref: [35])	25
13.	Block diagram of Fuzzy Logic Controller (FLC)	27
14.	Fuzzy sets considered for speed control	27
16.	MATLAB -Simulink implementation of FSTPI-BLDC motor drive	30
17.	Hall decoder for FSTP BLDC motor drive	31
18.	Hall decoder for SSTP BLDC motor drive	32
19.	Reference current generator and reverse switch for four quadrant operation	33
20.	Hysteresis current controller for two phases	34
21.	MATLAB model for proportional Integral (PI) Controller	35
22.	Starting speed response of SSTPI-BLDCM for $N_{ref}=1800$ rpm	36

23(a).	Starting speed response of SSTPI-BLDCM for $N_{ref}=1800$ rpm, $HHH_{initial} = 100$	37
23(b).	Showing voltages of two capacitors C1 and C2 with $HHH_{initial}=100$	37
23(c).	Showing voltages of two capacitors C1 and C2 with $HHH_{initial}=101$	38
24.	Depicting flat speed phenomenon at starting of machine	39
25.	Starting speed response of FSTPI-BLDCM for $N_{ref}= -1800$, $HHH_{initial}=101$	40
26.	Hall signals, phase currents, N and T_e of BLDC motor at starting $HHH_{initial}=101$	41
27.	Speed, phase current, T_e response for load perturbation of SSTPI-BLDCM drive	42
28.	Speed, phase current, T_e response for load perturbation of FSTPI-BLDCM drive	43
29.	Speed, phase current, T_e response for speed reversal of SSTPI-BLDCM drive	44
30.	Speed, phase current, T_e response for speed reversal of FSTPI-BLDCM drive	45
31.	Speed, T_e , i_{dc} and I_{dc} responses for regeneration of SSTPI-BLDCM drive	46
32.	Speed, T_e , i_{dc} and I_{dc} responses for regeneration of FSTPI-BLDCM drive	47
33.	Showing currents and back emf's of three phases of BLDC motor	48
34.	Showing six switch inverter with six switches and their anti parallel diodes	49
35.	Phase A current response at rated load 2 N-m, 500 rpm for SSTPI fed drive	50
36.	Phase A current response at rated load 2 N-m, 1800 rpm for SSTPI fed drive	50
37.	Current responses during mode 4 commutation at 500 rpm for FSTPI fed drive	53
38.	Current responses at 1800 rpm showing commutation for FSTPI fed motoring	54
39.	Current responses at 1800 rpm showing commutation for FSTPI fed regeneration	56
40.	Proposed commutation technique for FSTPI-BLDC forward motoring operation	58
41.	Torque response showing commutation torque ripple and hysteresis torque ripple	59
42.	Current responses of proposed technique of FSTPI-BLDC forward motoring	60
43.	Torque response of proposed technique have only hysteresis torque ripple	61
44.	Simulink implementation of sliding mode speed controller	62

45.	Starting speed response using sliding mode speed controller of FSTPI fed drive	62
46.	Blocks of a fuzzy controller	63
47.	Step Response of the speed	66
48.	MATALB model for Fuzzy Logic (FL) speed controller	66
49.	Membership function plots for input and output variables	67
50.	Starting speed response using fuzzy speed controller of FSTPI fed drive	68
51.	Starting, speed Reversal & Load Perturbation Response of SSTPID with PI controller	72
52.	Starting, speed Reversal & Load Perturbation Response of SSTPID with SM controller	73
53.	Starting, speed Reversal & Load Perturbation Response of SSTPID with fuzzy controller	73
54.	Starting, Reversal & Load Perturbation Response of FSTPID with PI controller, $H_{initial}=100$	74
55.	Starting, Reversal & Load Perturbation Response of FSTPID with PI controller, $H_{initial}=101$	75
56.	Starting, Reversal & Load Perturbation Response of FSTPID with SM controller, $H_{initial}=100$	76
57.	Starting, Reversal & Load Perturbation Response of FSTPID with SM controller, $H_{initial}=101$	77
58.	Starting, Reversal & Load Perturbation Response of FSTPID with fuzzy controller, $H_{initial}=100$	78
59.	Starting, Reversal & Load Perturbation Response of FSTPID with fuzzy controller, $H_{initial}=101$	79
60.	Current responses and torque response of FSTPI-BLDCM at 1800 rpm and 2N-m load	80
61.	Current and Torque responses of proposed technique to reduce commutation torque ripple	81

LIST OF TABLES

Table.1. Details of individual phase reference currents based on rotor position (hall signals)	19
Table.2. Logic rules for Fuzzy Logic (FL) speed controller	67
Table.3. Comparative results using Different Speed Controllers for SSTPI-BLDCM drive	72
Table.4. Results of FSTPID with PI controller with $H_{initial}=100$ for different capacitances	74
Table.5. Results of FSTPID with PI controller with $H_{initial}=101$ for different capacitances	75
Table.6. Results of FSTPID with SM controller with $H_{initial}=100$ for different capacitances	76
Table.7. Results of FSTPID with SM controller with $H_{initial}=101$ for different capacitances	77
Table.8. Results of FSTPID with fuzzy controller with $H_{initial}=100$ for different capacitances	78
Table.9. Results of FSTPID with fuzzy controller with $H_{initial}=101$ for different capacitances	79

CHAPTER 1

INTRODUCTION

1.0 GENERAL

Electrical machines have been playing a vital role in the world since its primitive stage. Scientists and Technologists put efforts to realize many electrical machines and they succeeded by developing very famous Induction machine and Direct Current (DC) machine etc. These have been supporting industries, consumer applications and many others. To talk about DC machine, in particular, it set a trend to achieve a superior speed control. Since it was developed, DC machine has become important machine in industry and many other applications. It is well known for its simple speed control in either direction with above and below rated speed. But at the same time it has got some drawbacks in its functioning like operating voltage limitation, commutation and needs constant maintenance of brushes etc.

Technologists started pondering about other way to implement the same design technique of DC machine with some major modifications to eliminate the limitations imposed by DC machine. The result of these extensive efforts has given birth to Brushless DC motor. In early times it faced many problems due to limited progress in power electronics, electronics for position sensing and permanent magnets. But in due course, advances in these areas accelerated the improvement of Brushless DC motor. Since then many advancements have taken place to meet application requirements. Many new control techniques have further improved the scope of these motors.

Brushless dc motor uses permanent magnets, which previously hindered its growth, are now supporting due to reduction of its cost and increasing its performance like possibility for high flux density even at high temperatures. Similarly, position sensing become very easy in the form of Hall sensors as Brushless dc machine does not need so sophisticated position sensing. All these are now making Brushless dc machine suitable for many new applications day by day. Normally six switch voltage source inverter is used in control of three phase motors.

1.1 CHARACTERISTICS AND APPLICATIONS OF BLDC MOTOR

A Brushless DC motor is a rotating self-synchronous machine with a permanent magnet rotor and with rotor position sensor for electronic commutation. A motor meets this definition whether the drive electronics are integral with the motor or separate from it [4]. When the motor was developed, it was aimed to get similar characteristics as that of conventional DC motor and it so designed. This motor speed is approximately proportional to primary DC supply voltage assuming there is no speed or torque regulator i.e. in open loop. This is one of the main characteristics of DC motor. Figure.1 shows an example of torque/speed characteristics. There are two torque parameters used to define a BLDC motor, peak torque (T_P) and rated torque (T_R). During continuous operations, the motor can be loaded up to the rated torque. In a BLDC motor, the torque remains constant for a speed range up to the rated speed. The motor can be run up to the maximum speed, which can be up to 150% of the rated speed, but the torque starts dropping [1].

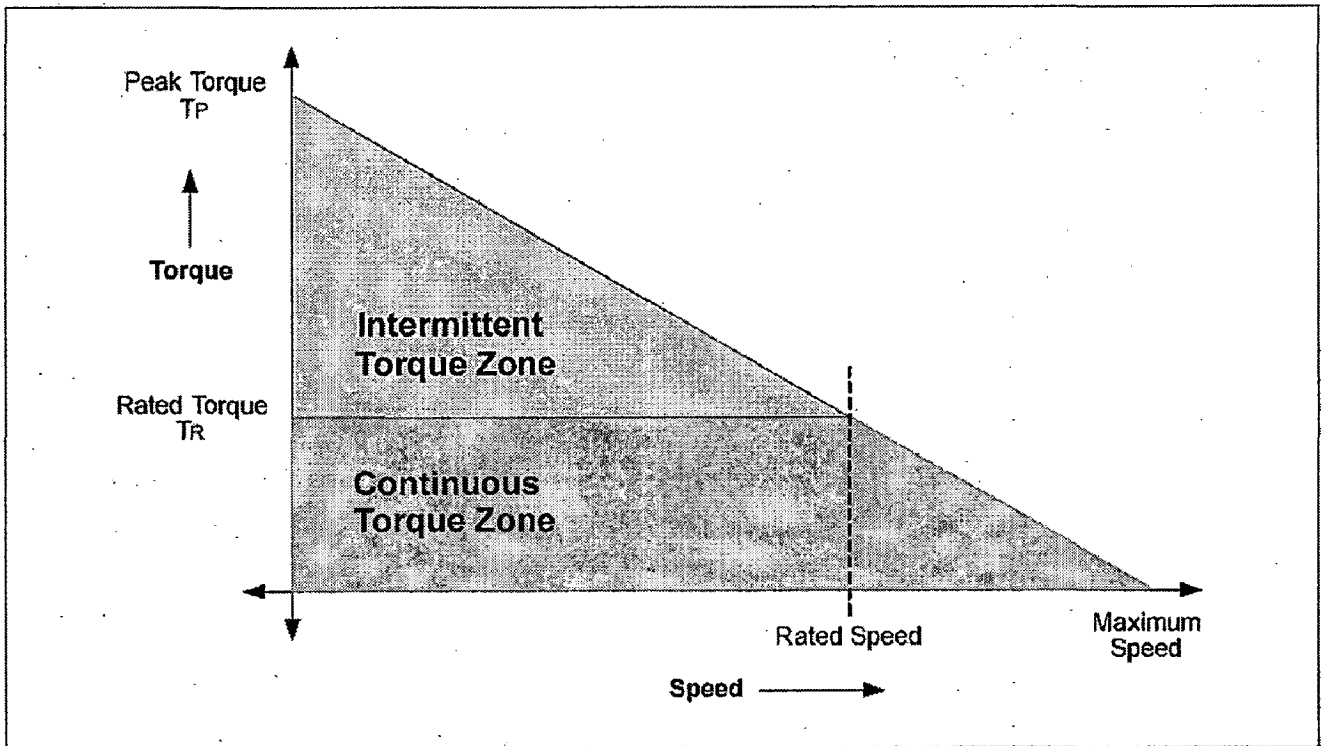


Figure.1. Speed-torque characteristics of typical Brushless DC motor (Ref: [1])

Applications that have frequent starts, stops and reversals of rotation with load on the motor, demand more torque than the rated torque to achieve fast action. This requirement comes for a brief period, especially when the motor starts from a standstill and during acceleration.

During this period, extra torque is required to overcome the inertia of the load and the rotor itself. The motor can deliver a higher torque, maximum up to peak torque, as long as it follows the speed torque curve [1].

BLDC motors find applications in many segments of the market. Automotive, appliance, industrial controls, automation, aviation and so on, have applications for BLDC motors. Out of these, we can categorize the type of BLDC motor control into three major types:

- Constant loads
- Varying loads
- Positioning applications

Constant load are the type of applications where a variable speed is more important than keeping the accuracy of speed at a set speed and these include fans, pumps and blowers demand low cost controllers mostly operating in open loop mode [1]. Varying load type applications have to handle continuously varying load over a speed range. These demand high speed control accuracy and good dynamic responses, includes applications like washers, dryers, compressors, fuel control automotive, fuel pump control, electronic steering control, engine control and electric vehicle control. In aerospace, there are a number of applications, like centrifuges, pumps, robotic arm controls, gyroscope controls and so on. Generally these applications use closed loop control and advanced algorithms making system expensive [1]. Most of the industrial and automation applications come under positioning applications which needs good dynamic response of speed and torque, subjected to frequent speed reversal. For these applications accelerating, constant speed range and decelerating periods are common with high performance closed loop control algorithms with separate loops for position, speed and torque control. Process controls, machinery controls and conveyer controls have plenty of applications in this category.

1.2 INVERTER TOPOLOGIES FOR THREE PHASE BLDC MOTOR DRIVE

Inverter is essential to drive a three phase BLDC motor and conventional six switch is the foremost choice. It has been found that the complete BLDC drive is expensive as BLDC motor itself is costly machine. Reducing cost of complete drive is the main objective for applications not requiring so sophisticated speed control. Researchers have found a possibility of four switch inverter fed three phase BLDC motor drive. Figure.2 shows the six switch inverter driving three phase BLDC motor without any controller.

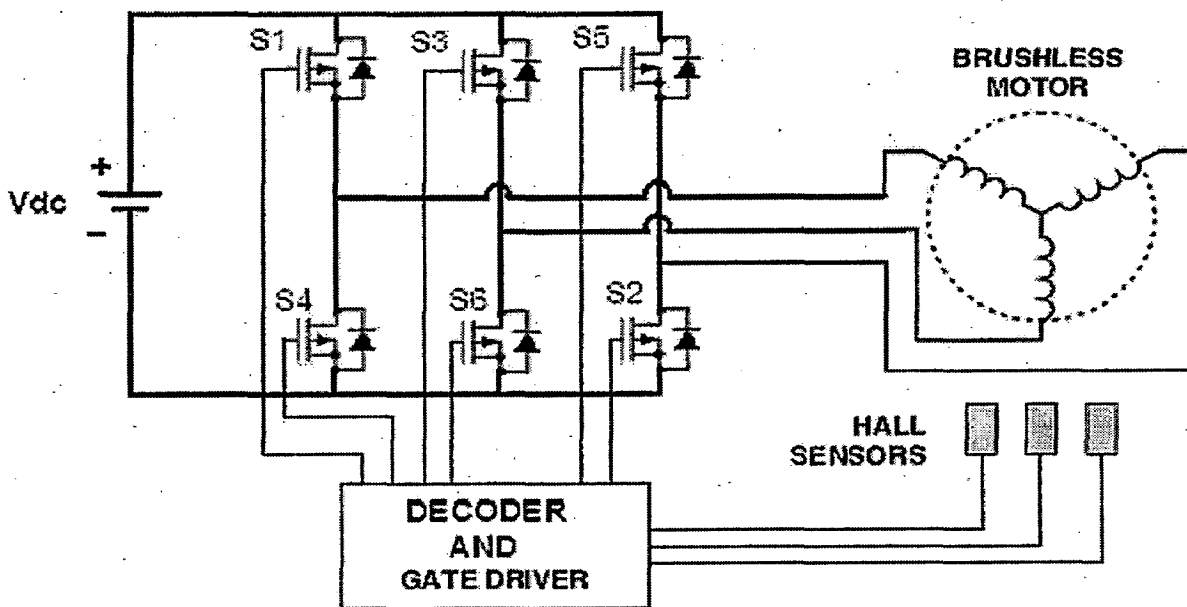


Figure.2. Basic circuit of six switch inverter fed BLDC motor

To produce a continuous torque, switching has to be done so that only two phases are 'on' based on rotor position information obtained from the hall sensors placed in the motor. The current flowing through phases has quasi square wave for constant ripple free torque. This is achieved using current controllers. This configuration is used for high performance applications requiring precise speed and torque control along with good dynamic response in closed loop form. It has good control over commutation torque ripple. Here, in this circuit, only two phases are 'on' at any time and the third phase is off. This leads to the concept and possibility of four switch inverter as two switches are redundant at any time. Figure.3 shows the configuration of four switch inverter driving three phase brushless dc motor without any controllers.

In this four switch inverter fed BLDC motor, the first leg two switches are replaced by two capacitors of equal value. There are total six switching states each for 60 degree electrical with two 2-switch controlled states and four 1-switch controlled states. During 1-switch controlled states only one of four available switches operates and the current will close its path through on of capacitor depend on which switch is 'on'. During 2-switch controlled states only two of four available switches operates with one switch from each leg and which must be one from high end other is from low end.

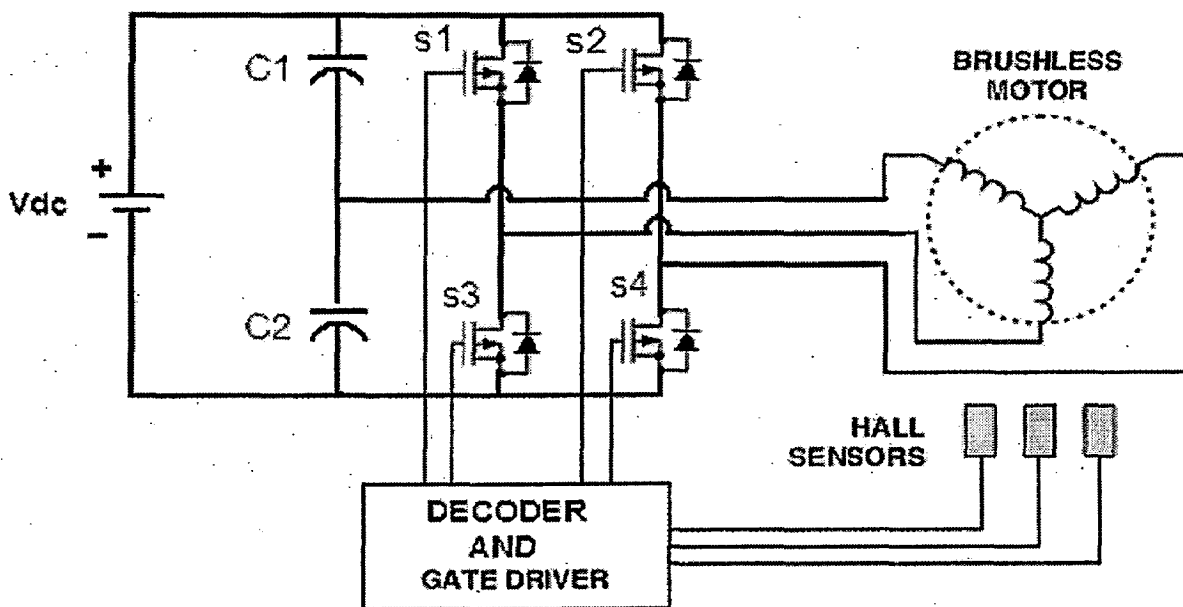


Figure.3. Basic circuit of four switch inverter fed BLDC motor

These 2-switch states are similar to the states in six-switch inverter where only six 2-switch states are available. During 1-switch states only one switch operates to control the current which makes the system to compromise its performance when compared six-switch inverter where only 2-switch states available leaving system for no compromise. The full details will be discussed in its specific chapter along with the advantages of four switch inverter. From this it is obvious that to run a Brushless DC motor it is must to have an inverter or another means to switching unlike induction motor where direct from mains can be run as it needs sinusoidal supply.

1.3 LITERATURE REVIEW

In the past decades, the development of motor control, power electronics and microelectronics technologies made the BLDC motor suitable for many applications. These motors have been investigated and described in the engineering literature for last few decades. Kusko and peeran have given a formal definition of a brushless dc motor. The definition includes the components of the motor and the types of circuits to energize the stator windings [4]. Generally six switch inverter is used for three phase BLDC motor. But later, it is found that there is possibility for four-switch inverter for its operation without reduction in quality. A little literature survey has been done regarding topologies and controlling techniques advances.

Yen-Shin Lai, and Yong-Kai Lin presented a paper to assess the Pulse-Width Modulation (PWM) techniques for BLDC motor drives. The criteria for assessment include driver circuit, reversal DC-link current, circulating current of floating phase.

Bhim Singh, A H N Reddy, S S Murthy proposed a new design of speed PI controller in which variable gain PI controller is used instead conventional fixed gain speed PI controller as it has got some short comings like they exhibit poor performance when applied to systems containing un known non-linearity like dead zones, saturation and hysteresis. In the proposed technique the speed PI controller gain is allowed to vary in a pre-determined range and therefore eliminates the problem faced by normal speed PI controller [24].

Byoung-Kuk Lee, Tae-Hyung Kim, and Mehrdad Ehsani, describes the feasibility of new inverter topology which reduces the price of drive unit, which is cost effective for commercial units where cost is the key role. It takes the advantage of idle leg of the traditional six switch inverter. Direct current control principle explained. The back emf in the idle phase is the again a problem and it is answered with a back emf compensated pwm control strategy [9].

Abolfazl Halvaei Niasar, Abolfazl Vahedi and Hassan Moghbelli presented a technique to eliminate commutation ripple torque. Due to unequal inductance of phases while rotor rotating, the change in current in different phases is different, particularly at switching time of phases causes commutation ripple torque. This problem is answered in above presentation [18].

B. K. Lee, B. Fahim, and M. Ehsan detailed overview of reduced parts converter topologies for AC Motor drives. In this they presented details of possibility for four-switch inverter for BLDC motor.

Joong-Ho Song, Ick Choy explained how to reduce commutation torque ripple using single current sensor in DC link [27] while Dae-Kyong Kim, Kwang-Woon Lee and Byung-II Kwon presented a technique to reduce commutation torque ripple in position sensorless Brushless DC motor drive [25].

Junyong LU, Deliang LIANG, Xiangyang FENG presented a simulation work in matlab-simulink about linear Brushless DC motor speed controlled system. Speed and thrust curves are presented for starting procedure and sudden load [23].

V.Donescu, D.O.Neacsu, G.Griva presented a design technique for fuzzy logic speed controller for brushless DC motor [22] while Fu Qiang, LinHui, Zhang Hai-tao explained the possibility for single current sensor based sliding mode driving strategy for four switch three phase BLDC motor.

1.4 AUTHORS CONTRIBUTION

A wide research is going on BLDC motor fed drives. Topological research of inverter feeding the BLDC motor is a emerging area in the research. One of the area's most research going on is four switch inverter fed drive and many performance improvement techniques presented. In this work four quadrant operation of four switch, three phase inverter fed BLDC motor has been implemented and its performance is evaluated and compared with its six switch counterpart. Decoder control logic for regeneration and reverse motoring is developed both for six switch and four switch inverter fed drives. Many things have been observed in forward and reverse regenerative region as these areas very less explored research area. At present, in particular, the most research happening area in four switch fed drive is commutation torque ripple reduction. In this work four switch inverter is facing problem with commutation torque ripple. To make the drive more suitable for many applications a novel technique is presented and it has improved torque response significantly. This novel technique is applied to forward and reverse motoring operation of the drive. The energy storing element, capacitor, its introduction in the inverter operation makes the working of inverter more complex. In this work these capacitors value affect on inverter performance is evaluated.

1.5 CONCLUSION

It is concluded from above that the Brushless DC motor is popularity gaining for many applications. Researchers and technologists have presented many speed controlling techniques, performance improved techniques and research is being done in a wide range. Cost reduction of drive and torque ripple reduction are main areas of research in present days both in sensor and sensor less mode. Apart from above presented popular inverter topologies there are other switching topologies are there which suits various applications. Popular current controlling techniques are presented in second chapter while third chapter devoted to mathematical modeling of BLDC motor. A novel technique is presented in this work to reduce the commutation torque ripple in the FSTPI-BLDC motor and different speed controllers and their performance evaluation is presented in further coming chapters with comparison.

CHAPTER 2

CURRENT CONTROL STRATEGIES OF VSI FOR BLDC MOTOR

2.0 INTRODUCTION

Most of the applications of three-phase voltage-source pulse width modulated (VS-PWM) converters—ac motor drives, active filters, high power factor ac/dc converters, uninterruptible power supply (UPS) systems, and ac power supplies—have a control structure comprising an internal “current feedback loop”. Consequently, the performance of the converter system largely depends on the current control strategy. Therefore, current control of PWM converters is one of the most important subjects of modern power electronics. In this chapter a most used current control methods are presented. In comparison to conventional open-loop voltage PWM converters, the current-controlled PWM (CC-PWM) converters have many advantages [30]. The quality of the current waveform generated by a current-controlled, voltage source inverter, depends basically on three factors: (a) The switching frequency of the PWM modulator. (b) The type of current waveform being generated and (c) the modulation method used.

For Brushless DC motor current waveforms are quasi square wave. One of the most popular current source inverters is the current controlled voltage source inverter (CCVSI). The CCVSI allows an easy control of power in the four quadrants, with current reversal [28]. There are three main current control techniques are being used for BLDC motor drives. They are as follows:

1. Triangular carrier method.
2. Hysteresis band method.
3. Periodical sampling method.

First two are very famous in controlling the current in BLDC motor [28]. These two are discussed in detail in the following sections.

2.1 ADVANTAGES OF PWM TECHNIQUES

Advantages of current controlled PWM converters:

- 1) Control of instantaneous current waveform and high accuracy.
- 2) Peak current protection.
- 3) Overload rejection.
- 4) Superior dynamic performance.
- 5) Compensation for semiconductor voltage drop and dead times of the converter.
- 6) Compensation for the dc-link and ac-side voltage changes.

2.2 TRIANGULAR CARRIER METHOD (TC)

This technique is also known as triangular Pulse Width Modulation (PWM). This technique is very famous for sinusoidal current control and it is also used in quasi square current control in BLDC motor applications. The following circuit shows the control strategy of the technique.

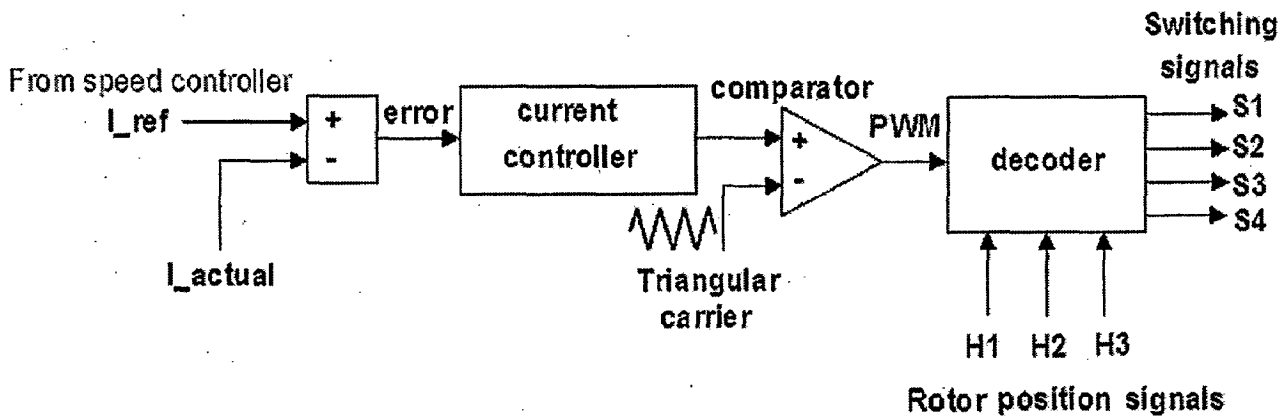


Figure.4. Triangular carrier (TC) PWM current control technique

The TC method shown in Figure.4, takes the error between reference current generated from speed PI controller and actual current sensed. Then the error will be processed through current Proportional (P) controller or Proportional plus Integral (PI) controller.

This controller needs to be designed properly. Empirical equations to find values for PI controller constants are available. Based on the type of current controller, P or PI, two types of triangular carrier PWM techniques available and those are TC-P and TC-PI. The output of this controller is compared with a fixed amplitude and frequency triangular wave: the triangular carrier. The values of K_p and K_i determine the transient response and steady state error of the TC method.

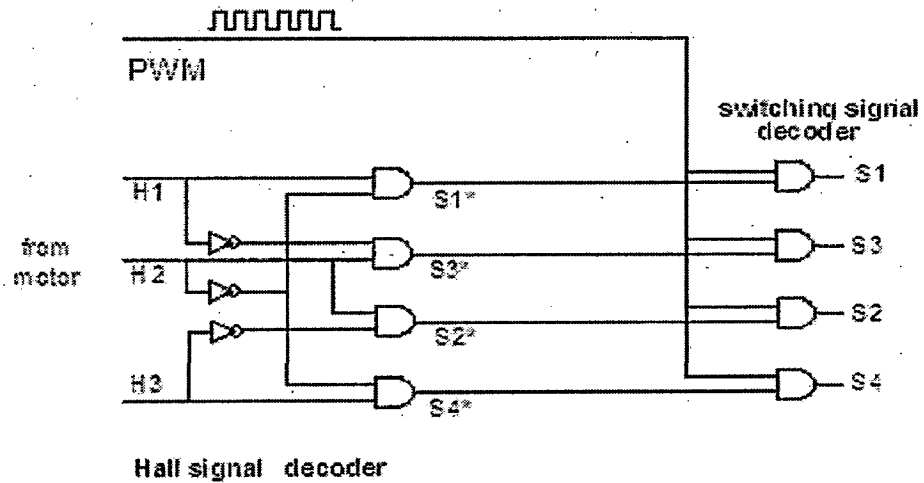


Figure.5. Decoder circuit for single quadrant BLDC motor

The Figure.5 shows the decoder circuit for a single quadrant BLDC motor. The Hall signals are decoded so that proper a continuous torque is developed in the motor by operating proper switches based on rotor position. The PWM signal from comparator will be logical 'AND'ed to have PWM effect on the switches there by supply voltage to control the current. TC-P gives better performance than TC-PI technique as latter one is strongly affected by the failure to follow the reference because the error accumulates in the integrator and finally produces an overshoot [28].

2.3 HYSTERESIS BAND METHOD (HB)

This controlling technique is most used for current controlling in BLDC motors and is also known as hysteresis current controller. Hysteresis control schemes are based on a nonlinear feedback loop with two level hysteresis comparators.

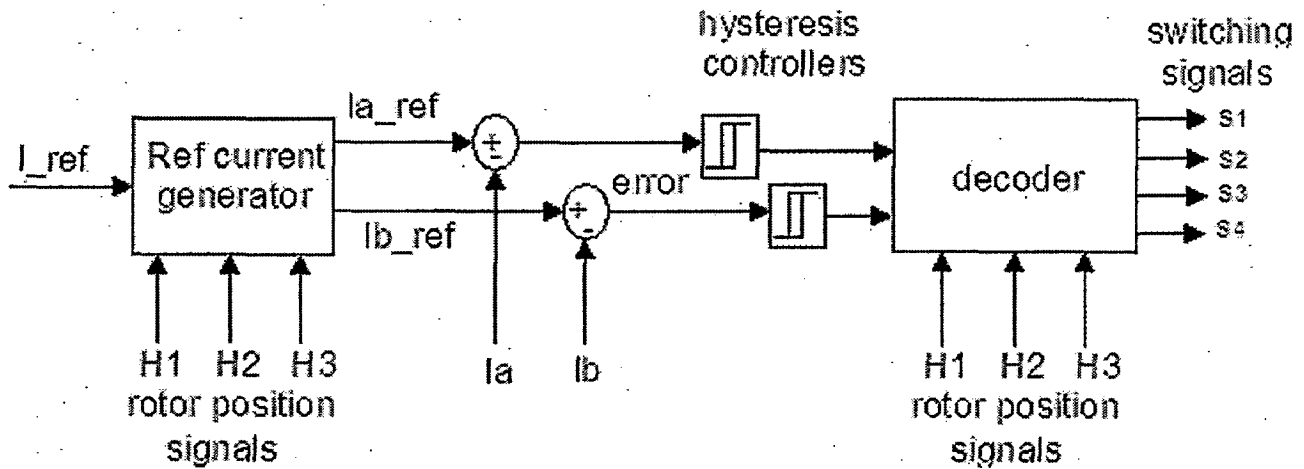


Figure.6. Hysteresis band current control technique

The reference current generated from the speed controller is fed to phase current reference generator, which actually generate individual phase currents based on rotor position. In four switch inverter only two phases are controlled. Generated phase reference currents i_{a_ref} and i_{b_ref} are compared with sensed actual phase currents i_a and i_b . The errors are then sent to hysteresis current controllers to produce PWM signal. PWM signal is then sent to the decoder circuit shown in Figure. 7. The HB method operates the switches when the error exceeds a fixed magnitude: the hysteresis band. This type of circuit needs comparator if it is implemented in analog circuits. In this case the switching frequency is not determined as in TC method, but it can be estimated [28]. In the case of TC-P, the generated current has a permanent error due to scaling factor. In the TC-PI case the error source is the overshoot of current [28].

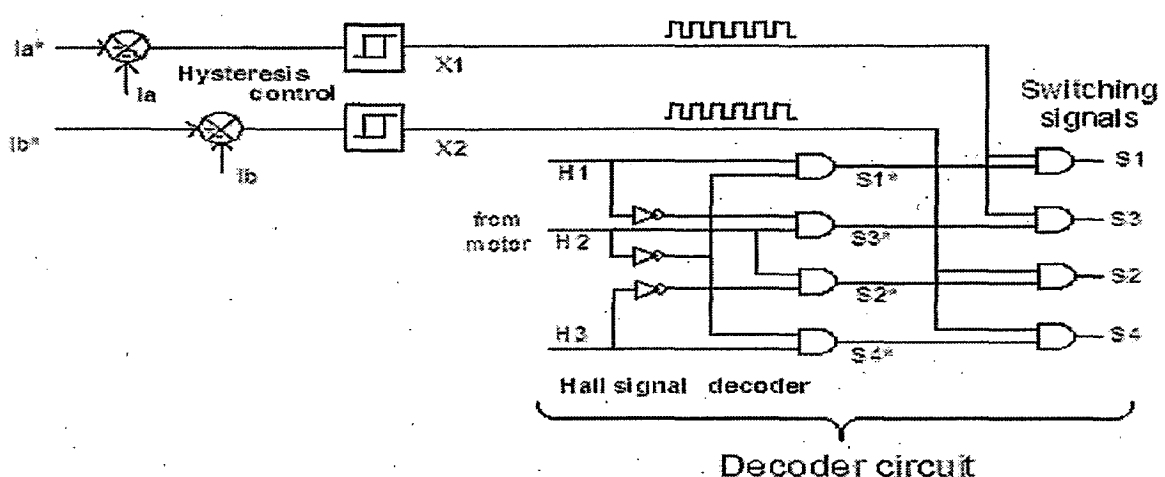


Figure.7. Hysteresis current controller and decoder circuit

Hysteresis current controllers are easy to implement and it has good performance for controlling currents in BLDC motor drives while TC methods best suits for sinusoidal current controlling. In BLDC motor drives hysteresis band and triangular carrier methods takes first and second place respectively while periodical sampling method is the last one in performance. Distortion is more in periodical sampling method and it is unable to follow the reference current as quickly as HB and TC do [28]. Hysteresis current controllers are used in 'direct current controlled PWM' technique very often used in BLDC motor drives. In this work direct current controlled PWM technique is used.

2.4 CONCLUSION

Like any other electric drives, BLDC motor drives need inner current feedback loop. So, the performance of the drive largely depends on the performance of current controller. Pulse Width Modulation based current controlling techniques have become popular due to its advantages. Triangular carrier (TC) PWM method unanimously best suit for sinusoidal currents while hysteresis band and triangular carrier methods are best suit for BLDC motor current control. The choice between them is decided by the inductance of the circuit. Most of the BLDC motor drives use HB current controllers for its current control. Direct current control PWM technique is mostly used current control technique in BLDC motors. Periodic sampling method is inferior to the above two methods.

CHAPTER 3

MODELING OF FOUR SWITCH THREE PHASE (FSTP) INVERTER FED BLDC MOTOR DRIVE

3.0 INTRODUCTION

A permanent magnet brushless dc (PMBLDC) motor drive is a combination of ac machine, rotor position sensor and inverter that results in a system producing a linear speed-torque characteristic similar to the conventional dc motor and due to this motor is named as brushless dc motor. It has 3-phase windings on the stator similar to 3-phase squirrel cage induction motor and magnets are placed on the rotor to provide air gap flux for brushless rotor construction. It has trapezoidal induced emf in stator phase windings when driven at any rotor speed. The quasi-square wave ac current is fed to stator phase winding through electronic commutator (using current controlled voltage source inverter and rotor position sensor), which results in constant torque. At any instant of time, two out of 3-phase stator winding of the motor carry currents in proper synchronization with rotor magnets position and develop electromagnetic torque. The output torque is dependent upon the amplitude of stator current and the flux produced by PM rotor. The use of high energy density permanent magnet material has resulted in reduced motor weight, increased efficiency, high torque, and low rotor inertia with associated fast response.

In this chapter a detailed description is given about direct current control PWM technique in the four switch inverter topology. Analysis and mathematical modeling of drive is presented. Mathematical modeling of different speed controllers used in this work is presented.

3.1 DIRECT CURRENT CONTROL PWM

As shown in Figure.8, the developed four-switch three-phase BLDC motor drive consists of two switch legs with switches S1, S2, S3, S4, and split capacitors. Two phases of the motor are connected to the switch legs and the other phase is connected to the midpoint of DC-Link capacitors. A PWM control strategy is used to control the three-

phase currents to take a form of quasi square waveform in order to synchronize with the trapezoidal back EMF to produce constant.

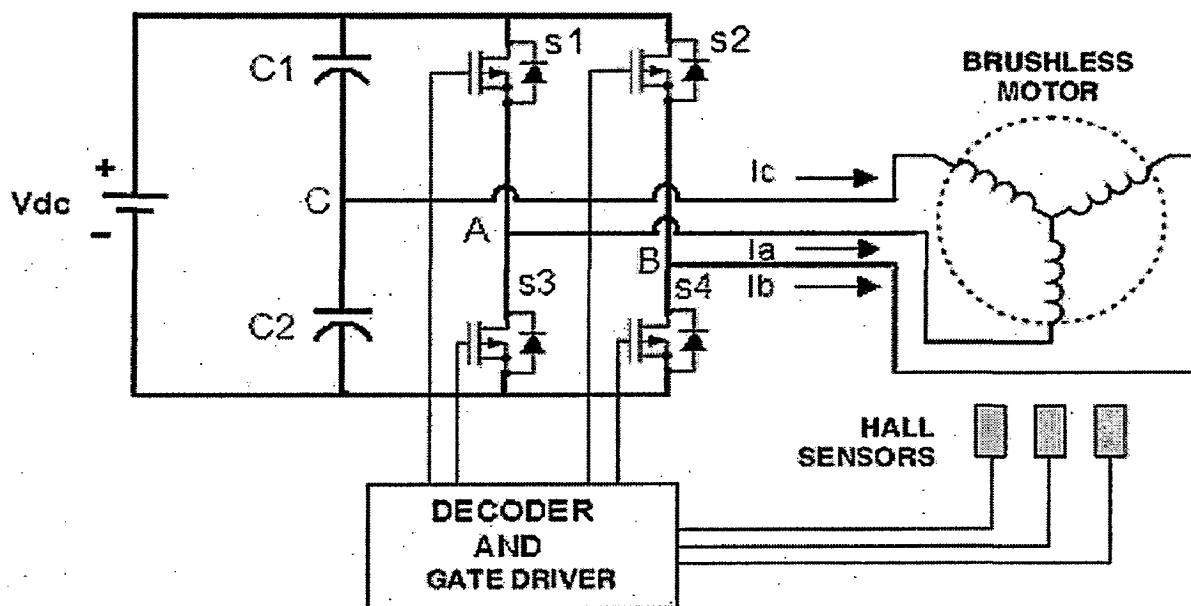


Figure.8. Four switch inverter for driving BLDC motor

For forward motoring operation, the BLDC motor is supplied by the four-switch inverter, ideal back EMF of three-phase BLDC motor and the desired current profiles are described as shown in Figure.9. From the detailed investigation of the four-switch configuration and back EMF and current profiles in Figures. 8 and 9, a PWM control strategy for the four-switch three-phase BLDC motor drives is explained as follows: Under the balanced condition, the three-phase currents always meet the following condition, such as

$$I_a + I_b + I_c = 0 \tag{1}$$

The above equation is re written as,

$$I_c = -(I_a + I_b) \tag{2}$$

Equation (2) implies that one of the three-phase currents equals the summation of the other phase currents. It means that control of the two-phase currents can guarantee the generation of the 120° conducting three-phase currents profiles. For completing this task, the two-phase currents are directly controlled using the hysteresis current control method for four switches, and is called as direct current controlled PWM scheme.

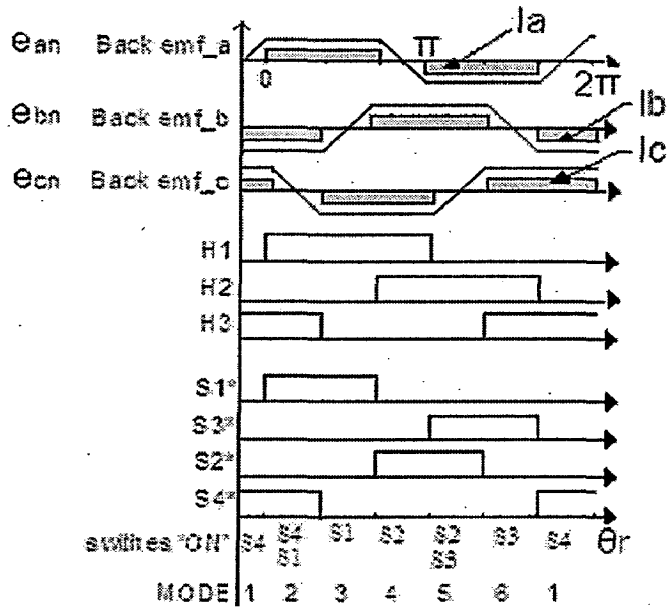


Figure.9. Hall sensor signals, switching signals, back emf and currents of three phases

Based on the direct current controlled PWM, the four-switch three-phase BLDC motor drive can be divided into six operating modes and the switching sequences are determined according to the operating modes. The detailed switching conduction status is depicted in Figures. 9 and 10. As an example of the phase A, the direct current control mechanism can be more clearly visualized with the help of Figure.10.

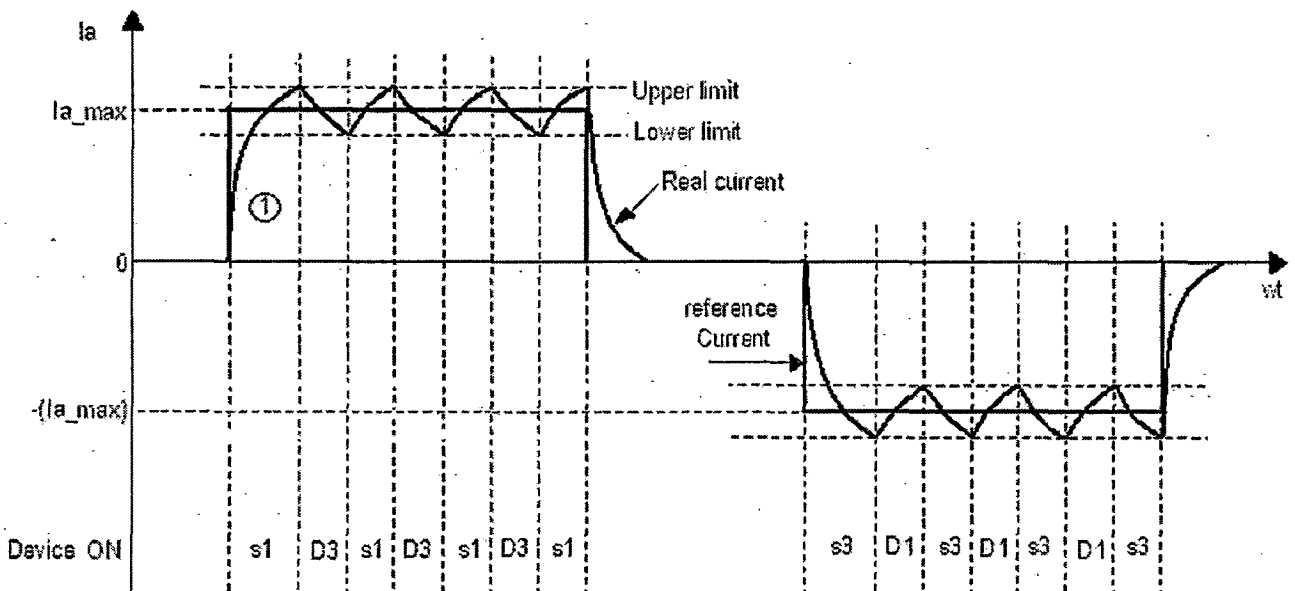


Figure.10. Implementation of direct current controlled PWM (Ref:[9])

(1)Case1: $I_a > 0$

- Period 1: $I_a < \text{Lower Limit (LL)}$ → Switch S1 is turned on.
- Period 2: $I_a > \text{Upper Limit (UL)}$ → Switch S1 is turned off and D3 is turns on.
- Period 3: $LL < I_a < UL$ and $\frac{dI_a}{dt} > 0$ → Switch S1 is turned on.
- Period 4: $LL < I_a < UL$ and $\frac{dI_a}{dt} < 0$ → Switch S1 is turned off and D3 is turns on.

(2)Case2: $I_a < 0$

- Period 1: $I_a > \text{Upper Limit (UL)}$ → Switch S3 is turned on.
- Period 2: $I_a < \text{Lower Limit (LL)}$ → Switch S3 is turned off and D1 is turns on.
- Period 3: $LL < I_a < UL$ and $\frac{dI_a}{dt} < 0$ → Switch S3 is turned on.
- Period 4: $LL < I_a < UL$ and $\frac{dI_a}{dt} > 0$ → Switch S3 is turned off and D1 is turns on.

The same explanation can be applied to the control of the phase B. Also, the voltage and current equations for each mode can be expressed as:

- Mode 1: $V_{c2} = 2RI_c + 2L \frac{dI_c}{dt} + e_{cb}$
- Mode 2: $V_{c1} + V_{c2} = 2RI_a + 2L \frac{dI_a}{dt} + e_{ab}$
- Mode 3: $V_{c1} = 2RI_a + 2L \frac{dI_a}{dt} + e_{ac}$
- Mode 4: $-V_{c2} = 2RI_b + 2L \frac{dI_b}{dt} + e_{bc}$
- Mode 5: $-(V_{c1} + V_{c2}) = 2RI_b + 2L \frac{dI_b}{dt} + e_{ba}$
- Mode 6: $-V_{c1} = 2RI_c + 2L \frac{dI_c}{dt} + e_{ca}$

As shown in Figure.9, special attention should be paid to the Mode 1 and Mode 5. In these modes, the phases A and B are conducting current and the phase C is regarded as a silent phase, so that it is expected that there is no current in the phase C. However, the back EMF of phase C can act as a source and causes the additional and unexpected current resulting in current distortion in the phase A and B. Therefore, in the direct current controlled PWM, the back EMF compensation problem should be considered.

As an example of Mode2, if the phase A current is controlled and determines the switching signals of S1 and S4, the phase A current can be regarded as a constant current source. In this case, the phase B current can be distorted by the phase C current. On the other hand, if the phase B is controlled, the phase B current can be a constant current source, and then the phase A current gets distorted. The same explanation can be applied to Mode V. But, if the phase A and B are regarded as independent current source, the back EMF of phase C cannot act as a current source, so that there is no current in the phase C. It means that in the direct current controlled PWM, the phase A and phase B currents should be controlled independently and the switching signals of S1 (S3) and S4 (S2) should be determined independently. This way direct current control eliminates the back emf problem [9].

3.2 ANALYSIS OF BLDC MOTOR DRIVE

The drive system considered here consists of speed controller, the reference current generator, hysteresis current controller, PMBLDC motor and inverter. Speed controllers used in this work are PI, sliding mode, fuzzy logic separately. Modeling of these speed controllers has been done in coming sections. Hysteresis current controller is used to implement direct current control PWM technique.

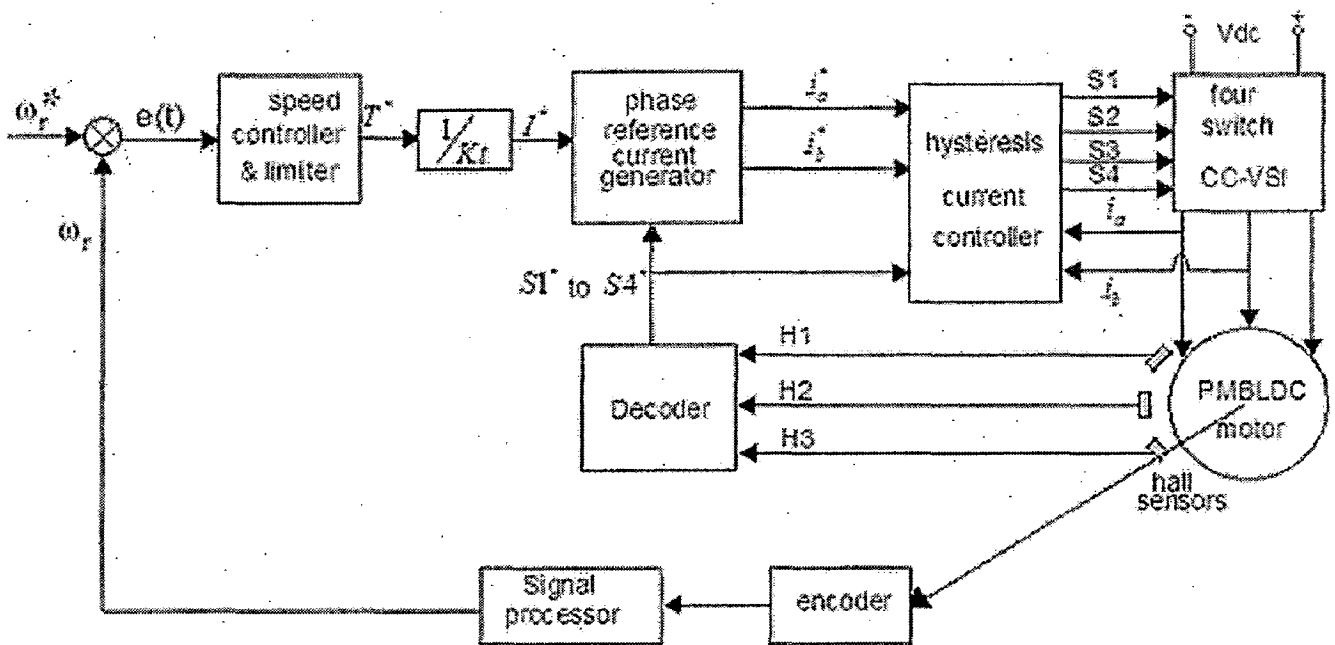


Figure.11. Basic block diagram of PMBLDC motor drive system

The input to the reference current generator is reference torque (T^*) and the rotor position signals. The magnitude of the three phases current (I^*) is determined by using reference torque (T^*) and the torque constant K_t is as:

$$I^* = T^* / K_t \quad (3)$$

Depending on the rotor position, the phase reference current generator generates the reference currents (i_a^*, i_b^*) by taking the value of reference current magnitude as I^* , $-I^*$ and zero as follows:

H1	H2	H3	Rotor position angle	$i_{a_reference}(i_a^*)$	$i_{b_reference}(i_b^*)$
1	0	1	$0^\circ - -60^\circ$	I^*	$-I^*$
1	0	0	$60^\circ - -120^\circ$	I^*	0
1	1	0	$120^\circ - -180^\circ$	0	I^*
0	1	0	$180^\circ - -240^\circ$	$-I^*$	I^*
0	1	1	$240^\circ - -300^\circ$	$-I^*$	0
0	0	1	$300^\circ - -360^\circ$	0	$-I^*$

Table.1. Details of individual phase reference currents based on rotor position (hall signals).

These reference currents are fed to the hysteresis current controller. Detail of hall signals and reference currents is given in Figure.9.

3.2.1 Modeling of back emf based on rotor position

Phase back emf in the PMSM motor is trapezoidal in nature and is the functions of the speed and rotor position angle. The normalized functions of back emf are shown in Figure.9. From this, the phase back emf can be expressed as:

$$\begin{aligned}
e_{an} &= E & \text{For } 0^\circ < \theta_r < 120^\circ \\
e_{an} &= (6E/\Pi)(\Pi - \theta) - E & 120^\circ < \theta_r < 180^\circ \\
e_{an} &= -E & 180^\circ < \theta_r < 240^\circ \\
e_{an} &= (6E/\Pi)(\theta - 2\Pi) + E & 240^\circ < \theta_r < 360^\circ
\end{aligned}$$

Where, $E = K_b \omega_r$ and e_{an} can be described by E and normalized back emf function shown in Figure.9. $e_{an} = E.f_a(\theta_r)$. Where, $f_a(\theta_r)$ is a back emf function. Similarly for other two phases e_{bn}, e_{cn} can be modeled.

3.3 MATHEMATICAL MODELLING OF PM BLDC MOTOR.

The PMLDC motor is modeled in the stationery reference frame using 3-phase abc variables. The general volt-ampere equations can be expressed as

$$v_{an} = Ri_a + p\lambda_a + e_{an} \quad (4)$$

$$v_{bn} = Ri_b + p\lambda_b + e_{bn} \quad (5)$$

$$v_{cn} = Ri_c + p\lambda_c + e_{cn} \quad (6)$$

Where v_{an}, v_{bn} and v_{cn} are phase voltages designed as

$v_{an} = v_{ao} - v_{no}$, $v_{bn} = v_{bo} - v_{no}$ and $v_{cn} = v_{co} - v_{no}$, where v_{ao}, v_{bo}, v_{co} and v_{no} are 3-phase and neutral voltages referred to the zero reference potential at the midpoint of two capacitors in the inverter. R is the resistance per phase of the stator winding, p is the time differential operator and e_{an}, e_{bn}, e_{cn} are phase to neutral back emf's. The λ_a, λ_b and λ_c are total flux linkages of phase windings a, b and c respectively. These values can be expressed as

$$\lambda_a = L_s i_a - M(i_b + i_c) \quad (7)$$

$$\lambda_b = L_s i_b - M(i_a + i_c) \quad (8)$$

$$\lambda_c = L_s i_c - M(i_a + i_b) \quad (9)$$

Where L_s and M are the self and mutual inductances respectively, the PMBLDC motor has no neutral connection and hence this results in

$$i_a + i_b + i_c = 0 \quad (10)$$

Substituting equation (10) into equations (7), (8) and (9) the flux linkages are given as

$$\lambda_a = i_a(L_s + M)$$

$$\lambda_b = i_b(L_s + M) \text{ and } \lambda_c = i_c(L_s + M) \quad (11)$$

By substituting equation (11) in volt-ampere equations (4)-(6) and rearranging these equations in a current derivative of state space form, giving

$$p i_a = (v_{an} - R i_a - e_{an}) / (L_s + M) \quad (12)$$

$$p i_b = (v_{bn} - R i_b - e_{bn}) / (L_s + M) \quad (13)$$

$$p i_c = (v_{cn} - R i_c - e_{cn}) / (L_s + M) \quad (14)$$

The developed electromagnetic torque may be expressed as

$$T_e = (e_{an} i_a + e_{bn} i_b + e_{cn} i_c) / (\omega_r) \quad (15)$$

Where ω_r is the rotor speed in electrical radian/sec. The torque expression runs into the computational difficulty at starting as induced emf is zero. The back emfs are expressed as function of position θ_r , which can be written as

$$e_{an} = k_b \cdot f_a(\theta_r) \cdot \omega_r \quad (16)$$

$$e_{bn} = k_b \cdot f_b(\theta_r) \cdot \omega_r \quad (17)$$

$$e_{cn} = k_b \cdot f_c(\theta_r) \cdot \omega_r \quad (18)$$

Where $f_a(\theta_r)$, $f_b(\theta_r)$, and $f_c(\theta_r)$ are functions of rotor position with a maximum of +1 or -1 are identical to induced emf in shapes as shown in Figure.9. Substituting equations (16) - (18) into equation (15), the torque expression becomes

$$T_e = k_b \{f_a(\theta_r)i_a + f_b(\theta_r)i_b + f_c(\theta_r)i_c\} \quad (19)$$

The mechanical equation of motion in speed derivative form can be expressed as:

$$p\omega = (p/2)(T_e - T_l - B\omega_r)/J \quad (20)$$

Where P is the number of poles; T_l , the load torque in N-m; B , is the frictional coefficient in N-ms/rad, and J is the moment of inertia, kg-m^2 . The derivative of the rotor position (θ_r) in state space is expressed as:

$$p\theta_r = \omega_r \quad (21)$$

Substituting equation (10) in the volt-ampere equations (4)-(6) and adding them together gives:

$$v_{ao} + v_{bo} + v_{co} - 3v_{no} = R(i_a + i_b + i_c) + (L_s + M)(pi_a + pi_b + pi_c) + (e_{an} + e_{bn} + e_{cn}) \quad (22)$$

Substituting equation (10) in equation (22) gives

$$v_{ao} + v_{bo} + v_{co} - 3v_{no} = (e_{an} + e_{bn} + e_{cn}) \quad (23)$$

Thus,

$$v_{no} = [v_{ao} + v_{bo} + v_{co} - (e_{an} + e_{bn} + e_{cn})]/3 \quad (24)$$

The set of differential equations mentioned in equations (12), (13), (14), (20) and (21) define the developed model in terms of the variables $i_a, i_b, i_c, \omega_r, \theta_r$ and time as an independent variable.

3.4 MODELLING OF SPEED CONTROLLERS

Feedback control is used in practice in many control applications. The benefits of this control method are that it is possible to keep some physical quantity at a strict level or change the value of the quantity, quickly and despite of the disturbances that might occur. The basic requirement that a control system should be able to fulfill is stability. This means that a control system should remain stable in all circumstances. The quality of the control can be measured by analyzing the accuracy, and robustness of a control system. If the output signal of the process grows, the measurement signal (feedback) grows as well. This means that the error signal becomes smaller and the control signal becomes smaller too. This makes the process output signal to go down, which means that error signal goes towards zero and the output of the process towards reference value. In this work, three speed controllers have been used. Each speed controller has been modeled separately as given below. Each speed controlled is followed by a limiter. Generally the speed error, which is the difference of reference speed and actual speed, is given as input to these controllers. These speed controllers process the speed error and give reference torque value as an output. Then the torque value is fed to the limiter which gives the final limited reference torque. The speed error at any n th instant of time is given a

$$\omega_{re(n)} = \omega_{r(n)}^* - \omega_{r(n)} \quad (25)$$

where $\omega_{r(n)}^*$ is the reference speed of the motor and $\omega_{r(n)}$ is the actual speed of the motor

Various speed controllers used in this work are explained in the following sections.

3.4.1 Proportional Integral (PI) speed controller

The PI speed controller is the simplest speed controller compared to any other speed controller. The general block diagram of the PI speed controller is shown in Figure.12. The output of the speed controller at n th instant is expressed as follows:

$$T_{(n)} = T_{(n-1)} + K_p \{\omega_{re(n)} - \omega_{re(n-1)}\} + K_i \omega_{re(n)} \quad (26)$$

where $T_{(n)}$ is the torque output of the speed controller at the n^{th} instant.

K_p and K_i are proportional and integral gain constants

$\omega_{re(n-1)}$ is the speed error at $(n-1)$ th instant

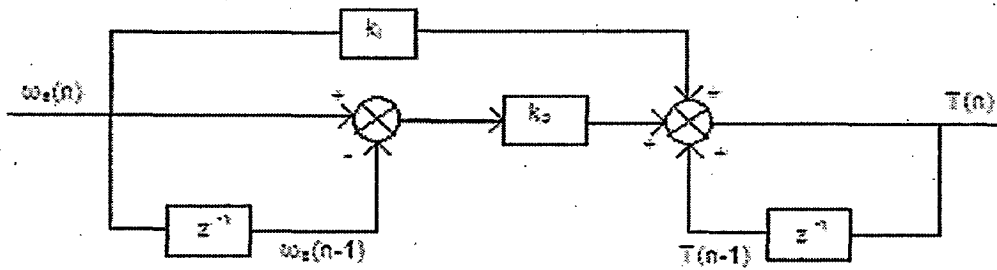


Figure.12 Block diagram of PI speed controller

The numerical values of these controller gains depend on the ratings of the motor and they are presented in the Appendix-A for the motor drive system used in this work. Tuning and Matlab implementation of speed PI controller is explained in coming sections. The purpose of *P* controller is to decrease the steady-state error, but it has the side effect, that is, larger overshoot and could give rise to the oscillation. The purpose of *I* controller is to eliminate the steady-state error.

3.4.2 Sliding Mode Speed Controller

The sliding mode controller (SMC) is a special case of variable structure control [35]. The problem associated with PI speed controller (PI parameter tuning) is overcome in the sliding mode controller. The SMC provides the robust performance in terms of system parameter variation and load changes. The system response in the phase plane is forced to a sliding line. In the time domain, the corresponding system output response is exponential. The block diagram of a sliding mode controller is given in Figure.12 (b). The response of sliding mode controller is insensitive to the parameter of the motor, and depends on the slope of the sliding line. The main drawback of the sliding mode controller is the chattering action in the controller output.

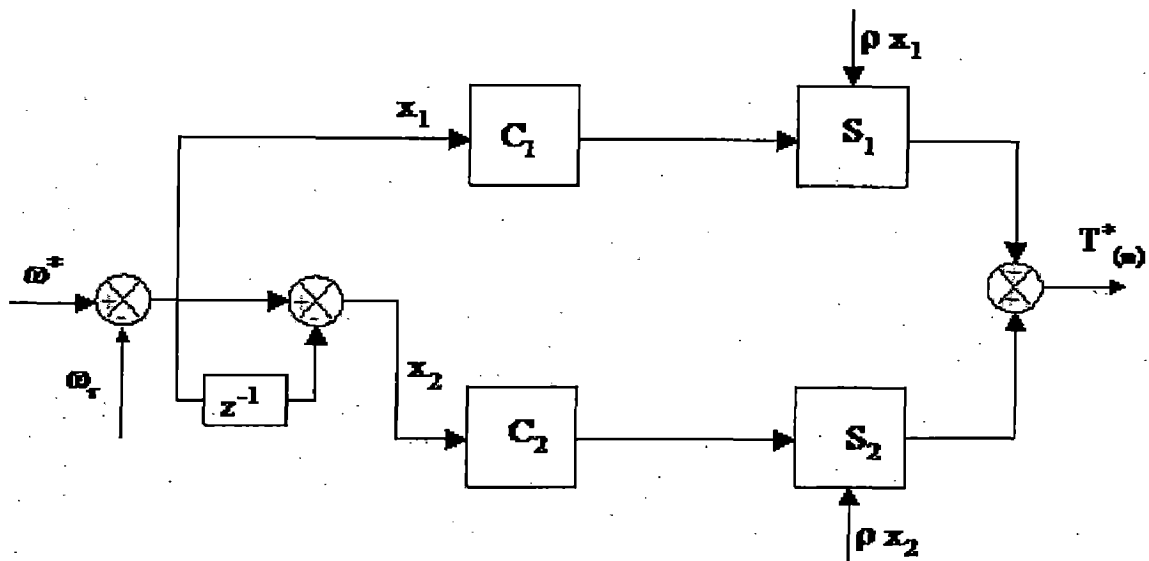


Figure.12 (b) Block diagram of sliding mode controller

3.4.3 Fuzzy logic speed controller

The conventional speed controllers for PM BLDC motor drives suffer from the problem of stability, besides these controllers show either steady state error or sluggish response to the perturbation in reference setting or during load perturbation. The motor control issues are traditionally handled by fixed gain PI and Proportional-integral-derivative (PID) controllers. However, the fixed-gain controllers are very sensitive to parameter variations, load disturbances, etc. Thus, the controller parameters have to be continually adapted. However, it is often difficult to develop an accurate system mathematical model due to unknown load variation, temperature variations, and unknown and unavoidable parameter variations due to saturation and system disturbances. In order to overcome the above problems, the fuzzy-logic controller (FLC) is being used for motor control purpose. The mathematical tool for the FLC is the fuzzy set theory introduced by Zadeh [28]. As compared to the conventional PI, PID, and their adaptive versions, the FLC has some advantages such as:

1. It does not need any exact system mathematical model.
2. It can handle nonlinearity of arbitrary complexity.
3. It is based on the linguistic rules with an IF-THEN general structure, which is the basis of human logic.

However, the application of FLC has faced some disadvantages during hardware and software implementation due to its high computational burden.

MODELING OF FUZZY LOGIC BASED SPEED CONTROLLER:

A. Variables of input and output for controller:

The block diagram of speed control system using a fuzzy logic controller (FLC) is shown in Figure.13. In order to establish the FLC, variables of the input and the output for the controller must be clearly defined. Though the FLC can have several observed values as inputs, the most significant variables entering the FLC have been selected as the speed error (ω_{re}) and its time derivative i.e. change in error ($\Delta\omega_{re}(n)$). The output of this controller is the reference torque, T.

At a sampling time n, the input variables are expressed as

$$\omega_{re}(n) = \omega_r^*(n) - \omega_r(n) \quad (28)$$

$$\Delta\omega_{re}(n) = \omega_{re}(n) - \omega_{re}(n-1) \quad (29)$$

Where ω_r^* and ω_r are reference speed command and the actual speed of the induction motor.

B. Fuzzy variables and control rules:

In order to obtain better control results, it is necessary to use appropriate number of fuzzy variables and to formulate appropriate control rules. In this study, we use the fundamental seven kinds of fuzzy variables as follows:

NB : Negative Big	PB : Positive Big
NM : Negative Medium	PM : Positive Medium
NS : Negative Small	PS : Positive Small
ZE : Approximately Zero	

The next step is to decide the appropriate shape of the membership functions for ω_e and ω_{re} . More fuzzy sets in ω_e and ω_{re} will lead to higher precision in this input space. Hence seven fuzzy sets are assigned to each of the inputs in their respective

universe of discourse. If the number of fuzzy sets in a particular universe of discourse is increased to infinity, then all fuzziness will be lost and it will be equivalent to a conventional input domain. To simplify mathematical computations, the shape of the fuzzy sets on the two extreme ends of the respective universe of discourse is taken as trapezoidal whereas all other intermediate fuzzy sets are triangular. This is illustrated in fig. 14.

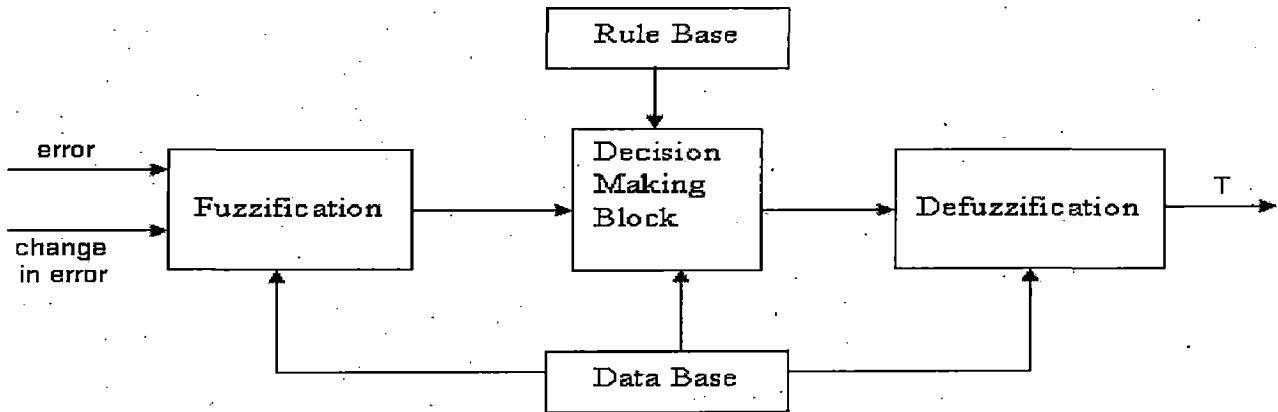


Figure.13. Block diagram of Fuzzy Logic Controller (FLC)

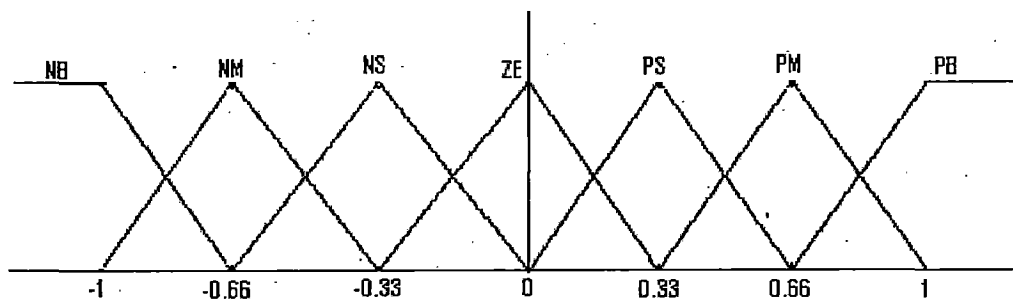


Figure.14. Fuzzy sets considered for speed control

The control rules for the FLC can be described by language using the input variables w_e and w_{re} , and the output variable, T. For example the i-th control rule can be usually written as:

Rule i : if w_e is F_i and w_{re} is G_i then T is H_i .

Where F_i , G_i and H_i are fuzzy variables.

3.5 CONCLUSION

In this chapter analysis of drive is presented to provide deep understanding of drive functioning. The current control technique "direct current controlled PWM" is explained. Mathematical modeling is the best way to understand a system. The mathematical modeling of BLDC motor is developed. Mathematical modeling of speed controllers used in this work are presented.

CHAPTER 4

MATLAB IMPLEMENTATION OF FOUR SWITCH THREE PHASE INVERTER FED BLDC MOTOR DRIVE

4.0 INTRODUCTION

Analysis of a BLDC motor drive provides an insight of the drive. But simulations provide more accurate and dynamic evidence of actual functioning of drive. Needless to mention that simulation work provides great flexibility to evaluate the functioning of drive. Due to many advantages of simulation of a system, it has been widely accepted. Much simulation software has been developed and MATLAB has become obvious choice for many researchers and technologists of electrical engineering. It provides lots of facilities to build a simulation model of a system. There different ways to build a simulation system. One of the choices is to use basic building blocks available in MATLAB-simulink and build a mathematical of drive. We can either develop a mathematical model of a machine or use its library block of the machine required. We can build a mathematical model of a machine either by using basic building blocks of library or by s-functions. In this work BLDC library model has been used and s-function based mathematical model of BLDC motor is also developed. In this work four switch inverter fed BLDC motor drive has been developed and its performance is investigated with different speed controllers but common hysteresis current controller, it gives better performance to implement quasi square wave currents using direct current control technique than any other method [28]. A reduced switch inverter fed drive is implemented in this work and its performance is compared with the conventional six switch inverter fed drive in four-quadrant operation.

4.1 FOUR QUADRANT OPERATION OF FSTP INVERTER FED BLDC MOTOR DRIVE

In this section a MATLAB –simulink model is developed for four switch inverter fed drive with four quadrant operations along with braking mode. In this three previously mentioned speed controllers have been presented with their conventional six switch counterpart for comparison. As mentioned, hysteresis current controller is effective for quasi square wave currents. This method is used in direct current controlling PWM technique.

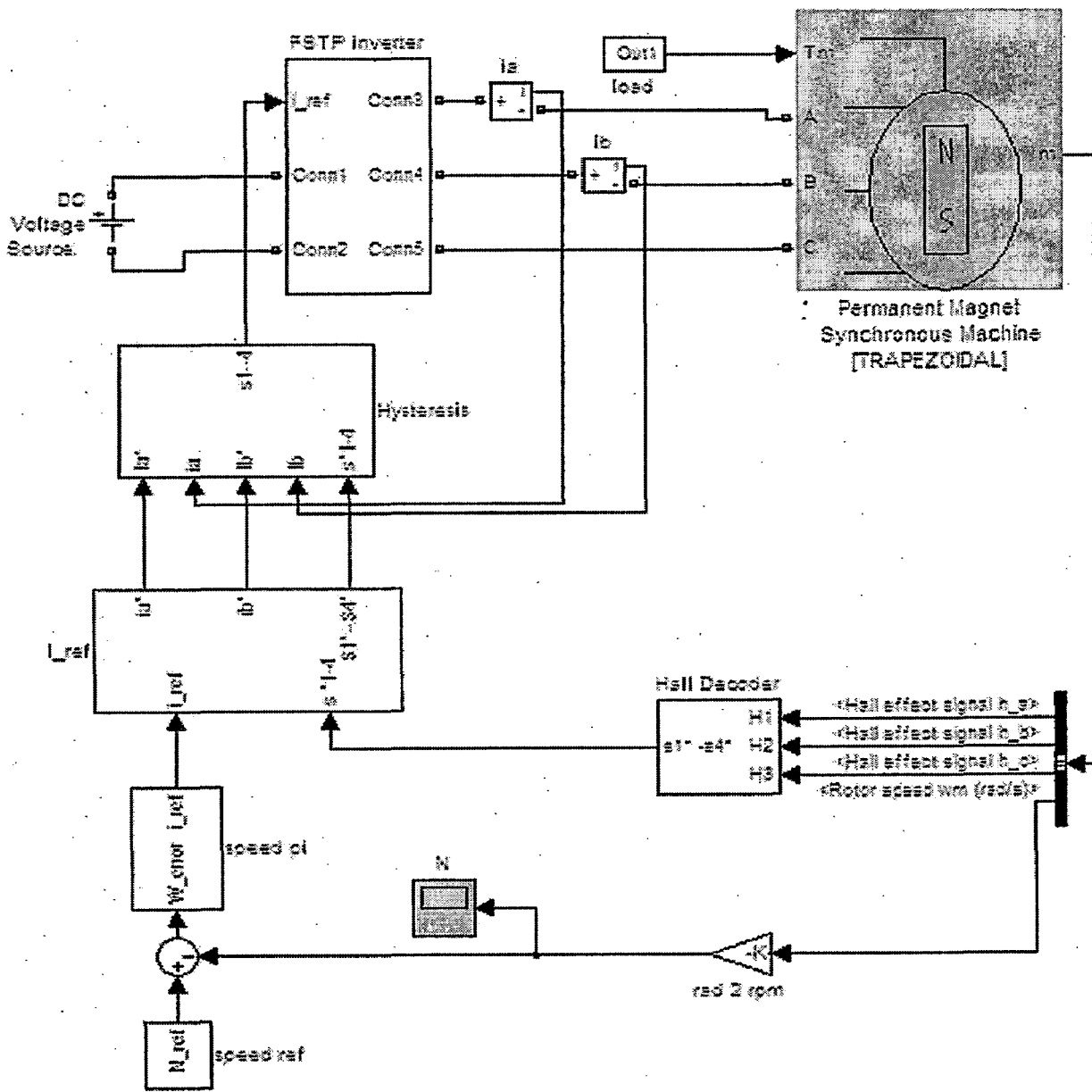


Figure.16.Simulation diagram of FSTPI-BLDC motor drive for four quadrant operation in MATLAB environment using simulink and Power System Block set (PSB) toolboxes

Fig.11 shows the simple block diagram of BLDC motor drive fed by four switch inverter and its implementation in MATLAB-simulink is shown in Fig.16. It needs two current sensors for current control of the machine. Previously detailed direct current control technique through

hysteresis controller is implemented. The Figure.17 shows the hall decoder circuit in MATLAB-simulink. This generates reference switch signals $S1^*$ -- $S4^*$. These signals are fed to phase reference current generator and hysteresis current controller.

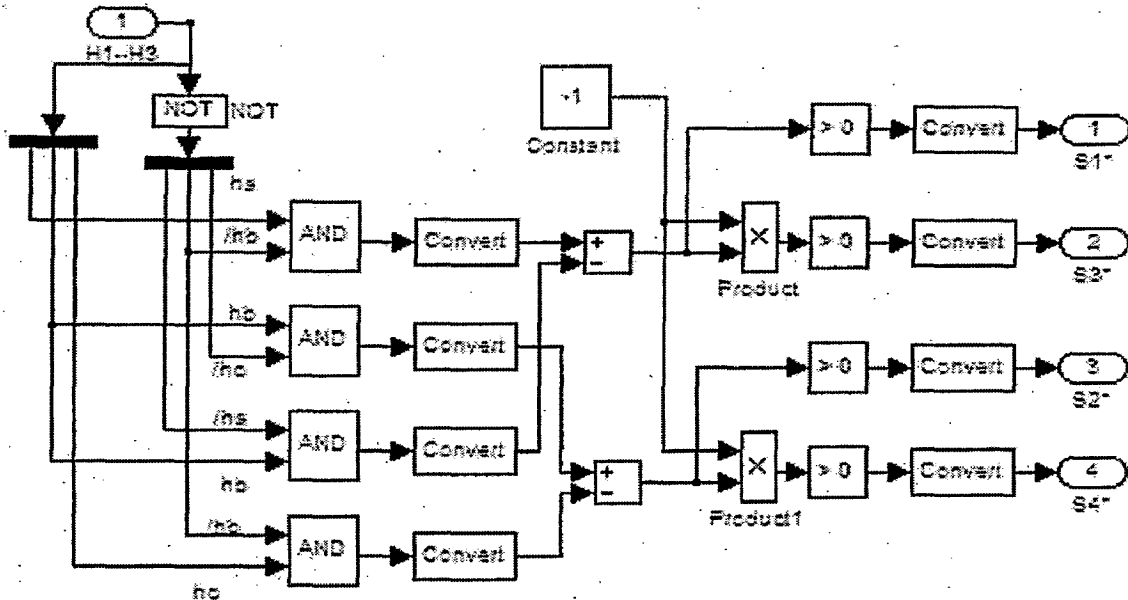


Figure.17. Hall decoder for FSTP BLDC motor drive

This logic is developed using the position signals with respect to three phases of BLDC motor. The individual phase position corresponds induced electro motive force (emf) of the motor. Three hall sensors are so positioned that a motor should give hall signals shown in Figure.9 with respect three stator windings. Signals $S1^*$ -- $S4^*$ are unit template of switching signals if the BLDC motor was operated on no current control techniques like hysteresis and PWM control i.e. in open loop. If the motor is to be controlled in a closed loop manner using inner current control loop to control current in the phases, these signals have to be fed to reference current generator. Logic is developed to implement four quadrant operation of motor. This uses the sign of reference current generated by speed controller and reverse switching technique using position signals. Figure.18 shows the decoder logic developed in MATLAB-simulink, similar to Figure.17 but for six switch inverter operation. Three hall signals from motor are the input to the decoder circuit.

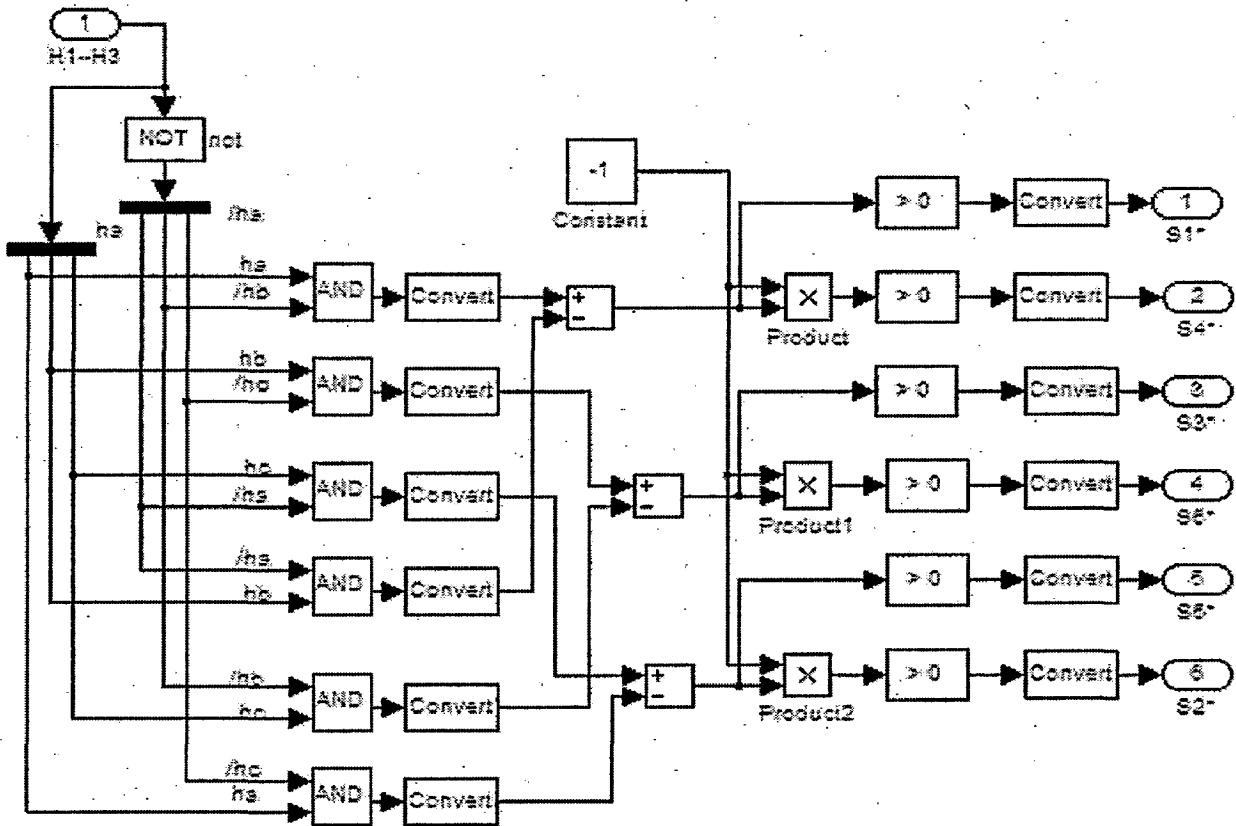


Figure.18. Hall decoder for SSTP BLDC motor drive

Hall signals from the motor will pass through the hall decoder to get $S1^*--S4^*$. These signals are then fed to phase reference current generator and hysteresis current controller in single quadrant operation. In four quadrant operation these decoded signals pass only to phase reference current generator circuit. The difference in the above two cases is because, the reference switching signals ($S1^*--S4^*$) will change as per sign of reference current generated from speed controller. This is implemented using a reverse switch as shown in Figure.19. It shows Phase reference current generator along with reverse switch for four quadrant operation. The outgoing signals from this circuit are two phase reference currents ia^* , ib^* and four reverse switch controlled reference switching signals ($S1^*--S4^*$). Hardware implementation of this circuit is included in the software part. Hall signal decoding is implemented through software in hardware implementation of the drive. Speed controller is also implemented in the programming. The reverse switch in the Figure.19 changes the $S1^*$ to $S3^*$ and vice-versa, $S2^*$ to $S4^*$ and vice-versa when sign of reference current is changed. Phase reference currents are sent to next part for current controlling based on the value of actual sensed currents.

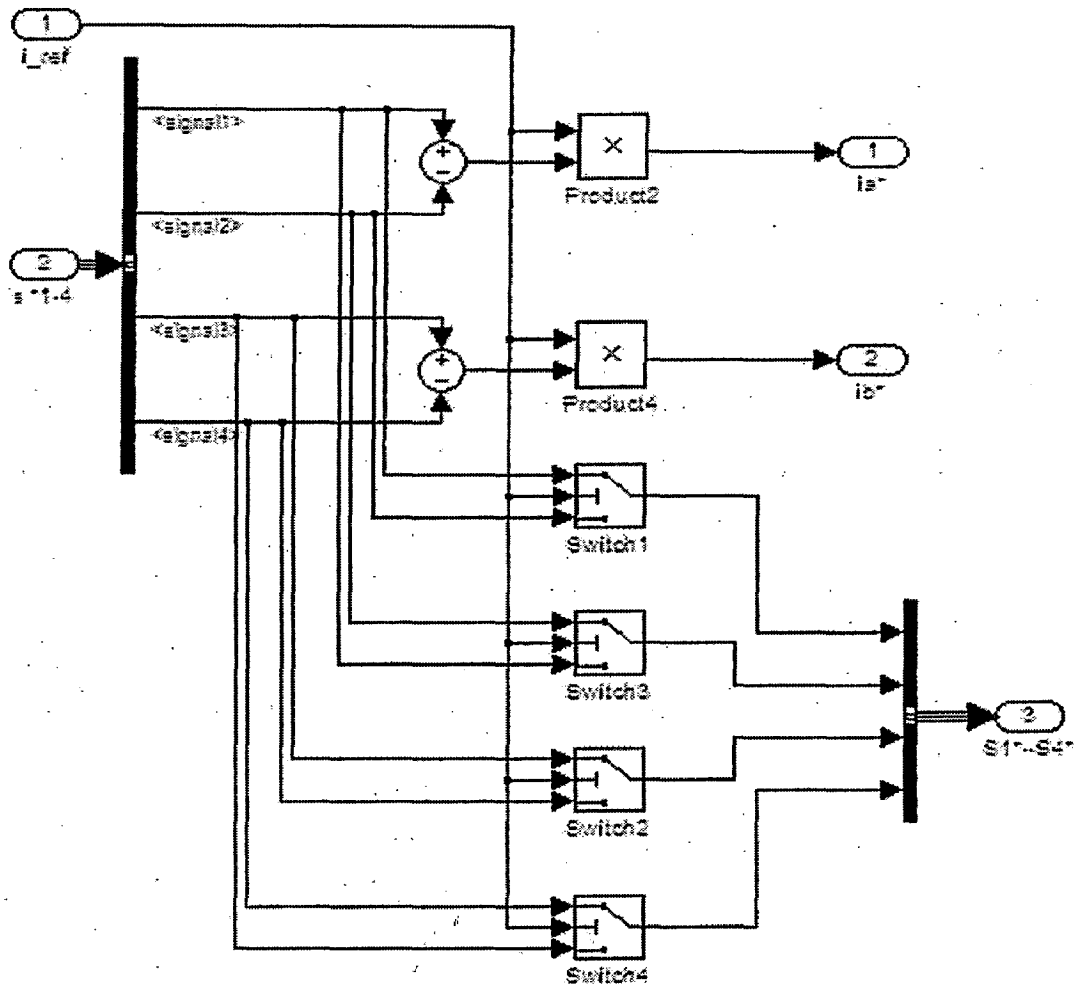


Figure.19. Phase reference current generator along with reverse switch for four quadrant operation.

One might question the importance of four reference switching signals ($S1^*--S4^*$) going to hysteresis current controller. This is because, any phase conducts positive current for 120° and negative current for 120° as shown in Figure.9. The rest of the 120° is divided into two 60° duration. During these two periods actually the current is zero. But due to back emf in that phase some current tries to flow in that phase causes the hysteresis current controller to trigger unnecessary switches which actually are not intended to switch 'on'. This leads to misfiring of power switches, and causes deterioration in performance. To avoid this problem a set of four reference switching signals ($S1^*--S4^*$) from hall decoder are used as shown in this Figure.20, these ensures proper operation of power switches. This is enough for a

single quadrant operation. To ensure four quadrant operation and to avoid above mentioned misfiring problem a set of four reverse switch controlled, reference switching signals ($S1^*$ -- $S4^*$) from phase reference current generator block (Figure.19) are given to Hysteresis block shown in Figure.20. All these are clearly depicted in Figure.9 and Figure.16.

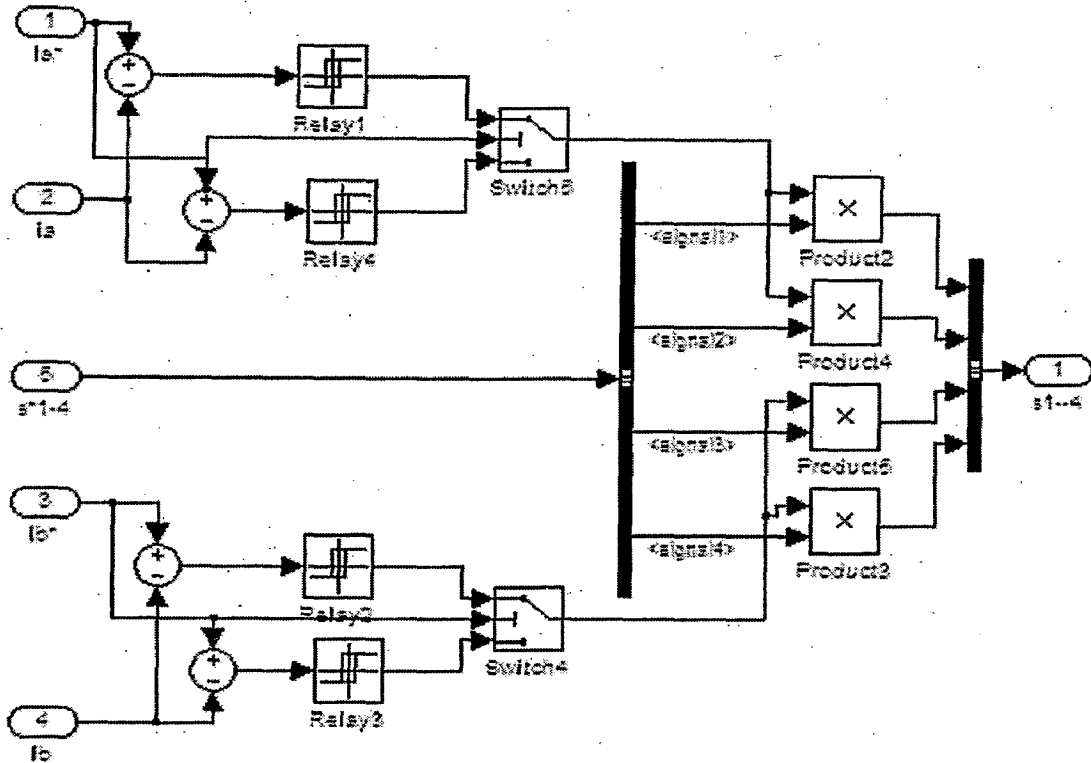


Figure.20. Hysteresis current controller for two phases

The Figure.20 shows the hysteresis current controller and also reference switching signals. This block generates PWM pulses to power switches. These signals are given to driver circuit of power switches to control current to required value.

4.2. PROPORTIONAL-INTEGRAL (PI) SPEED CONTROLLER BASED BLDCM DRIVE

This speed controller has been very popular for closed loop systems. The requirements set for a controller can be partly contradictory. A controlled closed loop system should be stable and the performance of the controller should be good, meaning that the control is fast and accurate. For example, the better the performance of the controller, the less stable the closed system. That is why one must make compromises to fulfill all the requirements. The goal is to make the system fast, but on the other hand, the system should not be taken close

to the oscillation boundary, where small changes in the system (e.g. noise) could make the system unstable. Motor performance is analyzed based on its speed and torque response.

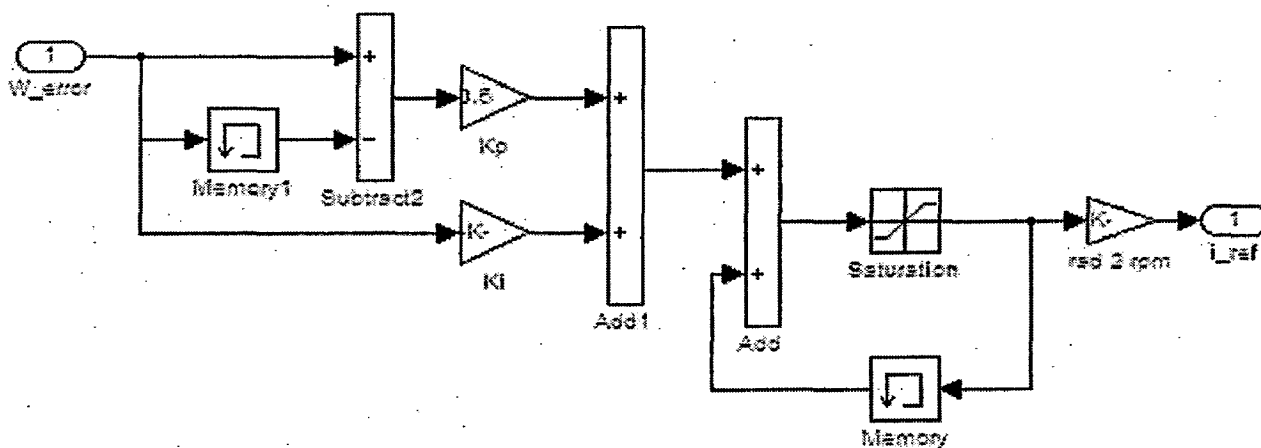


Figure.21.MATLAB model for proportional Integral (PI) Controller

4.2.1 Analysis of starting response

Starting response of conventional six switch inverter fed drive is obtained and then compared with four switch inverter fed drive. Starting speed response performance is evaluated for four switch inverter. Figure.22. show the simulated starting speed response of BLDC motor with six switch inverter. The motor used for simulation have rated speed of 1800 rpm. Reference speed is set for 1800 rpm. The rise time is 1.8175 seconds with an over shoot speed of 1.45 rpm (0.08%). The starting response of any motor is largely affected by moment of inertia, applied voltage and starting current of the motor. For any motor all these parameters are fixed. It is designer choice to limit the starting current, but it largely influences the starting time because starting torque is direct proportionally related to starting current. For a motor the starting current is generally in the order of three to six times the rated current. In this work motor starting current is limited to about three times its rated value. The rated current of this BLDC motor is 7.5 ampere and starting current is limited to 21 ampere. Motor is starts at 21 ampere to achieve fast starting. The same motor is implemented with four switch inverter. In four switch inverter two capacitors are used in one leg in which previously two switches were used.

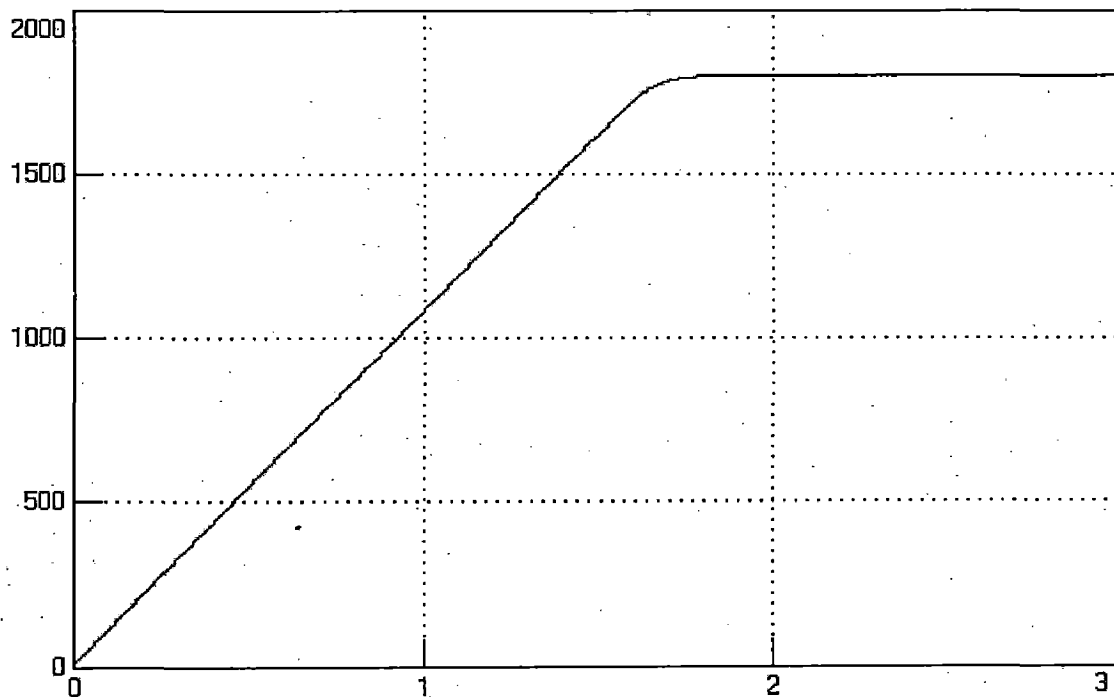


Figure.22. Starting speed response of BLDC motor fed with a six switch inverter for a reference speed of 1800 rpm

These two capacitors are initially charged to half of the DC supply voltage. Figure.23(a) shows the simulated starting speed response of the motor for the same reference speed with same maximum starting current. It can be seen from the Figure.23(a) that there is a difference in speed response during starting of drive. In this, an almost constant speed region is observed for very short duration.

The rise time is 2.1258 seconds with an over shoot speed of 3.2 rpm which is 0.17%, it is also negligible. Four switch three phase (FSTP) inverter fed drive takes 308.3 milliseconds more time than its six switch counterpart and have 0.09% more over shoot in speed. Reason for the delay in speed response can be explained as follows: Figure.24 shows the rotor position at starting by hall signals H1, H2, H3: 1 0 0. From Figure.9 it is known that for that rotor position only switch S1 is 'on' and phases A and C will be carrying current through switch S1 and lower capacitor C2 which is already charged to half the DC supply voltage at 77 volt for a DC supply of 154 volt. At zero speed of the motor, back emf is zero and motor takes more time to cover that 60° duration than time taken to charge the capacitor to DC supply voltage due to low speed of motor.

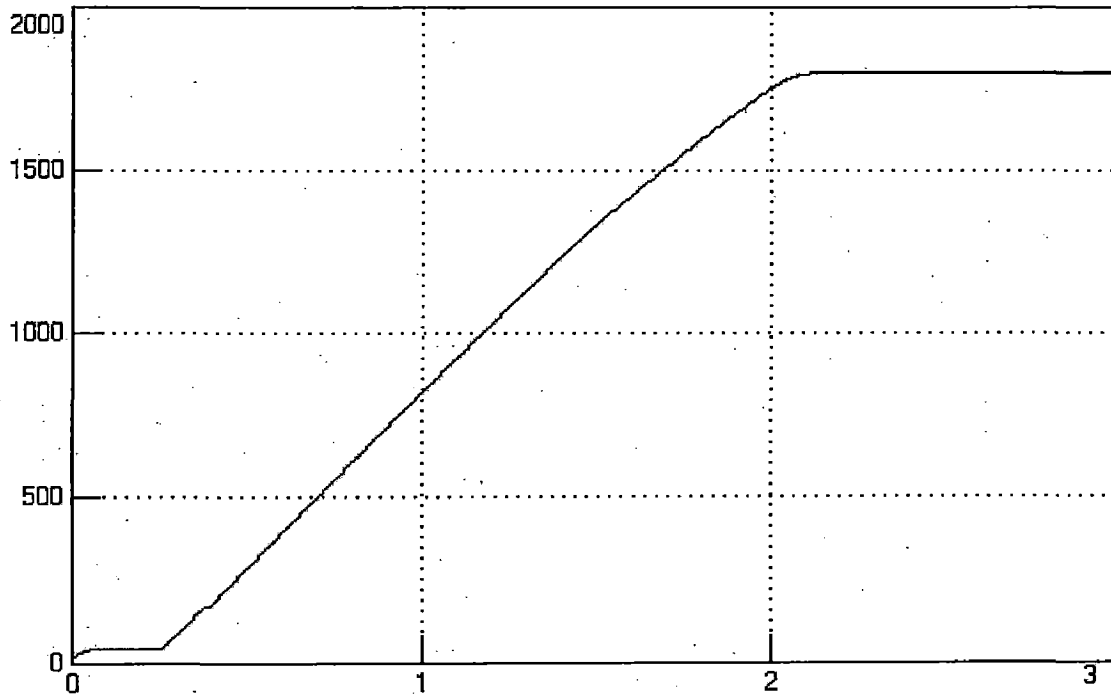


Figure.23(a). Starting speed response of BLDC motor fed with a four switch inverter for a reference speed of 1800 rpm with initial rotor position $HHH=100$

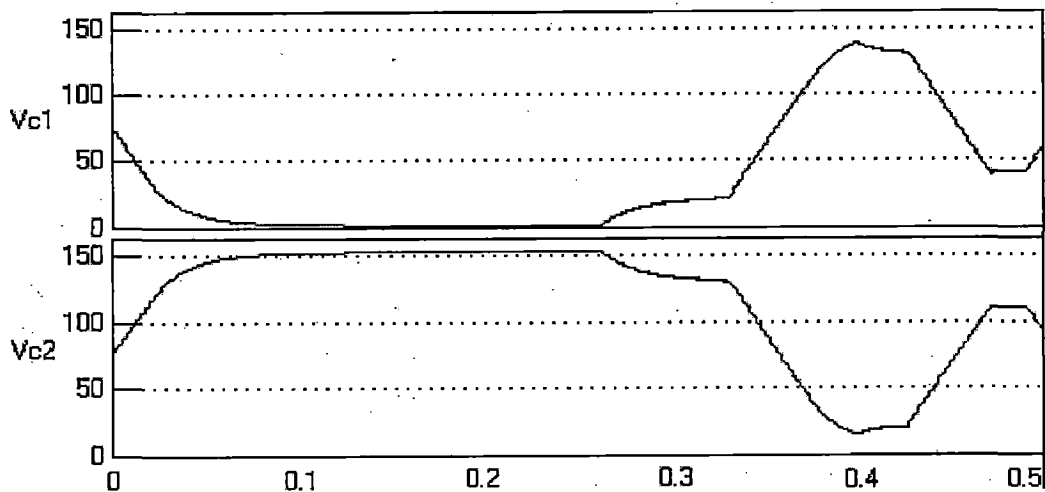


Figure.23(b). Showing voltages of two capacitors C1 and C2 with $HHH_{initial}=100$

So, during first 60° of conduction capacitor charges to nearly DC supply voltage in a very short time than the time taken for the 60° to complete. This causes the capacitor to block the further current after getting charged to nearly DC supply voltage.

This phenomenon is clearly depicted in Figure.23 (b) and 24. But due to starting torque and very low current in the motor causes it to move forward.

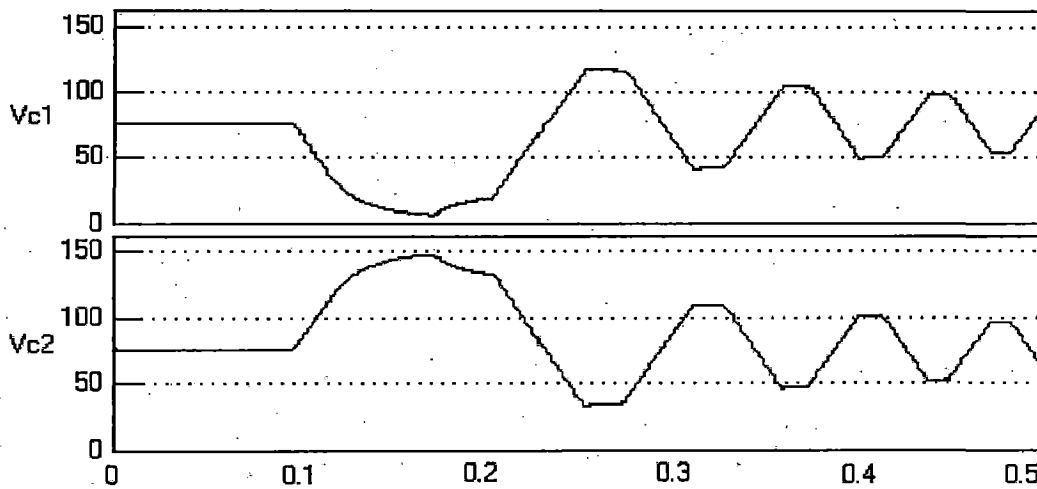


Figure.23(c).Showing voltages of two capacitors C1 and C2 with initial rotor position HHH=101

In Figure.24. h_a , h_b , h_c are hall signals H1, H2 and H3 respectively. As motor moves on forward, it will cover next 60° during which hall signals are 1 1 0 are H1, H2 and H3 respectively. During this period phase B and phase C have to conduct, but due to capacitor blocking, current becomes almost zero value but motor keep on moving forward. When the rotor reaches rotor position HHH=010, then phase A and phase B have to conduct current during that period of 60° . Phase A current is negative and phase B current is positive, this is easy to establish by operating switch 3 and switch 2. Maximum positive torque causes the motor to move forward just like other motor. Later back emf induced in the windings causes the motor to reduce charging of capacitor. As the speed increases the capacitor gets less time to charge, because 60° duration is covered fast. This flat speed time depends largely on the value of capacitor. As the value capacitor increases the flat speed time decreases and performance improves but cost of the inverter increases which is undesirable. The capacitor cost should not be more than the power switch module along with all auxiliaries.

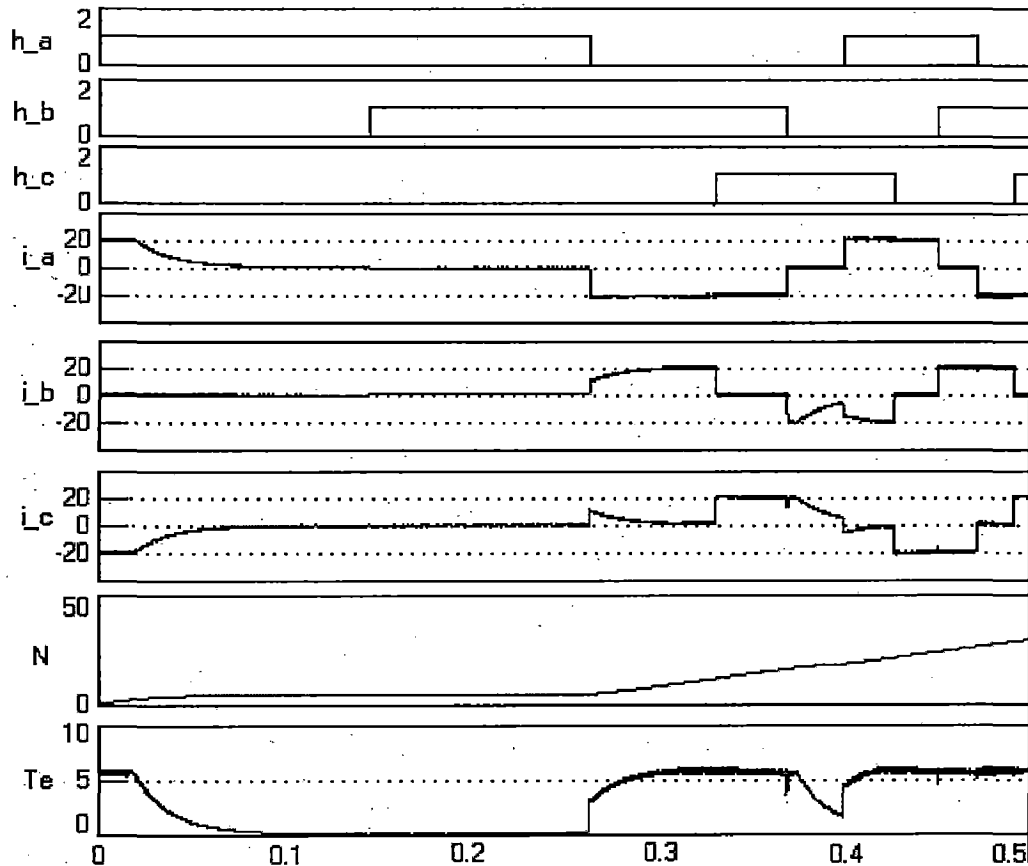


Figure.24. Depicting flat speed phenomenon at starting of machine

Here it can be identified that at zero speed of the motor the rotor position was HHH=100 and only one phase has to conduct of two phases A and B. Phase A conducts and the other phase must be phase C. This is responsible for constant speed. Same thing happens at starting if the rotor position is at either of the following: HHH=110,011,001 other than 100. But here there is difference in these positions. If the starting rotor position is 011, starting speed response of the motor is similar to the speed response 100 case. This is because after these (100 and 011) rotor position duration, coming rotor positions are 110 and 001 respectively. This causes motor current to flow in phase C which is not possible due to capacitor. So, if the starting rotor position is either 100 or 011, starting speed response is same. Regarding rotor positions 110 and 001, rotor positions next to these positions are 010 and 101 respectively, these (010 and 101) are starting torque supporting positions. So, if the rotor position is either 110 or 001, then starting speed response is better than the case for 011 or 100. This is because the rotor positions next to the rotor positions 110 and 001 are torque supporting rotor positions 010 and 101 respectively. Here better

speed response means that it has less rise time i.e. speed response is faster. But the common thing for all these (100,011,110,001) four rotor positions is that there will be considerable nearly constant speed region. In this work, nothing has been observed with rotor positions either 110 or 001 as starting rotor position. This is because the BLDC motor used in this simulated work is from MATLAB-simulink simpowersys library, which has a fixed starting rotor position 100. But, it can say that with rotor position either 001 or 110 as starting rotor position, motor gives faster response than starting rotor position either 100 or 011. This is because motor with starting rotor position either 101 or 010 gives starting speed response almost same as starting speed response with six switch inverter. This is clearly checked by running the motor in opposite direction, so that the starting rotor position becomes 101. Figure.25. shows the starting speed response of the motor with starting rotor position 101. This speed response is in negative direction. SSTP inverter fed drive rise time in negative direction is same as in forward direction and is equal to 1.8175 seconds while FSTP inverter fed drive takes 1.9275 seconds to rise with a difference 110 milliseconds which is less than 308.3 milliseconds for rotor position with either 100 or 011. From this it is found that motor with starting rotor position either 110 or 001 has less rise time than the motor with starting rotor position 100 or 011.

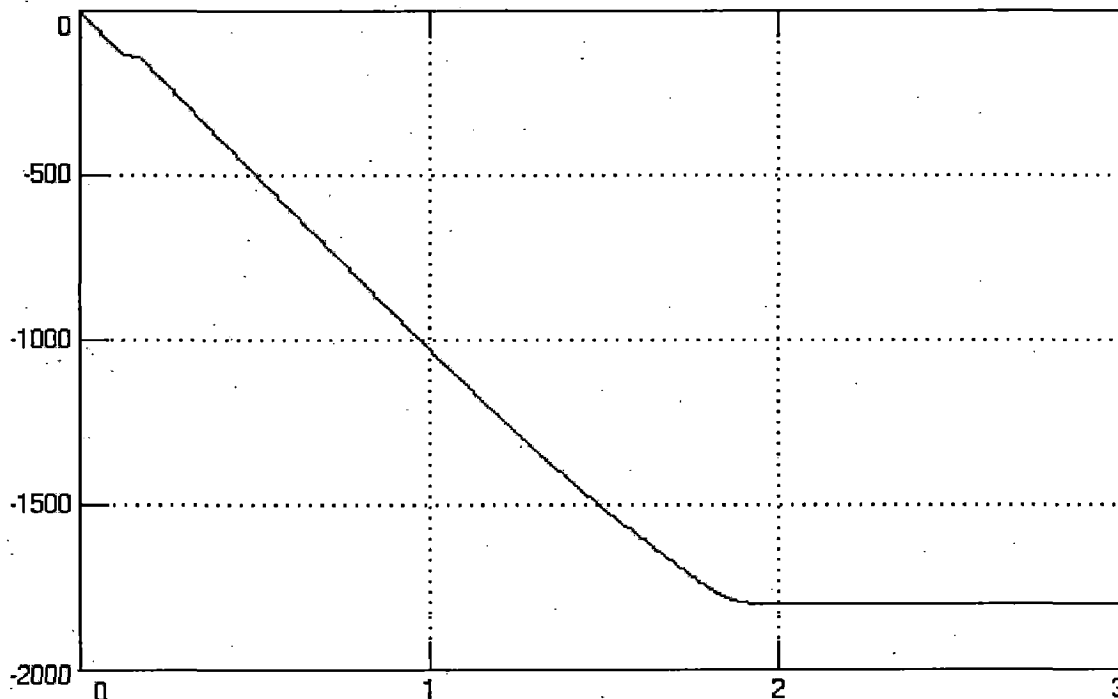


Figure.25 Starting speed response of BLDC motor fed with a four switch inverter for a reference speed of -1800 rpm with initial rotor position HHH=101

Figure.26 shows the current wave forms during starting. During first 60° i.e. during HHH=101 phase A and phase B are conducting current at maximum allowable value and torque will be maximum allowable. So, motor starts like six switch counterpart, but in the next duration (HHH=001) phase B and phase C have to conduct. The capacitor charges at maximum current, and falls down sharply due to its almost full charging to DC supply. But, due to long time starting torque (at HHH=101) motor runs faster than that in Figure.24 at the starting of constant speed region. Next duration HHH=011 and HHH=010 comes and then continuous torque will be generated.

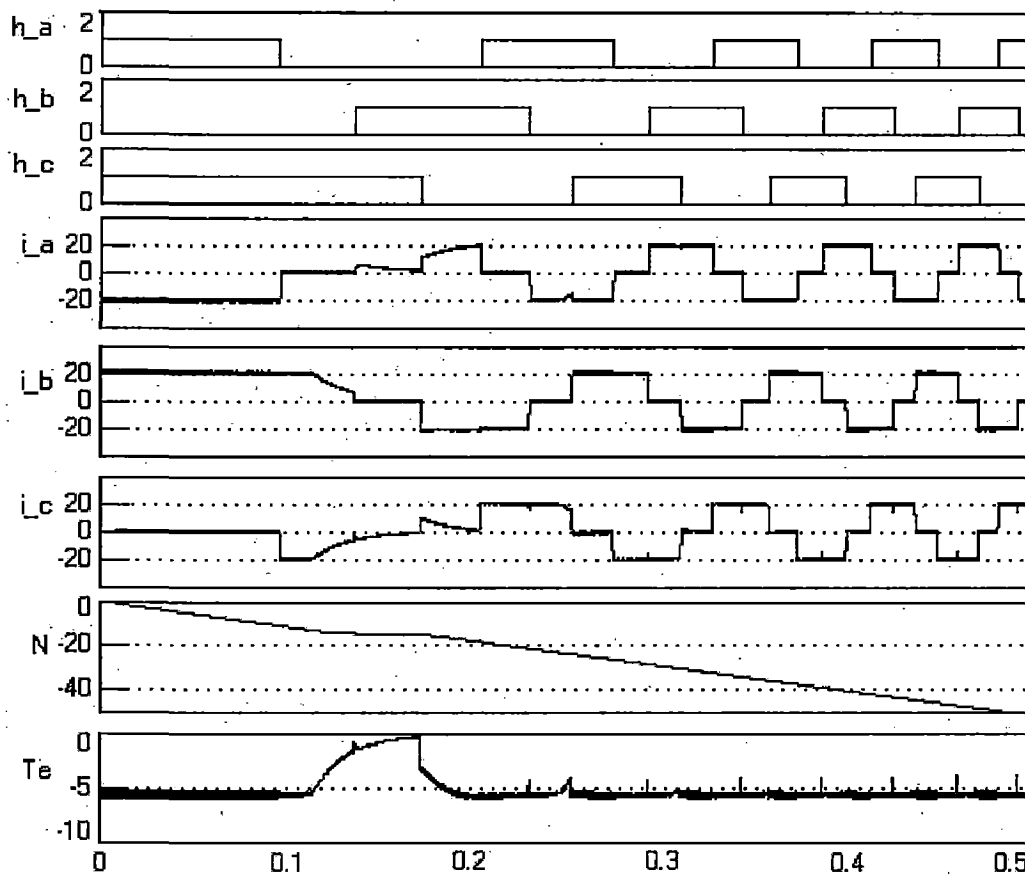


Figure.26. Hall signals, phase currents, speed and torque of BLDC motor during starting with initial position HHH=101

From this it can be observed that FSTP inverter fed BLDC drive takes maximum of 308.3 milliseconds and minimum of 110 milliseconds based on rotor position compared to six switch counterpart. In the above FSTP inverter used capacitor value $5000 \mu\text{F}$, 160 volt. There are two other ways to reduce this starting time: one is to increase the capacitor value. Second one is to increase the maximum allowable current. First option is not suitable,

because it increases the inverter cost. Second method is preferable but has some limitations. An exhaustive performance evolution is done for the starting response of the used motor for different values of capacitors and maximum allowable current. These details are arranged in the form of tables in the results section.

4.2.2 Analysis of load perturbation

Load perturbation is loading the motor if it was running on load, or removing the load if it is was on load or reduced load. Here both, applying load and removing load cases are analyzed. Motor will be running at rated speed before applying load on the motor.

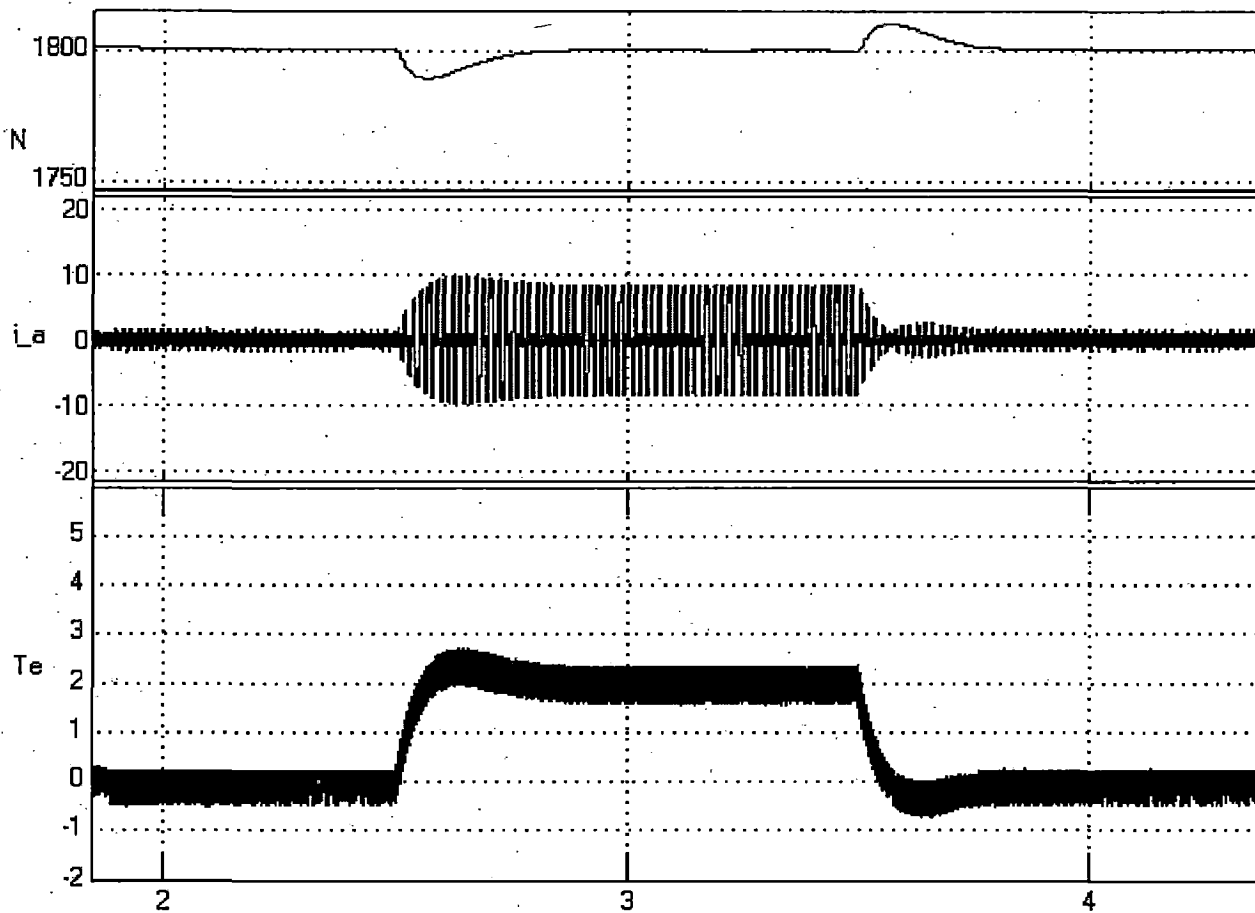


Figure.27. Shows speed, phase A current, torque response for load perturbation, loading 2 N-m at time 2.5 seconds and load removal at time 3.5 seconds for SSTP inverter case.

Figure.27 shows the load perturbation response of SSTP inverter fed BLDC motor drive. Motor is running on rated speed at 1800 rpm before applying load. While motor running on no-load it takes low value of no-load current to frictional and other losses. When load is applied, motor speed drops down due less no load torque and due to reduced speed,

controller increases the reference current to its rated value to drive the motor at rated speed. The speed regains back to its reference value. Dip in speed can be observed due to load application. Similarly when full load is removed due to its inertial energy in the rotor causes the motor to go beyond its rated speed. The controller limits the current to no load value. A rise in speed can be observed from the Figure.27 when load is removed. Increase in phase A current and torque when load is applied and decrease in phase A current and torque when load is removed is also can be observed from Figure.27. When load is applied, the dip in speed is by 10.69 rpm and the speed recovery time is 379 milliseconds. When load is removed, the rise in speed is by 10.23 rpm and the speed recovery time is 354 milliseconds. Figure.28 shows speed, current and torque response for load perturbation for FSTP inverter fed BLDC motor drive.

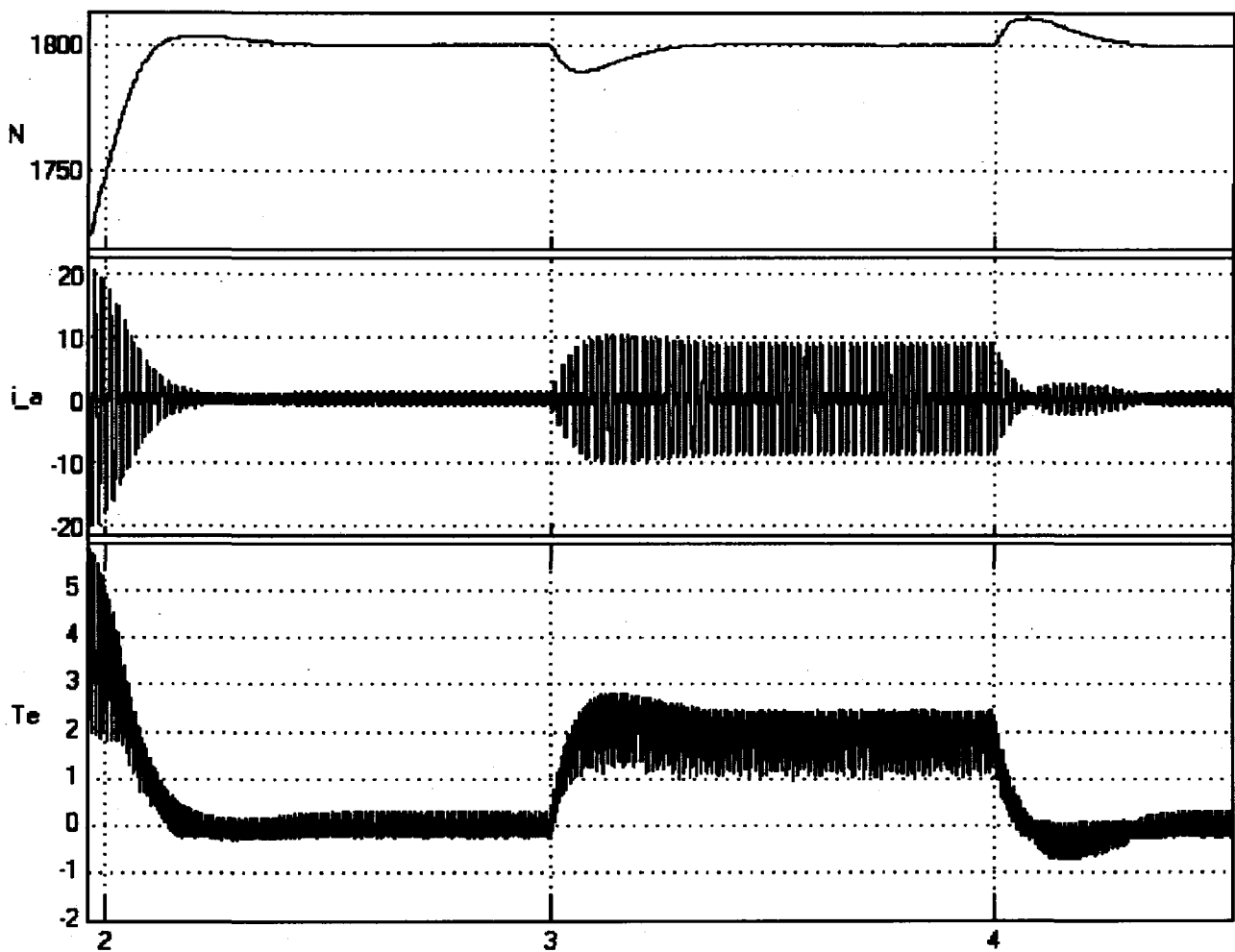


Figure.28. Shows speed, phase A current, torque response for load perturbation, loading 2 N-m at time 3rd second and load removal at time 4th second for FSTP inverter case

In FSTP inverter fed motor, load is applied at $t=3$ sec and load is removed at $t=4$ sec. When load is applied, the dip in speed is by 10.8 rpm and the speed recovery time is 360 milliseconds. When load is removed the rise in speed is by 10.5 rpm and the speed recovery time is 338 milliseconds. From the comparison between Figure.27 and 28, it is observed that ripple torque is more in FSTP inverter fed case. Its causes and analysis are given in detail in later section.

4.2.3 Analysis of speed reversal

It is very common in industrial drives or consumer applications or some other application to reverse its speed. This speed reversal should be fast, smooth and the rate of change in speed is also important in some applications.

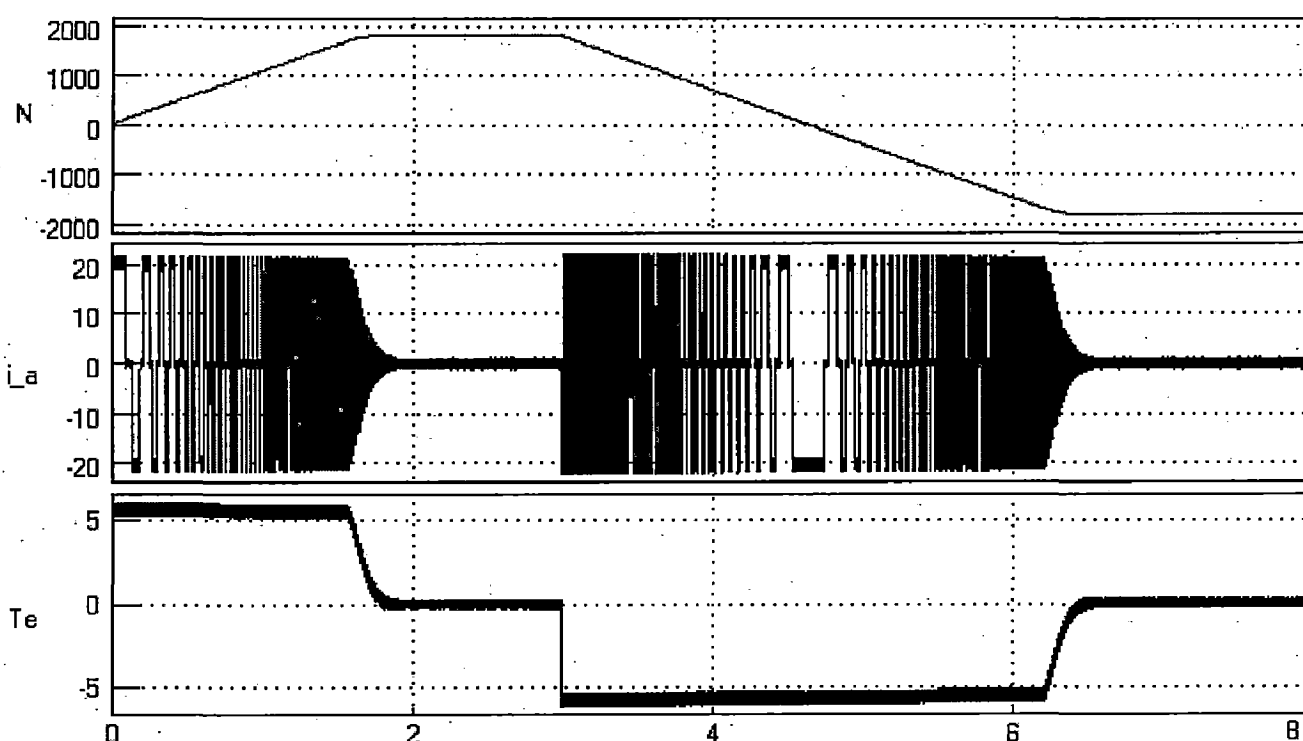


Figure.29. Shows speed, phase A current, torque response while speed reversal from 1800 rpm to -1800 rpm for SSTP inverter case

Figure.29 shows speed reversal response along with current and torque. Speed reversal started at $t=3$ sec, causes the speed controller to output negative reference current at its maximum allowable value to achieve fast speed reversal. The speed reversal is done at maximum allowable current 21 ampere. While changing speed from 1800 rpm to some speed zero speed braking is done. From zero speed to -1800 rpm negative motoring is

done. SSTP inverter fed BLDC motor drive takes 3.4565 seconds to reverse its speed from 1800 rpm to -1800 rpm on no load. Figure.30 shows speed, current and torque response during speed reversal for FSTP inverter fed BLDC motor drive. This drive takes 3.6576 seconds to reverse its speed from 1800 rpm to -1800 rpm.

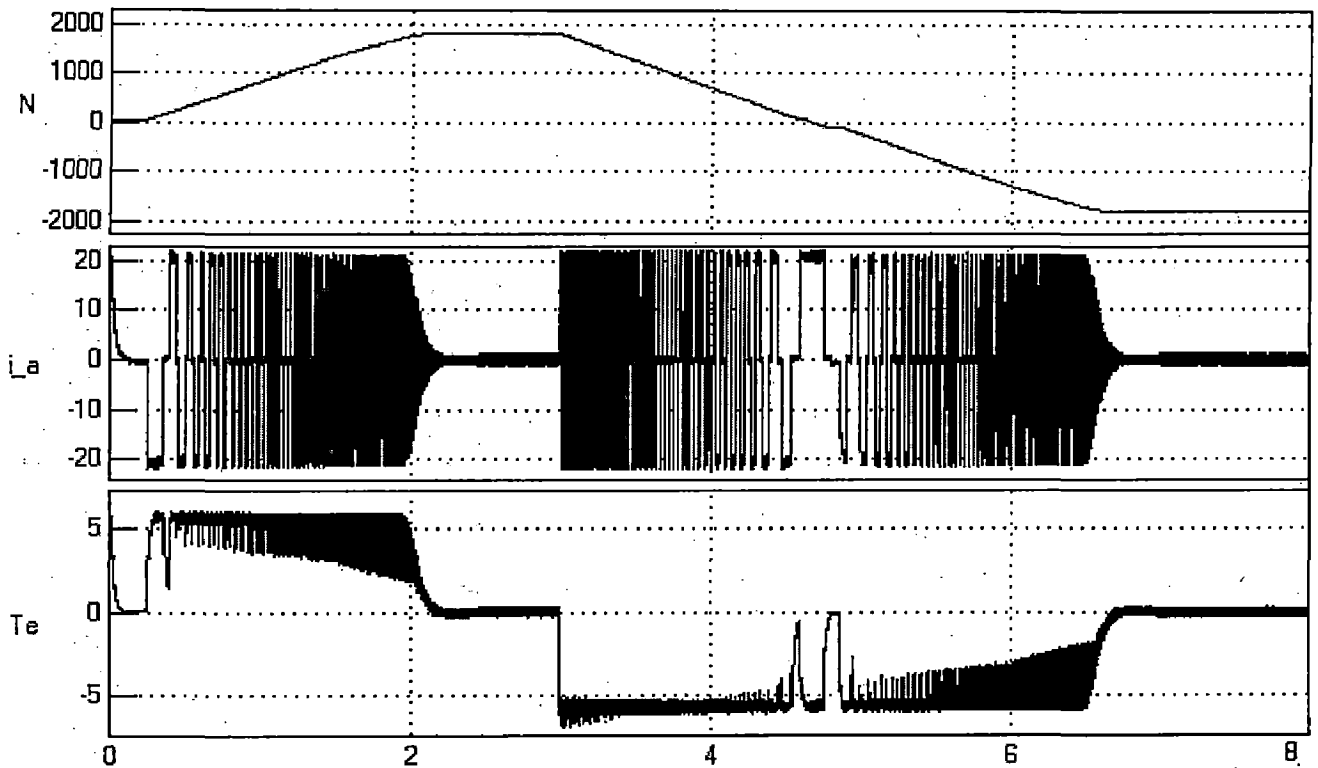


Figure.30. Shows speed, phase A current, torque response while speed reversal from 1800 rpm to -1800 rpm for FSTP inverter case

It takes 201.1 milliseconds more time than SSTP inverter. This is because of the constant speed phenomenon on either side of zero speed. This small flat speed region on either side to zero and at very low speed can be observed from speed response. During this flat speed region current goes to nearly no-load current of the motor due to capacitor blocking. This is also can be observed from the current response of phase A.

4.2.4 Analysis of regeneration

In many applications it is necessary regenerate the power back to source. If the motor is running in a condition where torque on the motor changes (i.e. active loads) as in case of vehicle or in hoist load, then it is possible to achieve regeneration by harnessing energy of active load. The amount of energy we can harness from active loads or other depends on the energy it posses. If the developed drive can be used for forward regeneration and

reverse regeneration then, drive can work in four quadrants and four quadrant operation is possible. The Figure.31 shows the possibility for regeneration in BLDC motor drive with active loads.

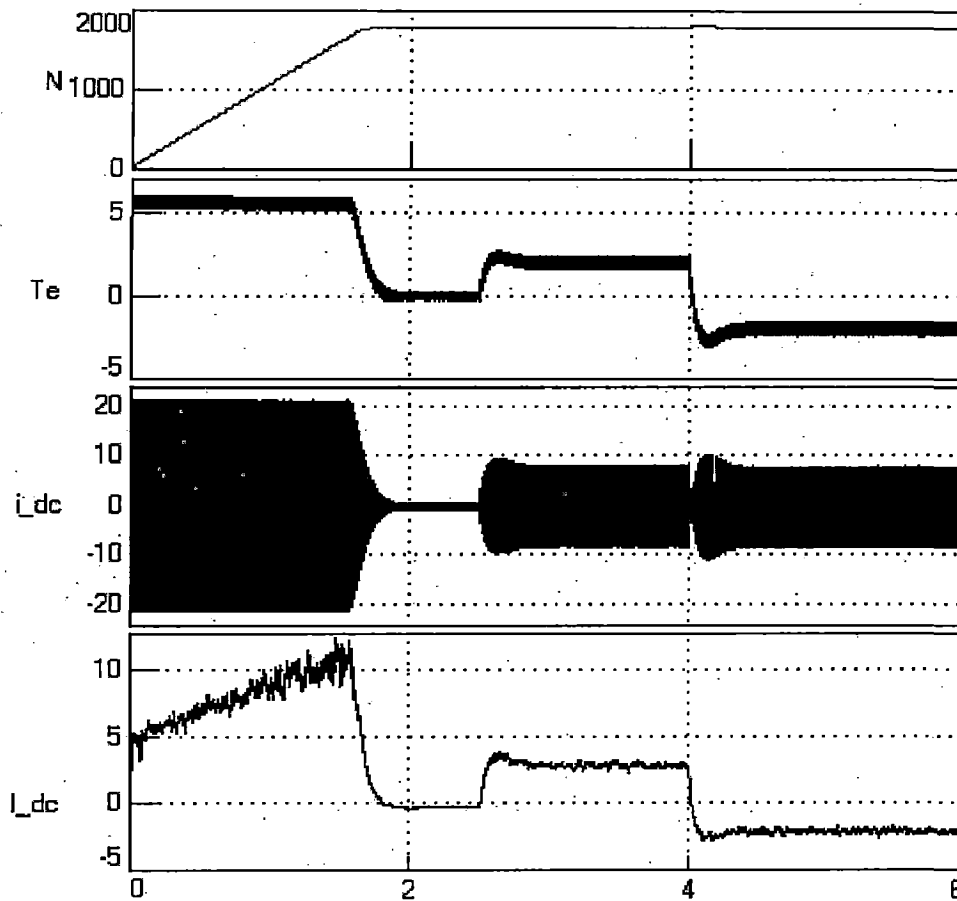


Figure.31. Shows the speed, torque, i_{dc} and I_{dc} of the BLDC motor for SSTP case

Figure.31 shows the speed, torque and dc supply current i_{dc} and average dc supply current I_{dc} for BLDC motor fed by SSTP inverter. Motor is run on forward motoring with full load at 1800 rpm from 2.5 seconds and load on the motor is reversed and becomes active load supplying torque at 2 N-m to the motor at $t=4$ sec. The power output from the motor at 1800 rpm and 2 N-m is 376.99 watt and power average power generated at 154 volt and 2.2 ampere is 338.8 watt. The same regeneration is also can observed from Figure.32 for FSTP inverter fed BLDC motor drive.

Figure.32 shows the waveforms for FSTP inverter fed BLDC motor drive. Motor is run on forward motoring with full load at 1800 rpm from $t=3$ sec and load on the motor is reversed and becomes active load supplying torque at 2 N-m to the motor $t=4$ sec. The power output from the motor at 1800 rpm and 2 N-m is 376.99 watt and power average

power generated at 154 volt and 2 ampere is 308 watt. There is difference in power generation in case of FSTP inverter fed drive to SSTP inverter fed drive. This difference is due to capacitor charging.

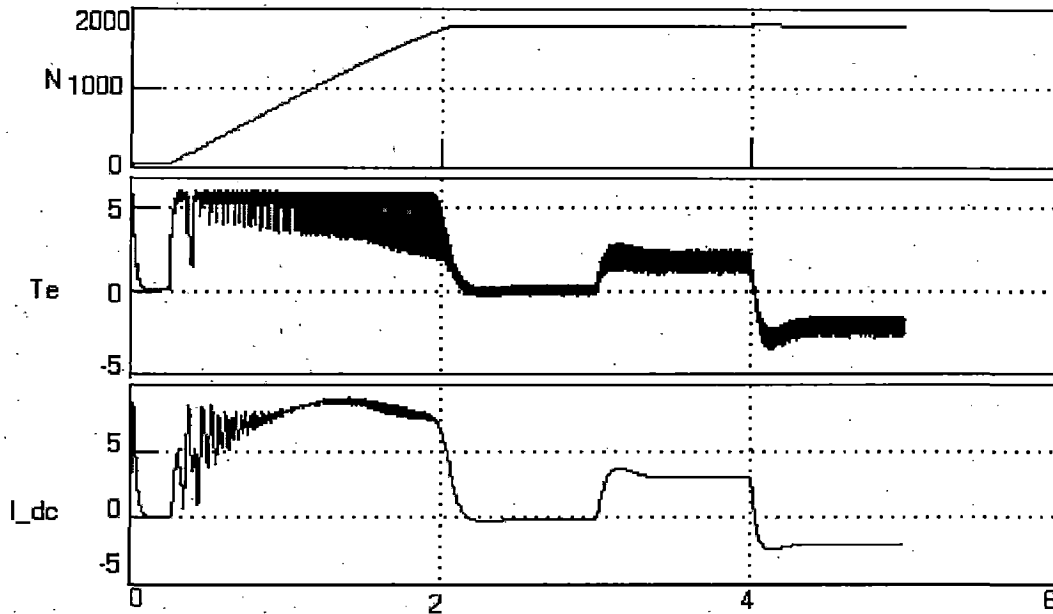


Figure.32. Shows the speed, torque and I_{dc} of the BLDC motor for FSTP case

4.2.5 Analysis of commutation torque ripple

In this section first SSTP inverter fed drive is analyzed briefly for commutation torque ripple and then, FSTP inverter fed drive is analyzed. As it can be observed from previous sections and their outputs that there are many torque ripples in torque response. Brushless DC motors have a trapezoidal back emf waveform and are fed with rectangular stator currents. On these conditions the torque produced is theoretically, constant. However, in practice, torque ripple exists, due to the machine itself but also to the inverter system. The causes of ripple due to the cogging torque and emf waveform imperfections and those coming due to the supply are current ripple (resulting of the pwm or hysteresis control) and phase current commutation [31]. Many ways have been proposed to attenuate cogging torque, mainly by slots skewing or by changing the magnets dimensions and positioning [32, 33]. Emf or static torque imperfections are analyzed and some original solutions have been proposed to overcome them [34]. In SSTP inverter fed drive, balanced voltages are applied for the machine. In any commutation duration one phase current vanishes and second phase current raises while third phase current is unaffected ideally as shown in Figure.33.

But, in actual system inductance in the system does not allow the current to rise or fall instantly and causes it to take some time to fall or rise. Any difference in the inductance of phases causes the current to rise or fall at different rates. This lead to either a dip or swell in the non-commutating phase current and causes ripple in torque. There are other factors affecting this variation current in commutation region other than inductance.

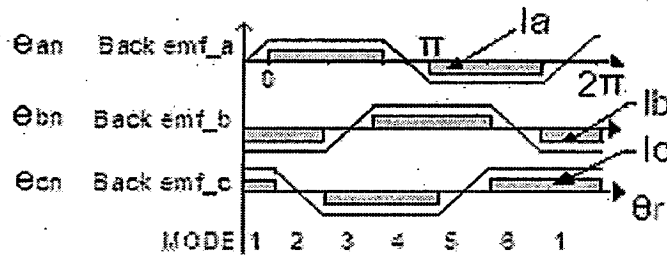


Figure.33. Showing currents and back emf's of three phases of BLDC machine

In this work, all phases are assumed to have same inductance. The following conditions are considered: neglecting winding resistance and keeping emf is constant during commutation period. Here only one period of total six periods of Figure.33 is observed and due to balance in supply voltage in SSTP drive, same analysis can be applied to other periods. Taking a case when i_a vanishing and i_b is rising while phase C is non-commutated by switching off the upper switch S1 of phase A and switching on the upper switch S3 of phase B as shown in Figure.34. This results in turn on off S3, S2 and D4. There are three possible based on the changing rate of current of commutating phases.

Case A: current i_a , vanishes at the same time the current i_b , reaches its final value and the commutation is finished; no torque ripple will be there.

Case B: current i_a , vanishes before current i_b , reaches its final value, but in this case the commutation will be achieved only when current i_b , will reach the final value. This causes a dip in the non commutated phase.

Case C: current i_b , reaches the final value before current i_a vanishes, but in this case the commutation will be achieved only when current i_a vanishes to zero. To achieve fast vanishing of current i_a , switches S2, S3 are turned off, this causes the diodes D4, D6 and D5 to conduct.

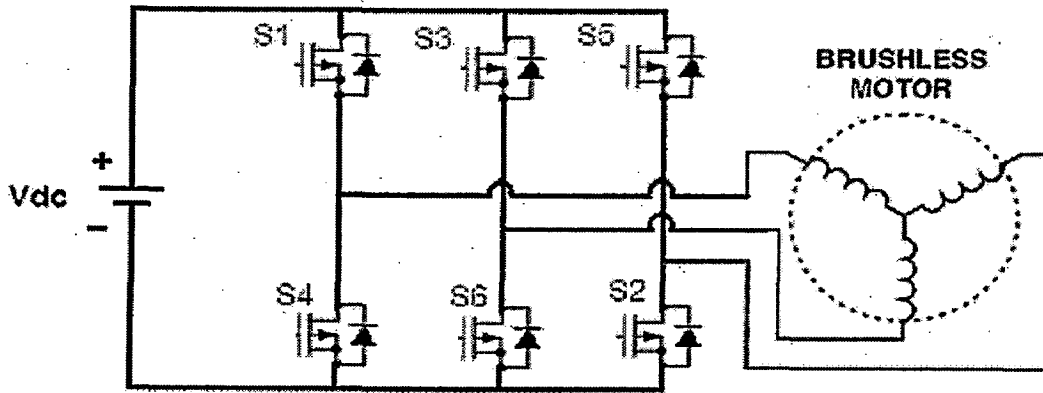


Figure.34. Showing six switch inverter with six switches and their anti parallel diodes

From the mathematical modeling of the machine and inverter, rate of change of current of three phases when S3, S2 and D4 are 'ON' (i.e. during commutation time), are given by

$$\frac{di_a}{dt} = -\frac{(V + 2E)}{3L} \quad (30)$$

$$\frac{di_b}{dt} = +\frac{2(V - E)}{3L} \quad (31)$$

$$\frac{di_c}{dt} = -\frac{(V - 4E)}{3L} \quad (32)$$

The equations during S2 and S3 turned off are given as follows:

$$\frac{di_a}{dt} = -\frac{(V + 2E)}{3L} \quad (33)$$

$$\frac{di_b}{dt} = -\frac{(V + 2E)}{3L} \quad (34)$$

$$\frac{di_c}{dt} = +\frac{2(V + 2E)}{3L} \quad (35)$$

From equation (32), it can say that case A is achieved when \$V=4E\$ and case B happens when \$V<4E\$ and case C happens when \$V>4E\$. Where \$E\$ = back emf in flat portion of the wave. Since the applied voltage is balanced in all modes and this is applied to all the six

modes of operation with variation in current notation [31]. Figure.35 shows the current response at rated load, 500 rpm in forward motoring mode for SSTP inverter fed drive.

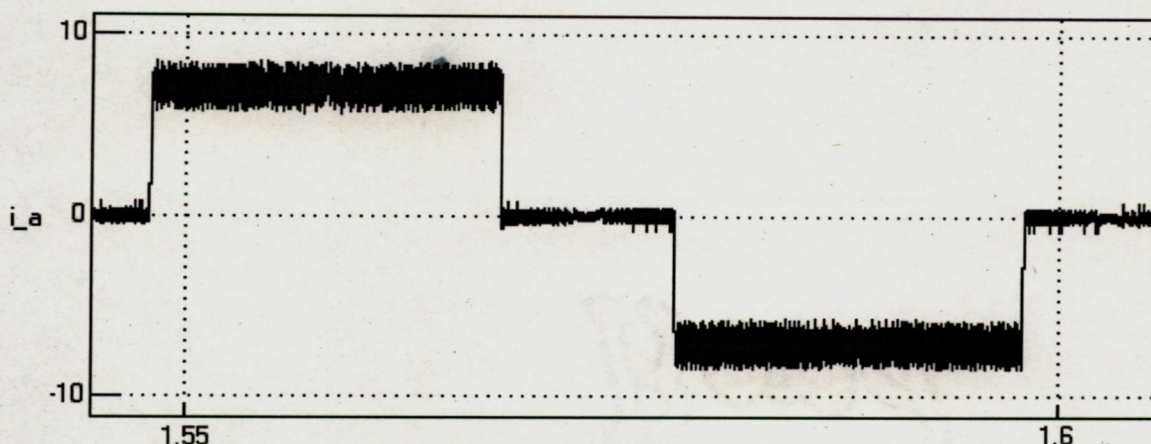


Figure.35. Phase A current response at rated load 2 N-m, 500 rpm for SSTP fed drive.

For this speed, case C is applicable because at low speeds condition for case C is satisfied. As per the above equation no swelling can be observed because swelling is controlled by switching off the switches S2 and S3. This is phase A current response and due to balanced voltage supply the other phases have same current response. Figure.36 shows the current response at rated load, 1800 rpm in forward motoring mode for SSTP inverter fed drive.

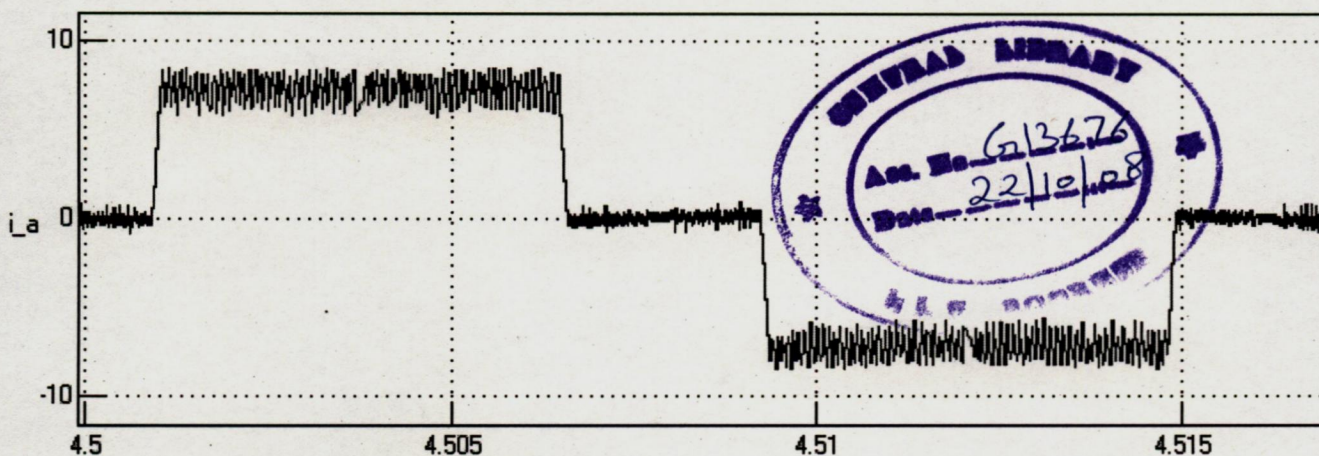


Figure.36. Phase A current response at load 2 N-m, 1800 rpm for SSTP fed drive

For this speed case B should happen because at high speeds condition for case B may be satisfied. As per the above equations case B should happen and a small dip in the current can be seen in the current in Figure.35. The magnitude of dip depends on the relative values of V and E . For the regenerative mode, at higher speeds there is a

possibility for a swell and amplitude of swell depends on the relative values of V and E . All this torque ripple analysis up to this is for SSTP inverter fed BLDC motor drive. In this case very less or no torque ripple is observed for this motor.

FSTPI-BLDC INVERTER:

Torque ripple generated in the commutation interval is one of the main drawbacks of BLDC motor fed by FSTP inverter. Phase commutations in six operation modes for a six-switch inverter BLDC motor drive are alike. But in four-switch inverter BLDC motor drive they are different. Depending on the operating condition (i.e. speed) above mentioned three cases occur. There are total six modes in a cycle shown in Figure.33. Mode 2 and mode 5 are similar in condition and commutation torque ripple generated in these two modes are similar. In these two modes case A, case B and case C are possible depending on the operating condition, just similar to six switch inverter. Case B is corresponding to high speed region of FSTPI-BLDC motor. In high speed range non-commutated current i_b has dip and so, torque decreases. Case C is corresponding to low speeds range of FSTPI-BLDC motor. In low speed range non-commutated current i_b has swell and so torque increases. But this can easily be avoided by switching off the switch S4. Other four modes are different from the SSTP inverter case, because of unbalanced voltage. According to Fig. 33, in mode 4, i_d , i_r and i_{nc} are corresponding to i_a , i_b and i_c , respectively. Commutation is from phase a to phase b. This current transfer is done by switching off S1 and switching on S2. It can be shown that in this mode, only case B will occur and that is the different with commutation in mode II or in six-switch inverter BLDC motor drive. To analyze of circuit in case B, by using KVL equations and with some simplifications, i_a and i_b derivatives are as:

$$\frac{di_a}{dt} = -\frac{(3V + 4E)}{6L} \quad (36)$$

$$\frac{di_a}{dt} = -\frac{(-3V + 4E)}{6L} \quad (37)$$

From this, it can be said, only case B is possible for mode 4 and mode 1. In this operation mode, i_d , i_r and i_{nc} are corresponding to i_b , i_c and i_a respectively. Commutation is from phase b to phase c and current transfer is done by switching off S2 and S3 is held on. In the similar manner mode 2, for three cases we have: case 'a' is possible for $V=8E$, case 'b' is possible

for $V < 8E$ and case 'c' is possible for $V > 8E$ [ref.18]. Simulation work is done to evaluate the torque ripple. All six modes are observed for 500 rpm and 1800 rpm speeds:

For the mode 2 at 500 rpm case 'c' is applicable and swell in the phase 'b' current is observed. But, hysteresis controller switches off the switch 'S4', causes the swell to disappear from phase 'b' current. In simulation work no swell in phase 'b' current has been observed as shown in Figure.37 located at mode 2 and a switching off of switch S4 has been also observed to avoid swell. This indicates the expected action of hysteresis controller. In mode 5, switch 2 operates to avoid swell in the phase b current.

For mode 6 at 500 rpm case 'c' is applicable and swell in the phase 'a' is observed. But at 500 rpm this is not observed. This is shown in Figure.37 located at mode 6 at very starting of current responses. For mode 3, current response is similar to mode 6.

For modes 4 and 1 case 'b' is possible for all speeds and for mode 4 current responses is shown in Figure.37 at speed 500 rpm.

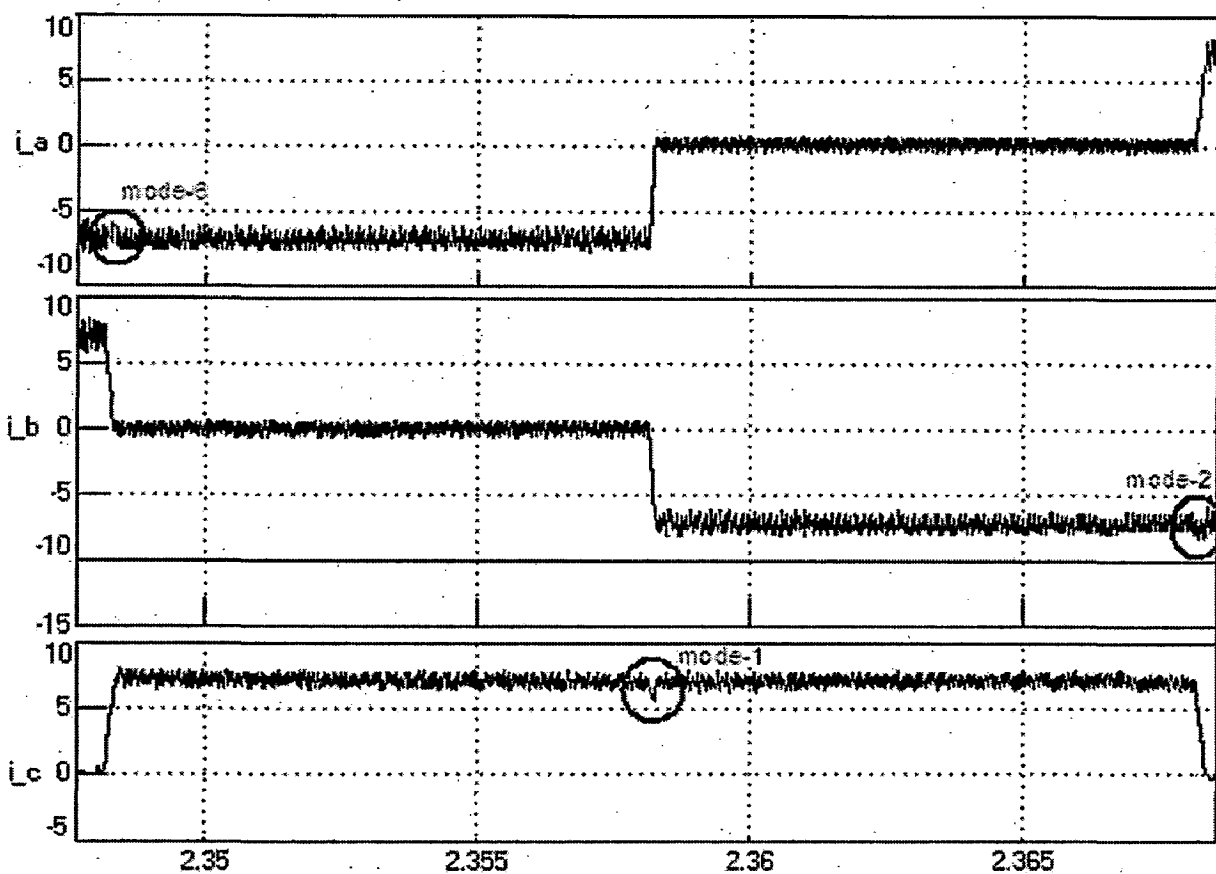


Figure.37. Current responses during mode 4 commutation showing a dip at 500 rpm for FSTPI-BLDC motor drive

A small dip during commutation (in the middle of figure at mode 1 indicator circle) time in Figure.37 indicates, starting of torque ripple production. As speed increases this torque becomes more for the same load. During mode 1 commutation time, i_a falls from positive value and i_b rises from zero to positive value and i_c will have a dip. As the speed increases the value of back emf changes, which changes the value of slope at which these current changes and causes more ripple in current thereby ripple in torque. Current responses for all six modes at 1800 rpm for forward motoring is shown in Figure.38. It shows the current ripple caused by commutation of currents. Regions of all six modes are indicated on the Figure.38. As it is analyzed, during mode 2 commutation a swell in phase 'b' current should be avoided due to hysteresis current controller action to avoid any increase in current beyond its range by switching off switch S4. This can be observed in phase 'b' current for more ripples at positive raising edge of phase 'a' current for mode 2 and for more ripples at negative raising edge of phase 'a' current for mode 5. From the previous analysis in mode 3 and mode 6, at higher speeds a dip in phase 'a' current is happens.

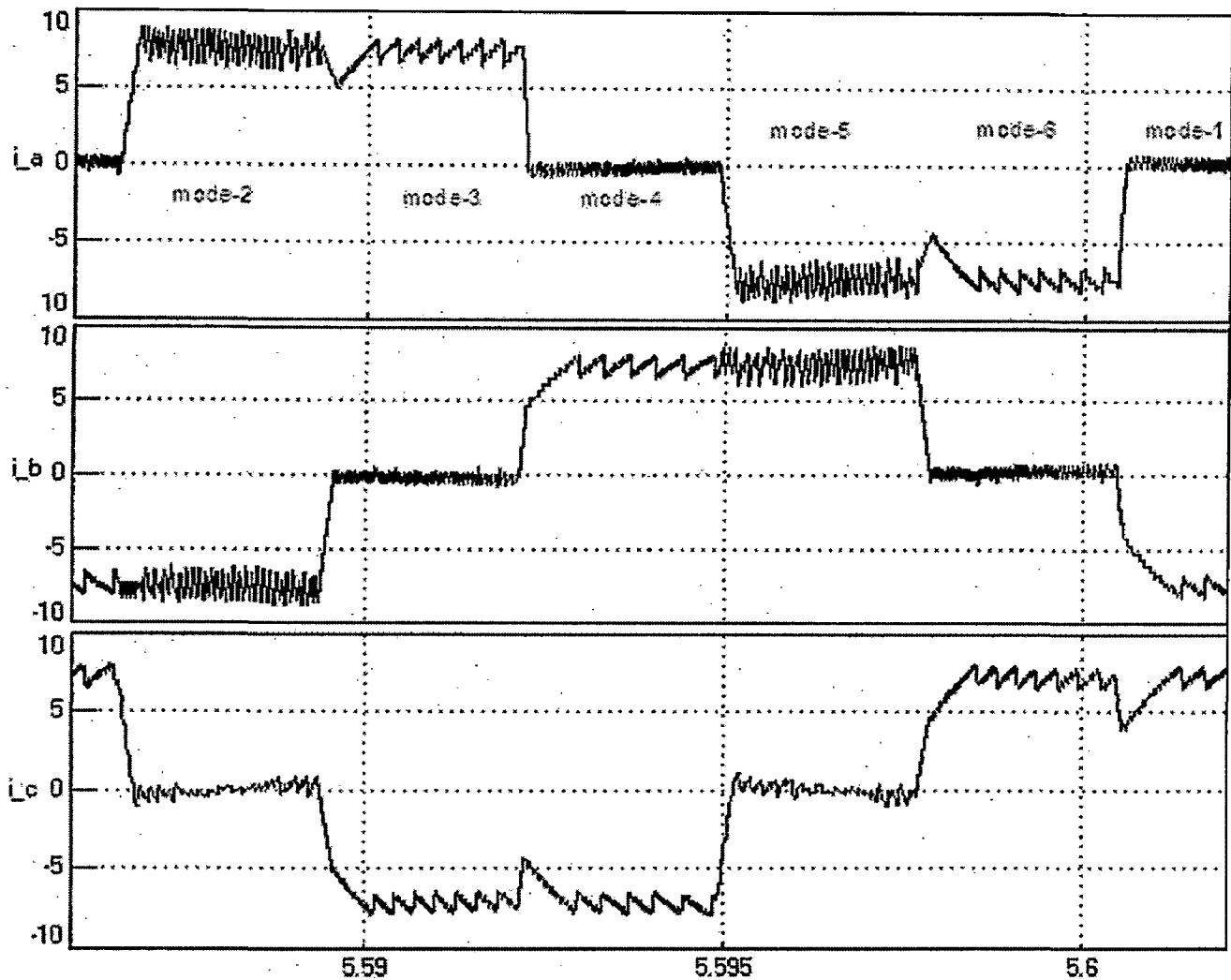


Figure.38. Current responses at 1800 rpm for FSTPI-BLDC motor drive during all six modes and it shows the current ripple due to commutation in all modes for forward motoring.

This is clearly observed from Figure.38. During mode 3 commutation, a sharp fall in current from negative maximum in phase 'b' current due to more back emf $-e_b$ and slow increase in phase 'c' current due to reduced voltage across two phases 'a' and 'c' causes dip in the un commutated phase 'a'. Similar phenomenon happens for mode 6. During mode 4 commutation, a sharp fall in current from positive maximum in phase 'a' current due to more back emf $-e_a$ and slow increase in phase 'b' current due to reduced voltage across two phases 'b' and 'c' causes dip in the un commutated phase 'c'. Similar phenomenon happens for mode 1. There is a basic difference in mode 3 and mode 4, the voltage applied across two phases in mode before mode 3 is DC supply voltage V and voltage applied across two phases in mode before mode 4 (i.e.mode3) is half the DC supply voltage V i.e. $V/2$ volt. This

causes the mode 4 and 1 to be a case 'b' for commutation. In the Figure.38 phase 'b' current is maintained constant while phase other two phases have ripples. In mode 3 commutation dip in phase 'a' can be avoided by reducing the slope of i_b by switching switch S4 using dead beat controller and also similar technique for mode 6. In mode 4 commutation dip in phase 'c' can be avoided by reducing the slope of i_a by switching switch S1 using dead beat controller and also similar technique for mode 1. Mode 2 and mode 5 do not need any special technique to avoid swell and hysteresis controller takes care of it. This is true for forward motoring mode but, for reverse motoring mode, phase 'a' current doesn't have any ripples while other two phases have ripples in their current response. One thing can observe from Figure.38 is that, most of the modes falling time is faster than the rising time. This is due to at higher speeds the back emf in the motor comparatively high and this causes the raising current to go at slow rate. Actually back oppose the current to rise. This results in the dips in the currents of phases. But, in many times motor needs to run in the regeneration mode. Figure.39 shows the current responses for forward regeneration in all six modes. In forward regeneration mode back is the same direction but phase current reverses in its windings. Here not only supply voltage but also back emf supports the current to rise fast. This leads to fast rates of rise in current than fall in current in phases. This in turn leads to different slope rates and causes swells in the phase currents and this happens most of the modes except in mode 3 and mode 6. Since the ripple torque problem is more in the higher speeds region Figure.39 depicts currents responses at 1800 rpm. In forward regeneration, during mode 2 and mode 5 faster rising current than falling current causes a swell in phase 'b' and this can be controlled by hysteresis controller by switching off switch S2 during mode 2 and S4 during mode 5. It does not need any special control. During mode 4 and mode 1 faster rising current than falling current causes a swell in phase 'c' and this can be avoided by using a dead beat controller which operates the switches S4 and S2 in modes 4 and mode 1 respectively. In reverse regeneration mode of operation, phase 'a' and phase 'b' current responses gets interchanged to Figure.39 while phase 'c' current response is same as Figure.39 regarding current ripple. All this ripple current in the phases results in the ripple in torque directly and causes noise and in some cases high ripple torque causes vibrations in the motor which may lead to mechanical resonance which is undesirable. Ripple torque analysis till now is steady state operation of the machine both at low and high speeds. In transient operation this ripple torque will more and even it reaches to 50 to 70% of maximum torque during transient time.

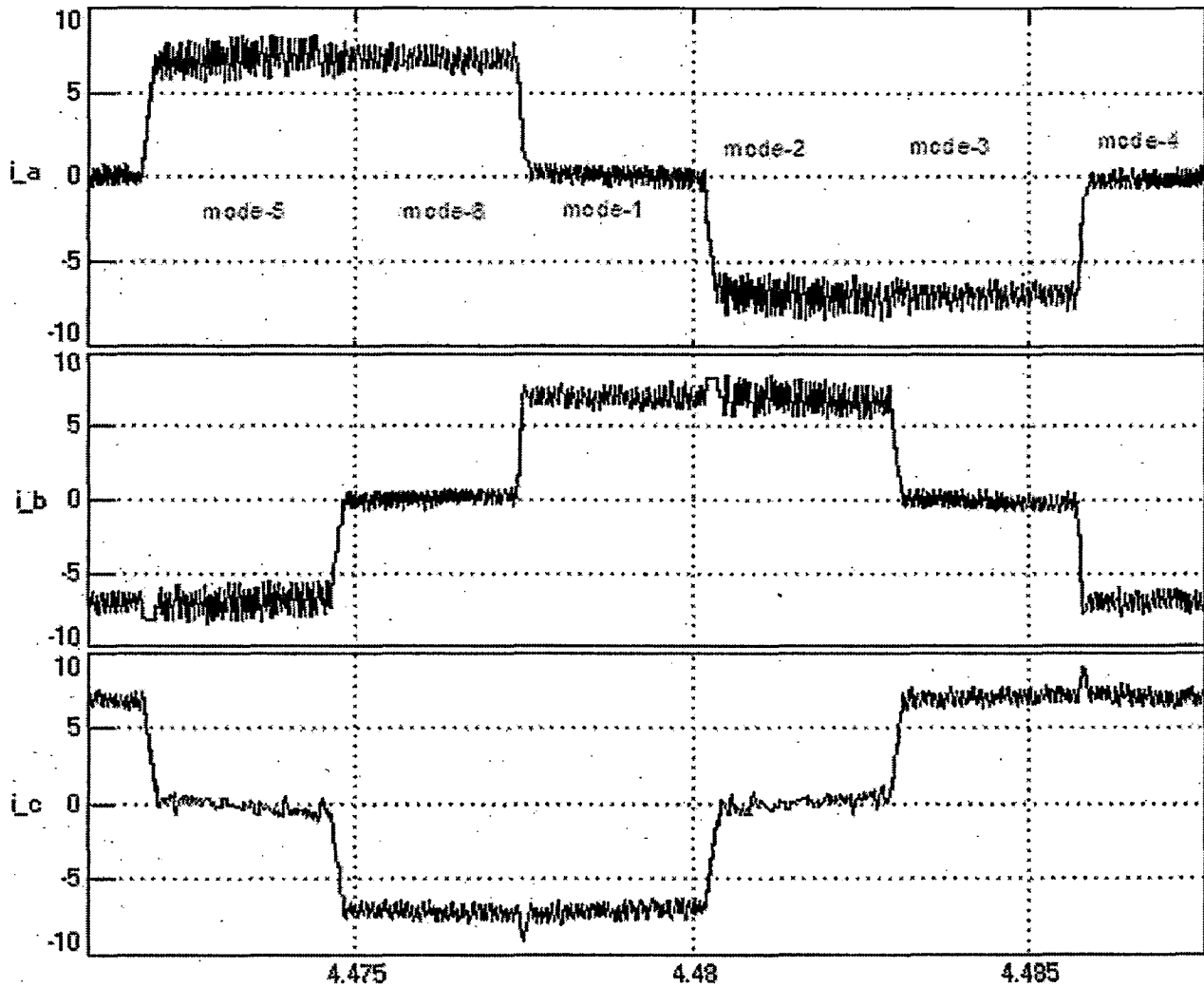


Figure.39. Current responses at 1800 rpm for FSTPI-BLDC motor drive during all six modes and it shows the current ripple due to commutation in all modes in forward regeneration mode

This ripple torque during transient time is mainly caused by high value of current s at a particular speed. The ripple torque during transient operation (change in speed or load) is caused due to high value of currents drawing from source and change in slopes of commutation currents. Fast charging and discharging of capacitors is the cause for ripple torque in transient condition due to high value of currents. Implementing the above mentioned solutions to avoid these ripple torque is carried out using new technique in this work.

4.2.6 Novel technique to reduce commutation torque ripple in FSTPI-BLDC motor.

It has been found that the dominance of ripple torque due to ripple current is more in the high speed region and many techniques are developed to avoid ripple torque [19, 31, 33, and 34] and some techniques used dead beat controller to avoid ripple torque. In this a new technique is developed to avoid torque ripple and is simulated in MATLAB-simulink to check its proper operation and compared it with normal control techniques for motoring forward mode. Same technique can be extended to four quadrant operation of the drive. Implementing the same technique for regeneration mode is much easier than motoring mode. This technique additionally needs one more current sensor in the phase 'c'. This technique improves its performance in a significant amount. Figure.38 shows the current response of normal FSTPI-BLDC motor drive at 1800 rpm in forward motoring mode and it shows the many commutation current ripples in at least two phases. From the solutions mentioned for the problem of current ripple for the Figure.38, one technique is proposed. The logic behind the novel technique is shown in Figure.40, showing the hysteresis current controller block similar to Figure.20 along with other control logic derived from the hall sensors and hysteresis current controllers. This technique needs one current sensor for phase 'c' and two hysteresis current controllers. Implementing the hysteresis current controllers in software is not a problem and effectively this technique needs one current sensor additionally. Even that other current sensor for phase can be avoided, because sum of the currents is equal to zero. We can get the value of phase 'c' current from equation (2). Since the problem of commutation torque ripple is more in high speed region of the motor, its performance is evaluated in the high speed region of the motor i.e. around 1800 rpm. Here, in Figure.40 control logic developed only for forward motoring and same technique can be extended to four quadrant operation of the machine.

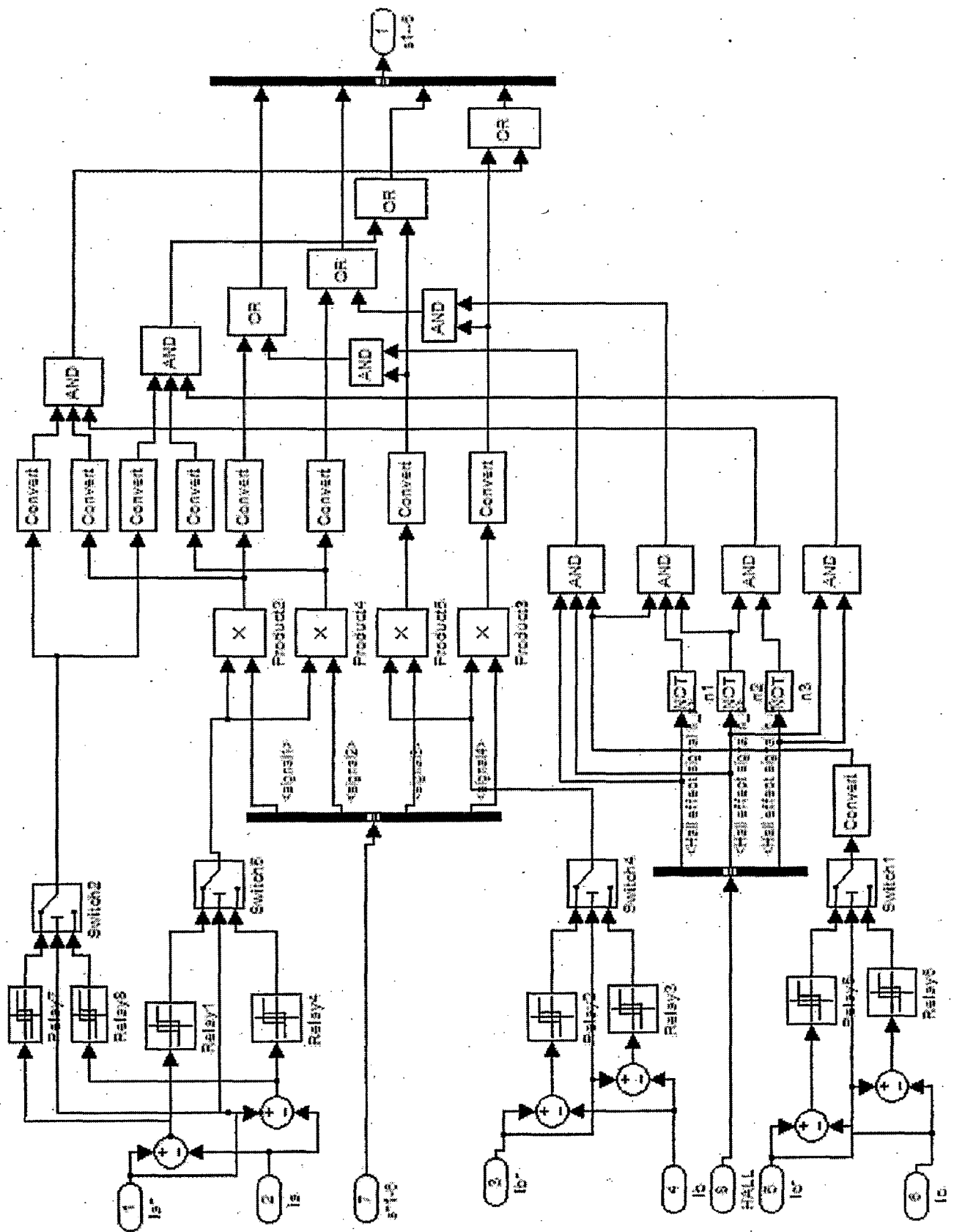


Figure.40. Control logic for proposed novel technique for FSTPI-BLDC motor forward motoring operation

Figure.38 shows the current responses having more current ripple and it results in the generation of ripple torque which is undesirable. Figure.41 shows the torque ripple produced for the same current responses. Basically it has two ripple torques, one is caused by the hysteresis current controller which is not a serious problem and other is ripple torque due to phase current commutation which is dominant and undesired.

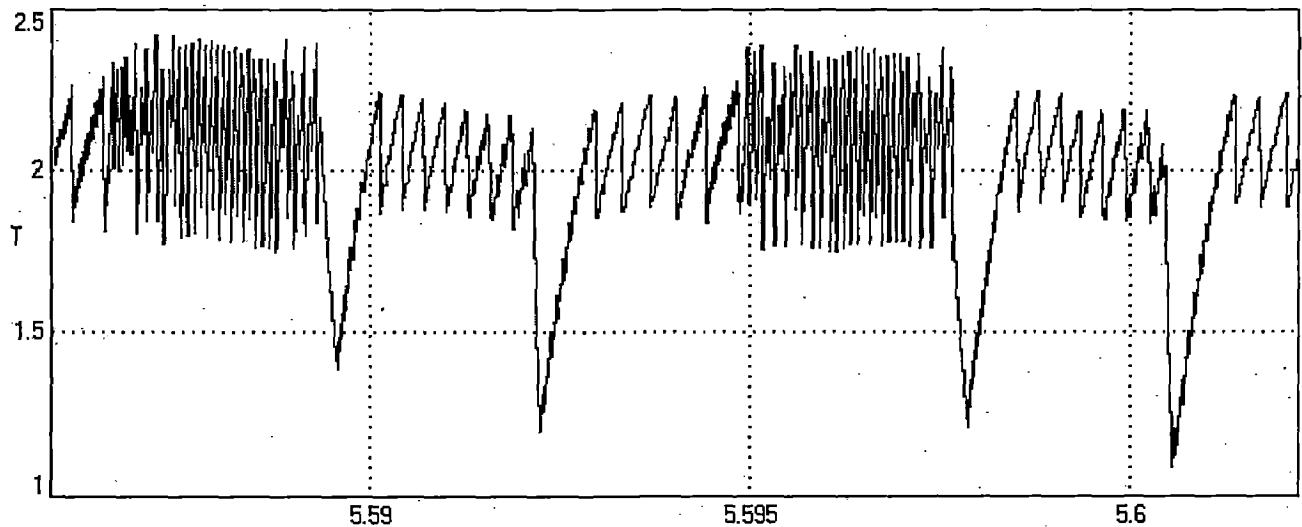


Figure.41. Torque response at 1800 rpm with 2 N-m load, showing commutation torque ripple and torque ripple due to hysteresis current controller

In Figure.41 high frequency ripples are due to hysteresis current controller and this torque ripple basically depends on the hysteresis band and fastness of the hysteresis controller. If the hysteresis current controller is fast and hysteresis band is low then low ripple torques caused by hysteresis action are possible, but there is limit of switching frequency and switching losses of power switch used. Hysteresis ripple torque can be controlled. In Figure.41, there are low frequency high torque ripples and there four torque ripple in this figure. These torque ripples are due to commutation of phase currents of unequal slopes. The novel technique presented answers to this problem. Generally hysteresis ripple torque is in the range of 5% to 15% of average torque depending on the fastness of hysteresis current controller and hysteresis band width. In steady state, the commutation torque ripple is from 26% to 50% of average torque at rated torque for FSTP-BLDCM drive. This needs to be avoided and these torques leads to noise in the system and sometimes causes mechanical resonance with the motor and bearing system leads heavy vibrations in the drive. All these problems are answered in the presented novel technique and Figure.42 shows the current response of the novel technique presented at 1800 rpm and load (2 N-m).

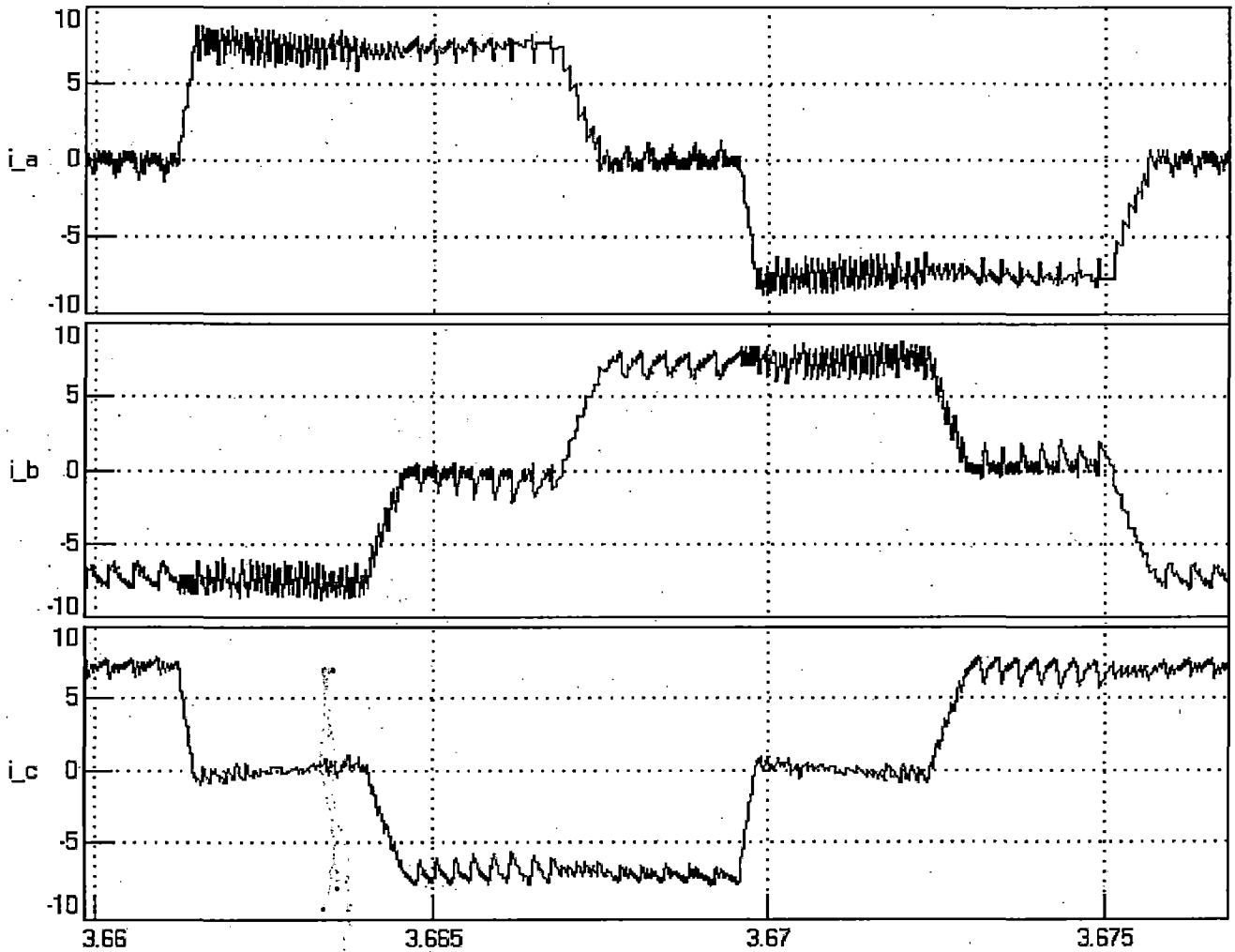


Figure.42. Current responses of FSTPI-BLDC motor using novel technique at 1800 rpm and 2 N-m for forward motoring

It shows the current waveforms much near to ideal wave forms of current. Here the falling is delayed using proper switching of power switches. Currents are actually conduct for 120° in the positive half cycle, so the rest of the 60° gives a possibility for delaying the proper switches and providing 60° of free time ensures the proper operation switches in the same leg by avoiding any short circuit. Figure.43 shows the torque response for the currents shown in Figure.42. It shows the proper generation of torque by avoiding commutation torque ripple by equalizing the slopes of currents undergoing commutation. The torque ripple in the novel technique is limited to only hysteresis torque ripple which is not a problem.

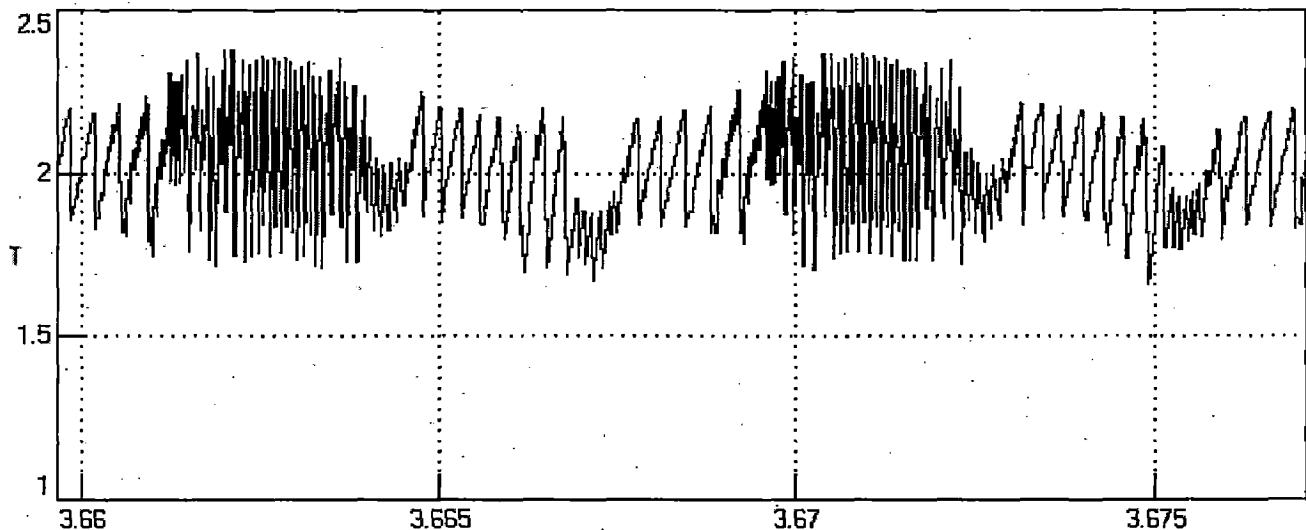


Figure.43. Torque response at 1800 rpm with 2 N-m load, have only hysteresis torque ripple.

Selection of new hysteresis current controller (other than three hysteresis current controllers for three phases in Figure.40) "hysteresis band" decides this technique performance. A proper "hysteresis band" has to be chosen for proper functioning of this technique. Commutation torque ripple is eliminated and the speed response is good. In some applications speed commutation torque ripple causes disturbance in the speed. This torque response is much better than the response shown in Figure.41.

4.3 SLIDING MODE SPEED CONTROLLER BASED FSTPI-BLDC MOTOR DRIVE

In BLDC motor drive using PI speed controller, there is overshoot in starting speed response and it is undesirable. It is need to use a controller which avoids overshoot for step response. In addition to invariance with respect to the system parameters and external disturbances as it is a very attractive feature of SLMC, in the time domain, the state response or corresponding response will be exponential. This nature of exponential state response leads to no overshoot in the system state (speed) response. A typical feature of implementing sliding mode control in speed control systems (i.e. SLMSC) is that it requires the state (speed) which is to be controlled and its derivative. Figure.44 shows the simulink implementation of Figure.12 (b) for sliding mode speed controller. Figure.45 shows the starting speed response of FSTPI-BLDCM with $HHH_{initial}=100$ and for a reference speed of 1800 rpm using sliding mode speed controller.

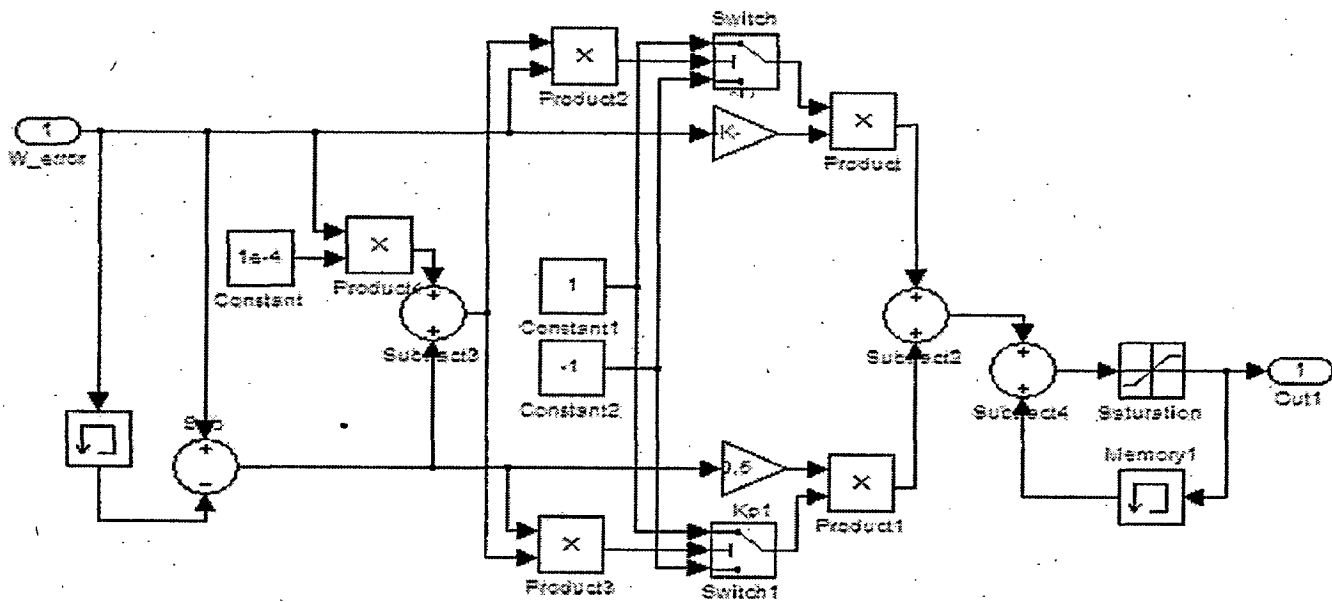


Figure.44. Simulink implementation of sliding mode speed controller

As the speed response is exponential, it takes more time to reach final value. It has steady state error but steady state error of PI controller speed response is zero. All the results at different initial rotor position and with different capacitance values are obtained are tabled in the results section.

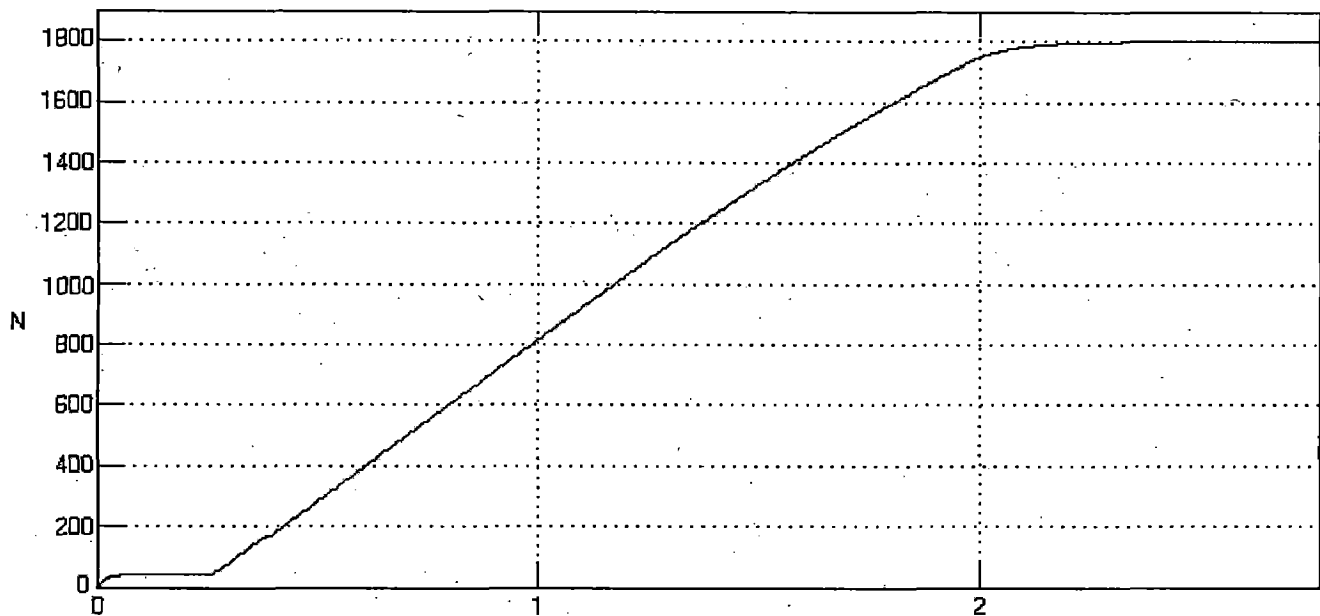


Figure.45. Starting speed response of FSTPI-BLDC motor using sliding mode speed controller for a reference speed of 1800 rpm with $HHH_{initial}=100$

4.4. FUZZY SPEED CONTROLLER BASED FSTPI-BLDC MOTOR DRIVE

4.4.1 Introduction

Due to continuously developing automation systems and more demanding control performance requirements, conventional control methods are not always adequate. The input output relations of the system may be uncertain and they can be changed by unknown external disturbances. New schemes are needed to solve such problems. One such an approach is to utilize fuzzy control. Fuzzy control is based on fuzzy logic, which provides an efficient method to handle in exact information as basis reasoning. With fuzzy logic it is possible to convert knowledge, which is expressed in an uncertain form, to an exact algorithm. In fuzzy control, the controller can be represented with linguistic If-then rules, the interpretation of the controller are the fuzzy but controller is processing exact input input-data and is producing exact output-data in a deterministic way.

4.4.2 Structure of a fuzzy controller

Fuzzy control is a control method based on fuzzy logic. Fuzzy logic can be described as "computing with words rather than numbers, "and" control with sentences rather than equations". There are specific components characteristic of a fuzzy controller to support a design procedure. In the block diagram in Figure.46 the controller is between preprocessing and post processing blocks.

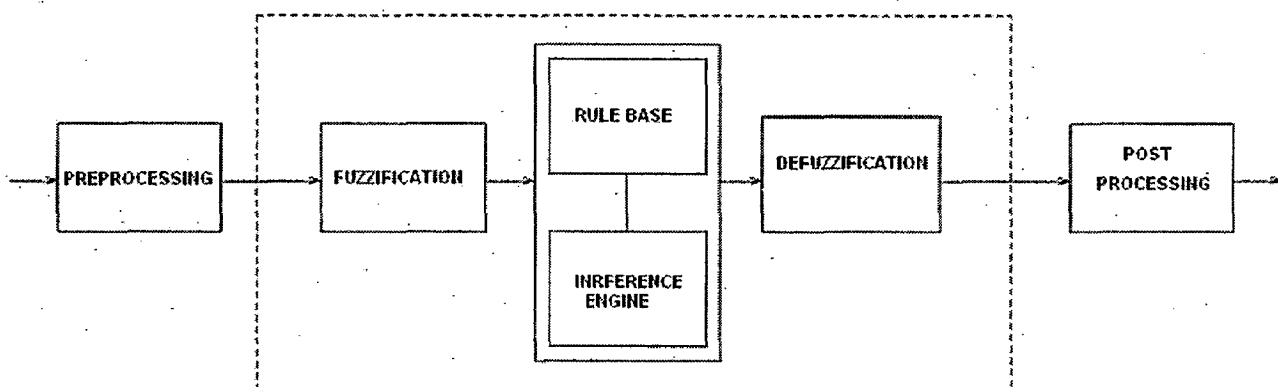


Figure.46. blocks of a fuzzy controller

Preprocessing:

The inputs are most often hard or crisp measurements from some measuring equipment, rather than linguistic. Pre processor conditions the measurements before they enter the controller and the control strategy is a static mapping between input and control signal. A dynamic controller would have additional inputs like derivatives, integrals. These are created in preprocessor thus making the controller multidimensional, which requires many rules and makes it more difficult to design. The preprocessor then passes the data on to the controller.

Fuzzification:

The first block inside the controller is fuzzification, which converts input data to degrees of membership by lookup in various membership functions. The fuzzification block thus matches the input with the conditions of the rules to determine how well the condition of each rule matches that particular instance. There is a degree of membership for each linguistic term that applies to that input variable.

Rule Base:

The rule base is to do with the fuzzy inference rules. It will be usually in an If-then format.

E.g. Inputs – error, change in error.

Rules: IF error is ___ AND change in error is ___ THEN output is ___.

Inference Engine:

(1) Aggregation: This operation is use to find the degree of fulfillment or firing strength of the condition of a rule k. if μ_1 , μ_2 are the membership functions of rules 1&2, then the aggregation is their combination:

$$\mu_1 \text{ AND } \mu_2$$

Similarly for other rules aggregation is equivalent to fuzzification, when there is only one input to the controller.

(2) Activation: Activation of a rule is the deduction of the conclusion.

(3)Accumulation: All activated conclusions are accumulated

Defuzzification:

The resulting fuzzy set must be converted to a number that can be sent to the process as a control signal is called defuzzification. There are several defuzzification methods.

- (a) Mean of max
- (b) Bisector of area
- (c) Centre of gravity

Post processing:

Output scaling is also relevant. In case the output is defined on a standard universe this must be scaled to engineering like meters, volts. This block often contains an output gain that can be tuned, and sometimes also an integrator.

4.4.3 Advantages of fuzzy

The principal advantages of fuzzy control are:

1. The fast convergence with adaptive step size of the control variable: This means that the machine flux decrement starts in the beginning with a large step size, which then gradually decreases so that the optimum flux condition is attained quickly.
2. The additional advantage of fuzzy control is that it can accept inaccurate signals Corrupted with noise.
3. The neural network adds the advantage of fast control implementation, either by a dedicated hardware chip or by digital signal processor (DSP)-based software.
4. The fuzzy estimator improves the stator flux estimation accuracy leading to a smooth trajectory and therefore reducing the torque ripples. This estimator is particularly suited in applications needing high torque at low speed and improves the performance of control strategy in applications where thermal impact on resistance variation is no more negligible.

4.4.4 Controller design and tuning

In general, it is difficult to formulate control rules for an unknown system. However, we already know the system and can predict a step response of the motor speed. Therefore it is comparatively easy to formulate control rules.

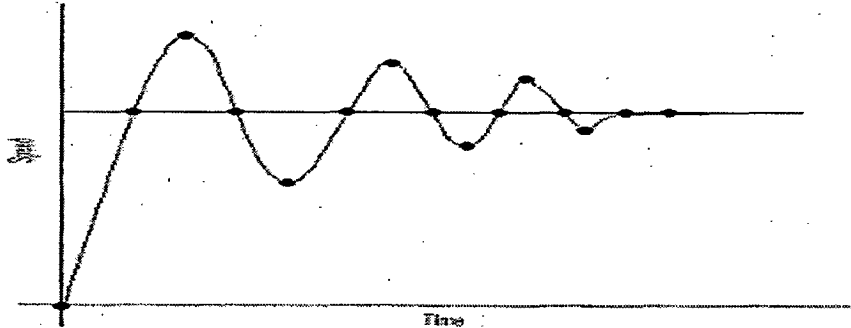


Figure.47. Step Response of the speed

The typical step response of the speed from 0 rpm to a set value is shown in Figure.47. The characteristic points are shown with dots in this figure. To formulate control rules, it is necessary to examine the condition at each characteristic point and to consider the relation among E_r , E_r (dot) and ΔT_c , so as to bring the step response close to the set speed value. The fuzzy rule table used in this work is given in the coming sections. Figure.48. shows the simulink model block diagram for the FL speed controller. The two inputs namely speed error and change in speed error are properly scaled and fed to the MATLAB fuzzy logic controller. The defuzzified output of the FL block is scaled by proper scaling factor and after limiting, forms the reference torque for the current controller.

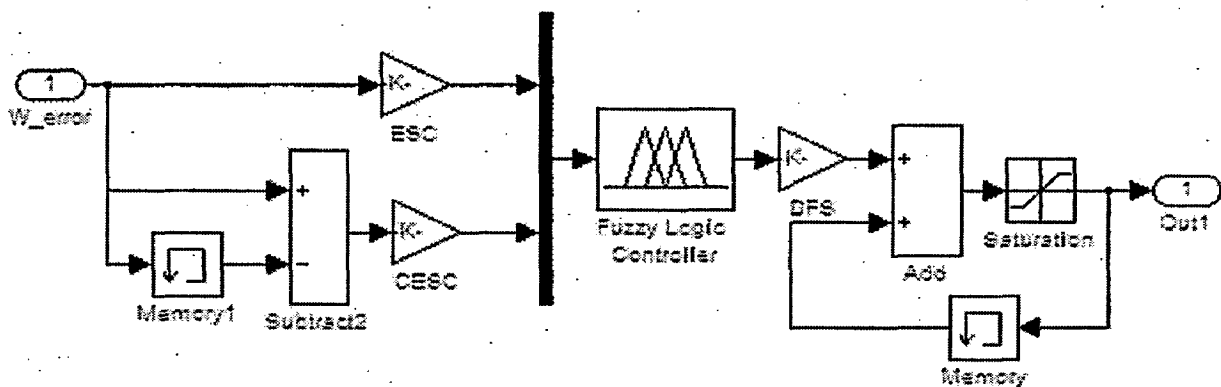


Figure.48. MATAALB model for Fuzzy Logic (FL) speed controller

ω_{err}								
$\Delta\omega_{err}$								
	NB	NM	NS	ZE	PS	PM	PB	
NB				NB	NB			
NM	NB			NB	NB			
NS	NB			NM	NM	NM	PM	
ZE	NB	NM	NS	ZE	PS	PM	PB	
PS	NM		PS	PS	PM			
PM				PM	PB	PB		
PB			PM	PM	PB			

Table.2. Logic rules for Fuzzy Logic (FL) speed controller

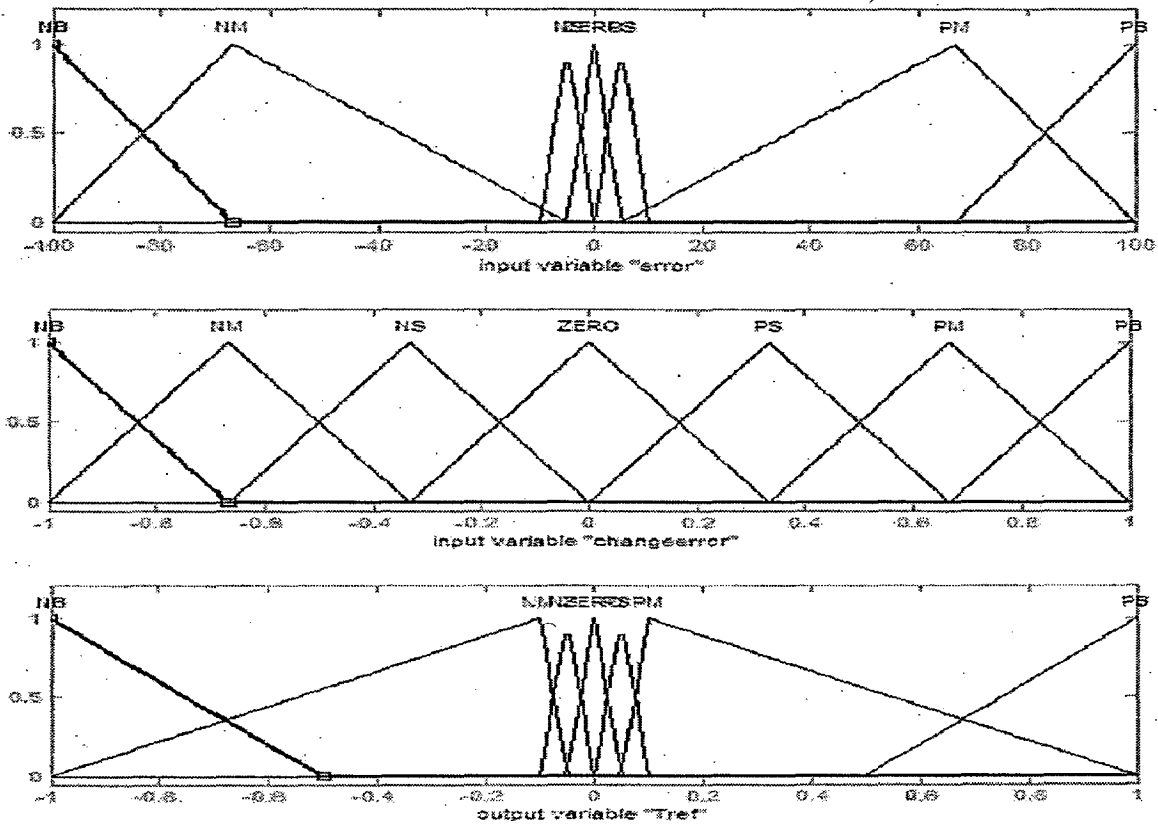


Figure.49. Membership function plots for input and output variables.

The tuning of fuzzy controller is based on Figure.47 and trial and error tuning process for membership function limits for input and output variables so as to reduce both speed error and overshoot. In PI controller based drive speed over shoot is more and steady state error

is while and in sliding mode drive speed overshoot is zero but it takes more time to reach reference speed while it provides some steady state error. Now, a controller is needed to achieve reduced overshoot, starting time and steady state error. Complete drive analysis has been done in previous sections with PI speed controller. Same drive can be used for fuzzy logic based drive except speed PI controller is replaced by fuzzy speed controller in Figure.16. Here only starting speed response using fuzzy controller is analyzed for both directions while the rest of the performance evolution is documented in the form of tables. Other results are put in the results section. Figure.50 shows the starting response when using fuzzy speed controller. Performance results of SSTPI-BLDC motor using fuzzy and FSTPI-BLDC motor using fuzzy for all modes of operation is presented in the results section. That can be compared with the other technique. Performance evaluated at different capacitor and maximum current values using fuzzy technique. The Figure.50 shows the Starting speed response of FSTPI-BLDC motor using fuzzy speed controller for a reference speed of 1800 rpm. Rise time of the motor speed is 2.0866 seconds with overshoot of 1 rpm which is negligible. There is very little steady state error in its speed response which is less than half rpm with no-load it would be more with load.

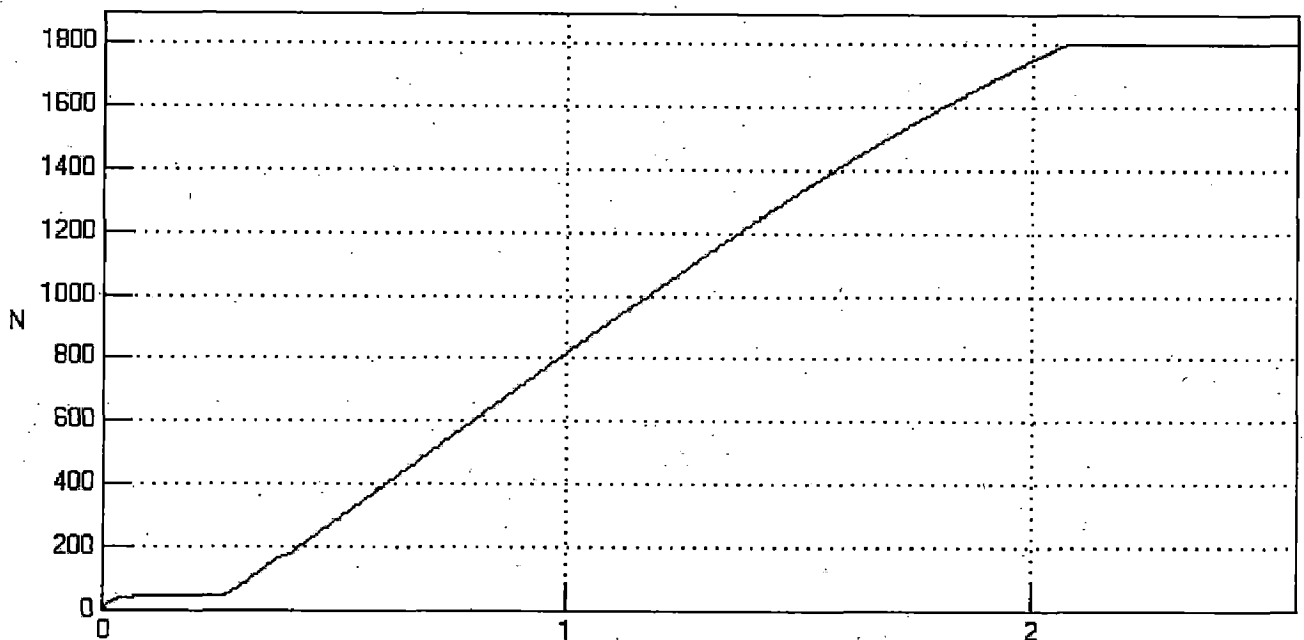


Figure.50. Starting speed response of FSTPI-BLDC motor using fuzzy speed controller for a reference speed of 1800 rpm with HHH=100

The speed response of Figure.50 is with starting rotor position HHH=100. But for rotor starting position with 101, 010, 001, or 110 takes less time than for the case shown or HHH=011.

4.5 CONCLUSION

A four quadrant operated simulation model in MATLAB-simulink is developed and its working is analyzed in four quadrants of operation for FSTPI-BLDCM drive. For comparison, SSTPI-BLDCM drive is developed and its operation is compared with four switch counterpart. Capacitors affect is analyzed as this is the main cause for delayed starting. Capacitor charging affect is also analyzed for different rotor initial positions. Commutation torque ripple is the main problem of FSTPI-BLDCM drives and the main reason for this is commutation of devices. Commutation torque ripple effect is analyzed and a new way to reduce the commutation torque ripple is presented. Speed response using all speed controllers is analyzed. Fuzzy speed controller is better in overall performance compared to PI or sliding mode speed controller.

CHAPTER 5

RESULTS AND DISCUSSIONS

The performance of BLDCM drive system is simulated using model developed in MATLAB environment along with simulink and Power System Block set (PSB) toolboxes under different dynamic conditions such as starting, load perturbation i.e. load application and load removal and speed reversal. As the choice has affect on the operation of BLDC motor, simulation work is carried out at different values of capacitance and these results are put in table. Results of novel technique presented for reduction of commutation torque ripple is presented at rated load of the machine at 2N-m and rated speed 1800 rpm. First, A set of responses consists of reference speed (N_r), motor speed (N) in rpm, reference current generated from speed controller (i_{ref}) in amperes, phase 'A' winding current (i_a) in Amperes and developed electromagnetic torque (T_e). The performance of BLDC motor under different modes of operation is investigated. The simulation results of BLDC motor corresponding to 0.5 hp motor and all parameters taken from reference[22] where a six switch inverter performance was examined for fuzzy logic controller. In this section first, results of commutation torque ripple reduction is presented. After this, the response for SSTPI-BLDCM for all controllers is presented along with comparative results. Next, the response for FSTPI-BLDCM for all controllers in possible modes is presented along with comparative results. Comparative results are presented for different capacitor values of FSTPI drive. Simulated results of novel commutation torque ripple reduction technique and normal FSTPI-BLDCM system is presented at the end for comparison.

5.1 STARTING DYNAMICS

At starting using rotor position signal based on the type of inverter used a proper switches are operated to start the machine and then machine starts to reach reference speed. In this work the reference speed is set at 1800 rpm as the base speed. The torque limit is set at thrice the rated value and hence the starting current is limited with in thrice the rated value when the motor builds up the required starting torque. When the speed error reaches nearly zero rpm, the winding current also reduces to no load value and the developed toque equals the load torque as observed in the starting response as shown in Figures.[51-59]

5.2 REVERSAL DYNAMICS

When the reference speed is changed from 1800 rpm to -1800 rpm, the motor tends to run in reverse direction. When the controller observes this change, reference current is reversed to brake the motor. As the drive is in the same dynamic state (on no load) just before and after the reversal phenomenon, the steady state values of the inverter current (phase 'A') are observed to be same in either directions of the rotation of the motor. However the switching sequence will be different.

5.3 LOAD PERTURBATION

The study of the performance of BLDCM drive under load variations is really important as the speed of the motor should not change under any load conditions. In this work this study is performed by applying load and removing the load on the motor when it running at a steady speed of 1800 rpm. Sudden application of load on the rotor causes an instantaneous fall in the speed of the motor. In response to this drop in speed value, the output of the controller responds by increasing the reference torque value. Therefore, the developed electromagnetic torque of the motor increases causing the motor speed settles down to the reference speed with the increased winding currents. Similarly, when the load is removed suddenly from the motor, a small overshoot in the speed of the motor occurs. Because of this small increase in speed, the torque output of the speed controller reduces thereby reducing the speed of the motor. Thus the motor settles at the reference speed value. After the load removal, the stator currents also set to the steady state value. In this manner the controller keeps the motor running at a constant speed under the load variations.

5.4 COMPARATIVE STUDY AMONG DIFFERENT SPEED CONTROLLERS

The dynamics of the motor discussed in the sections 5.1-5.3 are observed using different speed controllers namely PI, SLIDING MODE, and FUZZY and the responses are shown in Figures [51-59] for 0.5 hp BLDC motor. Table.3 also shows a comparative performance of these different speed controllers for SSTPI operation and next FSTPI operation responses are shown in Figures.[54-59]. The observations from the tables are discussed below. The advantages of PI controller are simple in operation and zero steady state error when operating on load. But the disadvantages of this PI controller is the occurrence of overshoot while starting, undershoot while load application and overshoot while load removal. To eliminate overshoot in the speed response at starting, sliding mode speed controller is used.

This controller eliminates over shoot but starting time and recovery times for load disturbances is more than PI speed controller and more steady state error is introduced in the sliding mode control. Only advantage we get from sliding mode control is overshoot is zero. Fuzzy controller has good dynamic response makes it to achieve reference speed in short time than other two speed controllers. Over shoot is less than PI controller but more than sliding mode controller. Speed change for load variations is lesser than other two controllers. Overall performance is good for fuzzy speed controller even it has little steady state response (SSE). But the disadvantage of the steady state speed error is observed in case of FL speed controller. All this performance evaluation is for SSTPI fed drive.

Controller type:		Pi (SSE=0)	Sliding mode (SSE=0.3)	Fuzzy (SSE=0.1)
$T_{start}(sec)$		1.7902	2.5	1.6935
Overshoot (%)		0.0794	0	0.012
Full load apply	ΔN	10.6809	10.8619	2.9098
	$T_{recover}$	0.375	1.2616	0.1112
Full load removal	ΔN	10.1901	10.0241	2.7367
	$T_{recover}$	0.8	0.8983	0.1319
$T_{reversal}(sec)$		3.4017	4.1486	3.2556

Table.3. Comparative Performance of Different Speed Controllers for SSTPI-BLDCM drive with reference speed of 1800rpm, reversal speed to -1800rpm and $T_L=2Nm$

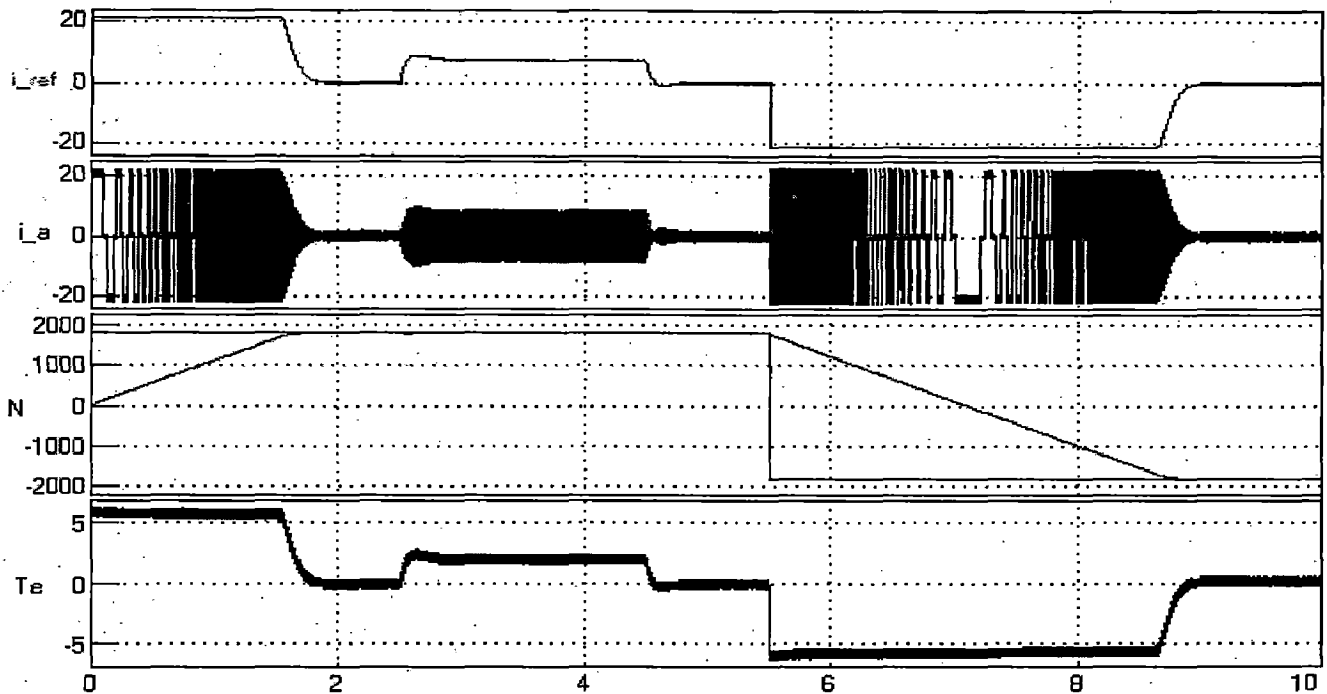


Figure.51. Starting, Speed Reversal and Load Perturbation Response of SSTPI-BLDCM system with Proportional Integral (PI) Speed Controller. (x-axis is time axis in seconds)

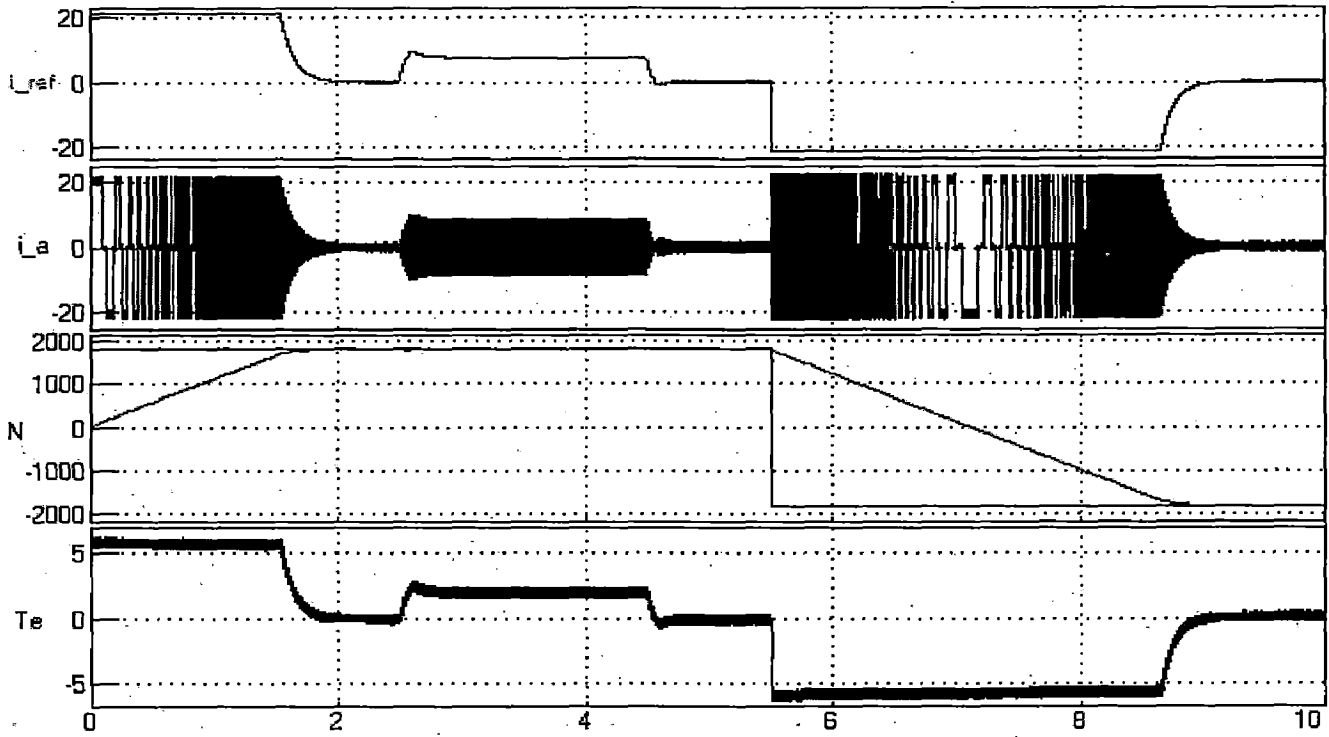


Figure.52. Starting, Speed Reversal and Load Perturbation Response of SSSIPI-BLDCM system with sliding mode Speed Controller. (x-axis is time axis in seconds)

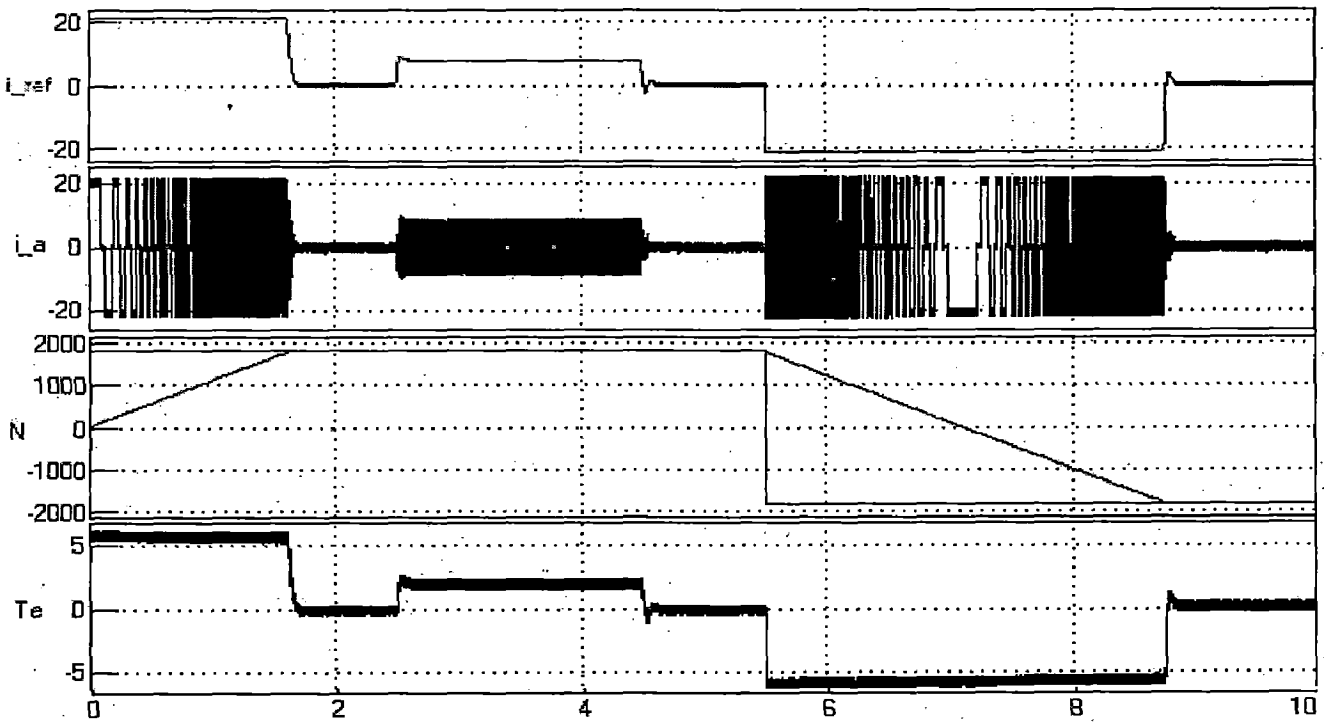


Figure.53. Starting, Speed Reversal and Load Perturbation Response of SSSIPI-BLDCM system with fuzzy Speed Controller. (x-axis is time axis in seconds)

It is known from previous sections analysis that the starting response depends on the initial rotor position (HHH). Table.4 shows results for initial rotor position HHH=100 or 011 and for different capacitance values for FSTPI-BLDCM system while figure.54. shows the responses for capacitance value 5000 μ f for PI speed controller. Steady state error (SSE) is zero.

Capacitance:		5000 μ f	4000 μ f	3000 μ f	2000 μ f
$T_{start}(sec)$		2.1258	2.1822	2.3313	2.6095
Overshoot (%)		0.17	0.17	0.17	0.167
Full load apply	ΔN	10.8	10.82	10.76	10.83
	$T_{recover}$	0.36	0.344	0.36	0.36
Full load removal	ΔN	10.5	10.53	10.54	10.52
	$T_{recover}$	0.338	0.344	0.344	0.3431
$T_{reversal}(sec)$		3.6576	4.3647	3.9437	4.0498

Table.4. Comparative Performance of FSTPI-BLDCM drive with $N_{ref}=1800$, reversal speed of -1800rpm and $T_L=2Nm$ for different capacitances using PI speed controller $HHH_{initial}=100$



Figure.54. Starting, Speed Reversal and Load Perturbation Response of FSTPI-BLDCM system with PI Speed Controller, capacitance=5000 μ f and $HHH_{initial}=100$ or 011. (x-axis is time axis in seconds)

Table.5 shows results for initial rotor position HHH=101 or 010 and for different capacitance values for FSTPI-BLDCM system while figure.55. shows the responses for capacitance value 5000 μ f for PI speed controller. Steady state error (SSE) is zero.

Capacitance:		5000 μ f	4000 μ f	3000 μ f	2000 μ f
$T_{start}(sec)$		1.9275	1.9434	1.9798	2.0772
Overshoot (%)		0.17	0.17	0.17	0.17
Full load apply	ΔN	10.8	10.8	10.78	10.795
	$T_{recover}$	0.36	0.36	0.363	0.358
Full load removal	ΔN	10.51	10.53	10.526	10.51
	$T_{recover}$	0.343	0.343	0.3421	0.3416
$T_{reversal}(sec)$		3.6222	4.0156	3.7308	4.0873

Table.5. Comparative Performance of FSTPI-BLDCM drive with $N_{ref}=1800$, reversal speed of -1800rpm and $T_L=2Nm$ for different capacitances for PI speed controller $HHH_{initial}=101$

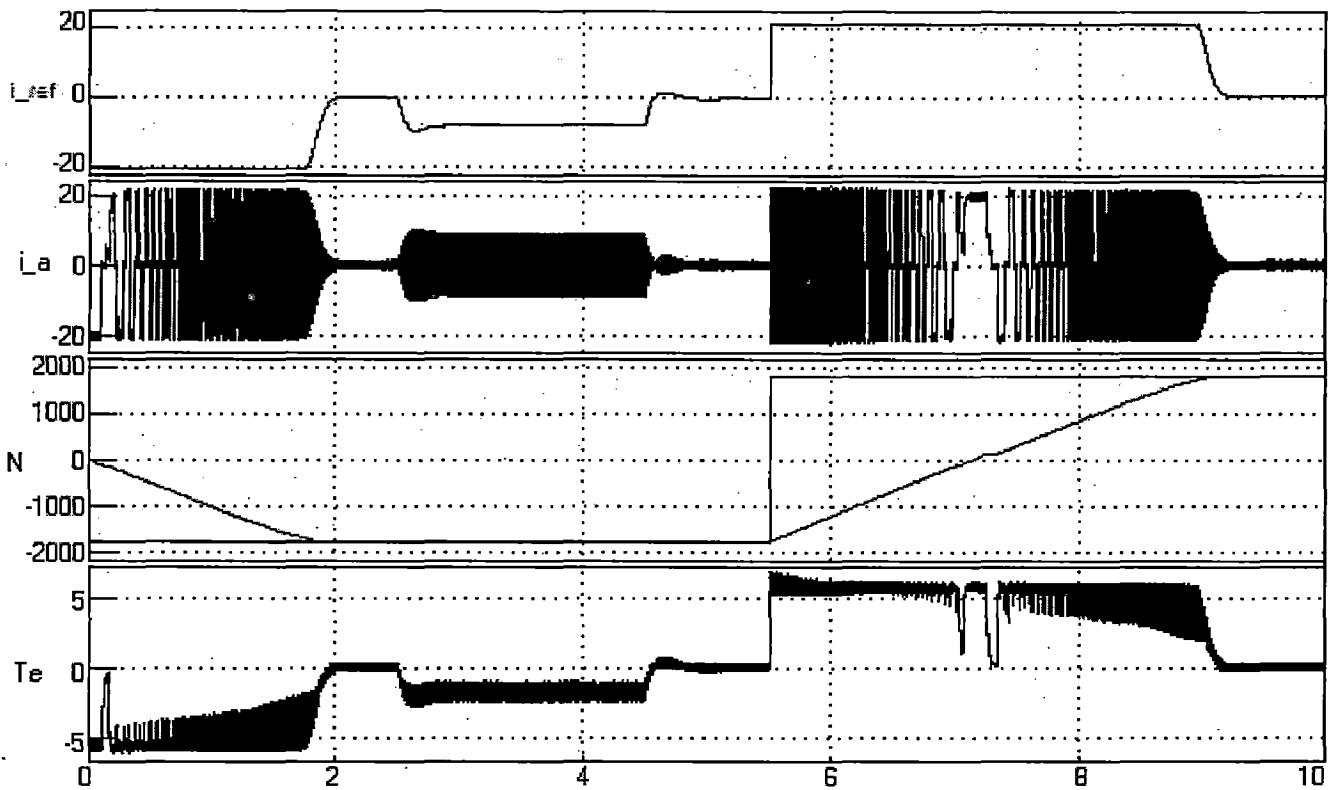


Figure.55. Starting, Speed Reversal and Load Perturbation Response of FSTPI-BLDCM system with PI Speed Controller, capacitance=5000 μ f and $HHH_{initial}=101$ or 010. (x-axis is time axis in seconds)

Table.6 shows results for initial rotor position HHH=100 or 011 and for different capacitance values for FSTPI-BLDCM system while figure.56 shows the responses for capacitance value 5000 μ f for sliding mode speed controller. Steady state error (SSE) is 0.3.

Capacitance:		5000 μ f	4000 μ f	3000 μ f	2000 μ f
T_{start} (sec)		2.6	2.75	2.844	3.1089
Overshoot (%)		0	0	0	0
Full load apply	ΔN	11.0024	11.0158	10.9025	10.8303
	$T_{recover}$ (error)	1.3(0.5)	1.3444(0.5)	1.2208(0.5)	1.2604(0.5)
Full load removal	ΔN	10.1737	10.1533	10.1389	10.1414
	$T_{recover}$	0.4998	0.498	0.4742	0.5212
$T_{reversal}$ (sec)		4.2957	4.1323	5.4806	5.0058

Table.6. Comparative Performance of FSTPI-BLDCM drive with $N_{ref}=1800$, reversal speed of -1800rpm & $T_L=2Nm$ for different capacitance for sliding mode speed controller $HHH_{initial}=100$.



Figure.56. Starting, Speed Reversal and Load Perturbation Response of FSTPI-BLDCM system with sliding mode Speed Controller, capacitance=5000 μ f and $HHH_{initial}=100$ or 011. (x-axis is time axis in seconds)

Table.7 shows results for initial rotor position HHH=101 or 010 and for different capacitance values for FSTPI-BLDCM system while figure.57 shows the responses for capacitance value 5000µf for sliding mode speed controller. Steady state error (SSE) is 0.3.

Capacitance:		5000µf	4000µf	3000µf	2000µf
T _{start} (sec)		2.411	2.438	2.4587	2.5779
Overshoot (%)		0	0	0	0
Full load apply	ΔN	10.894	10.9153	10.8373	10.8329
	T _{recover} (error)	1.2045(0.5)	1.3654(0.5)	1.4587(0.5)	1.4428(0.5)
Full load removal	ΔN	10.1799	10.1839	10.1778	10.1606
	T _{recover}	0.4991	0.5018	0.5042	0.4889
T _{reversal} (sec)		4.1991	4.3163	4.3373	5.6125

Table.7. Comparative Performance of FSTPI-BLDCM drive with N_{ref}=1800, reversal speed of -1800rpm & T_L=2Nm for different capacitance for sliding mode speed controller HHH_{initial}=101.

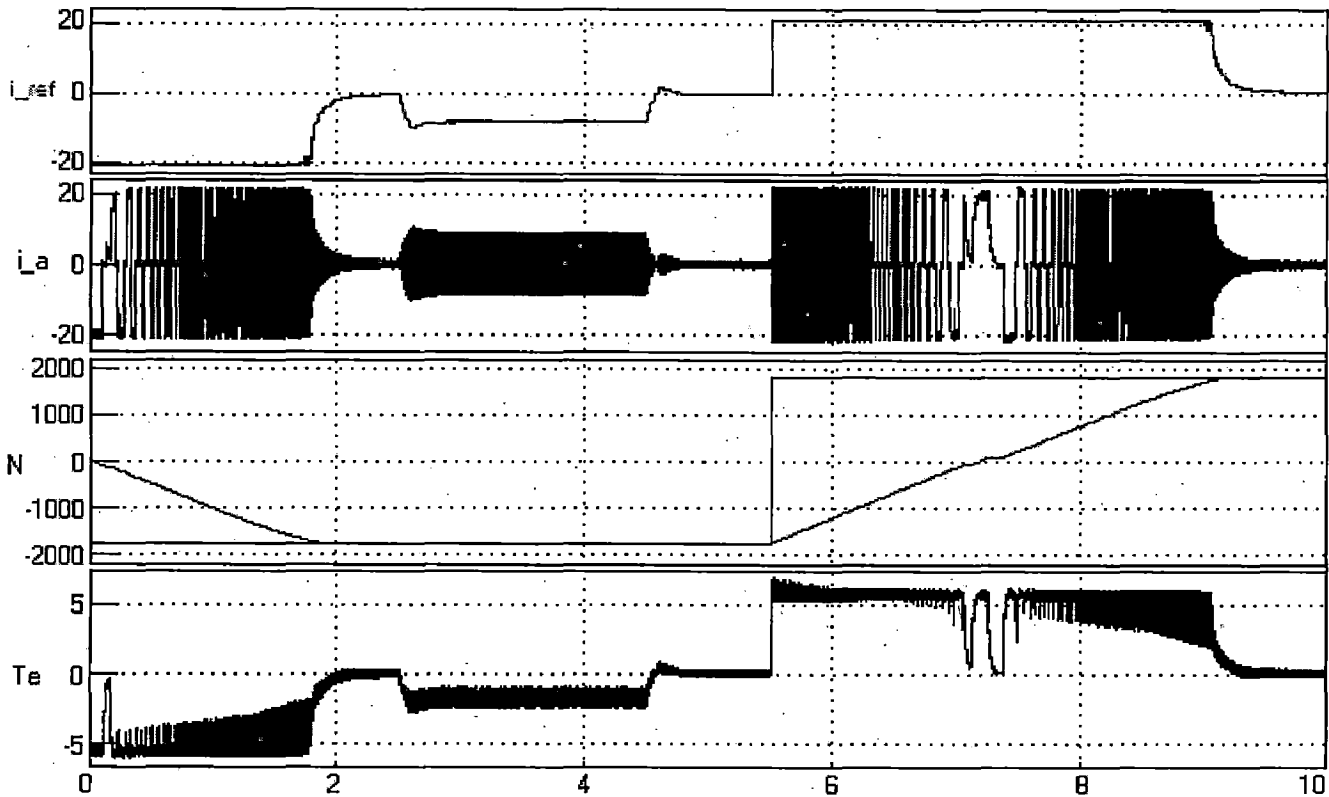


Figure.57. Starting, Speed Reversal and Load Perturbation Response of FSTPI-BLDCM system with sliding mode Speed Controller, capacitance=5000µf and HHH_{initial}=101 or 010. (x-axis is time axis in seconds)

Table.8 shows results for initial rotor position HHH=100 or 011 and for different capacitance values for FSTPI-BLDCM system while figure.58 shows the responses for capacitance value 5000 μ f for fuzzy speed controller. Steady state error (SSE) is 0.1.

Capacitance:		5000 μ f	4000 μ f	3000 μ f	2000 μ f
$T_{start}(sec)$		2.0873	2.1616	2.2925	2.569
Overshoot (%)		0.035	0.0347	0.03230	0.0341
Full load apply	ΔN	2.9364	2.9576	2.972	2.988
	$T_{recover}$	0.101	0.1002	0.1006	0.106
Full load removal	ΔN	02.85	2.841	2.7895	2.796
	$T_{recover}$	0.1455	0.1473	0.1473	0.1474
$T_{reversal}(sec)$		3.6028	4.3428	3.8801	3.9921

Table.8. Comparative Performance of FSTPI-BLDCM drive with $N_{ref}=1800$, reversal speed of -1800rpm & $T_L=2Nm$ for different capacitance for fuzzy speed controller, $HHH_{initial}=100$ or 011



Figure.58. Starting, Speed Reversal and Load Perturbation Response of FSTPI-BLDCM system with fuzzy Speed Controller, capacitance=5000 μ f and $HHH_{initial}=100$ or 011. (x-axis is time axis in seconds)

Table.9 shows results for initial rotor position HHH=101 or 010 and for different capacitance values for FSTPI-BLDCM system while figure.59 shows the responses for capacitance value 5000 μ f for fuzzy speed controller. Steady state error (SSE) is 0.1.

Capacitance:		5000 μ f	4000 μ f	3000 μ f	2000 μ f
T_{start} (sec)		1.868	1.8796	1.9203	2.0162
Overshoot (%)		0.4182	0.4185	0.4207	0.4182
Full load apply	ΔN	2.9166	2.9011	2.914	2.94
	$T_{recover}$	0.1461	0.14	0.1418	0.144
Full load removal	ΔN	2.8952	2.9187	2.9002	2.87
	$T_{recover}$	0.0959	0.0972	0.0968	0.0958
$T_{reversal}$ (sec)		3.5255	3.6348	3.6806	4.0093

Table.9. Comparative Performance of FSTPI-BLDCM drive with $N_{ref}=1800$, reversal speed of -1800rpm & $T_L=2Nm$ for different capacitance for fuzzy speed controller, $HHH_{initial}=101$ or 010

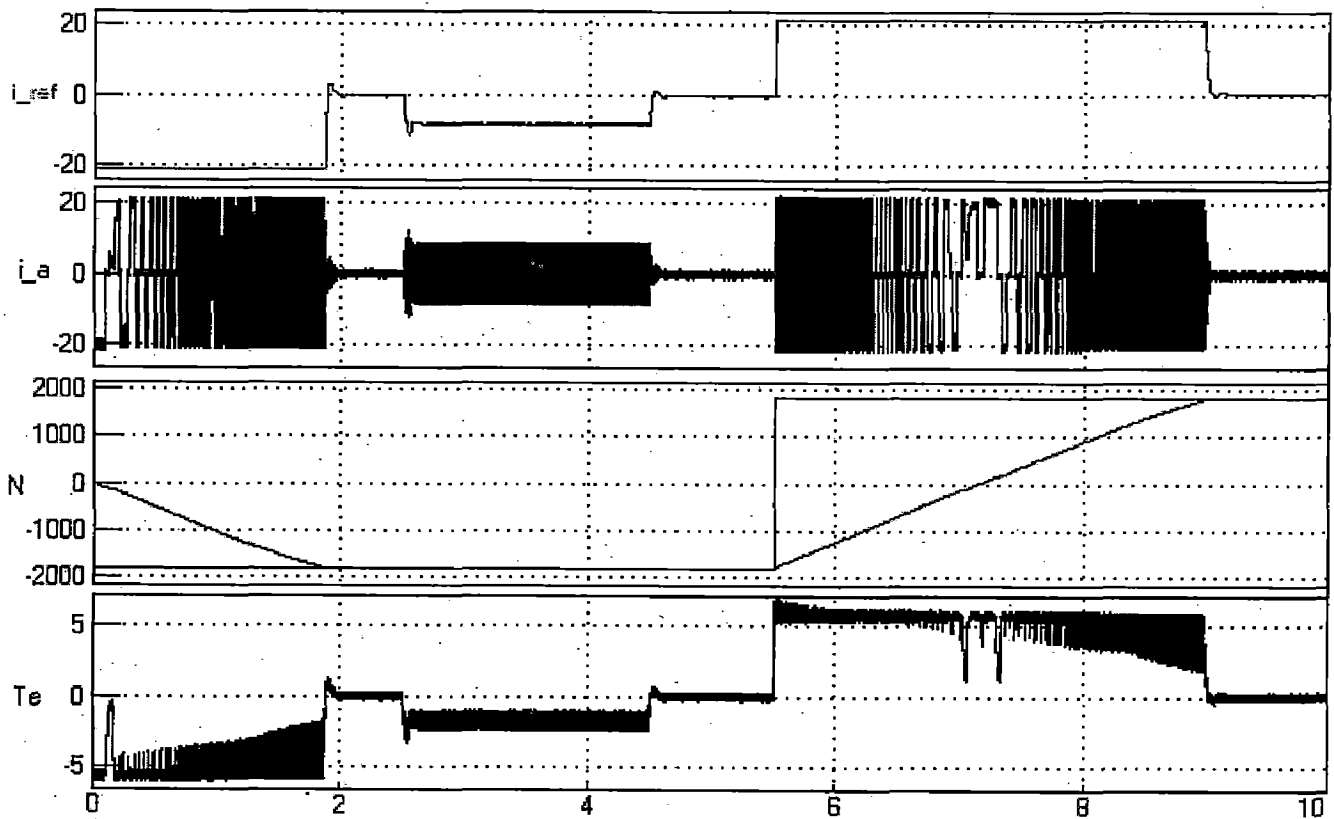


Figure.59. Starting, Speed Reversal and Load Perturbation Response of FSTPI-BLDCM system with fuzzy Speed Controller, capacitance=5000 μ f and $HHH_{initial}=101$ or 010. (x-axis is time axis in seconds)

5.5 COMPARATIVE RESULTS FOR COMMUTATION RIPPLES

In normal FSTPI-BLDCM drive at higher speeds commutation torque ripple is more and Figure.60 shows the three phase current responses and torque response of machine at 1800 rpm of the machine at full load (2N-m). In the previous sections a novel technique is presented which reduces the torque ripple to a significant amount causes the smooth and silent operation of the motor.

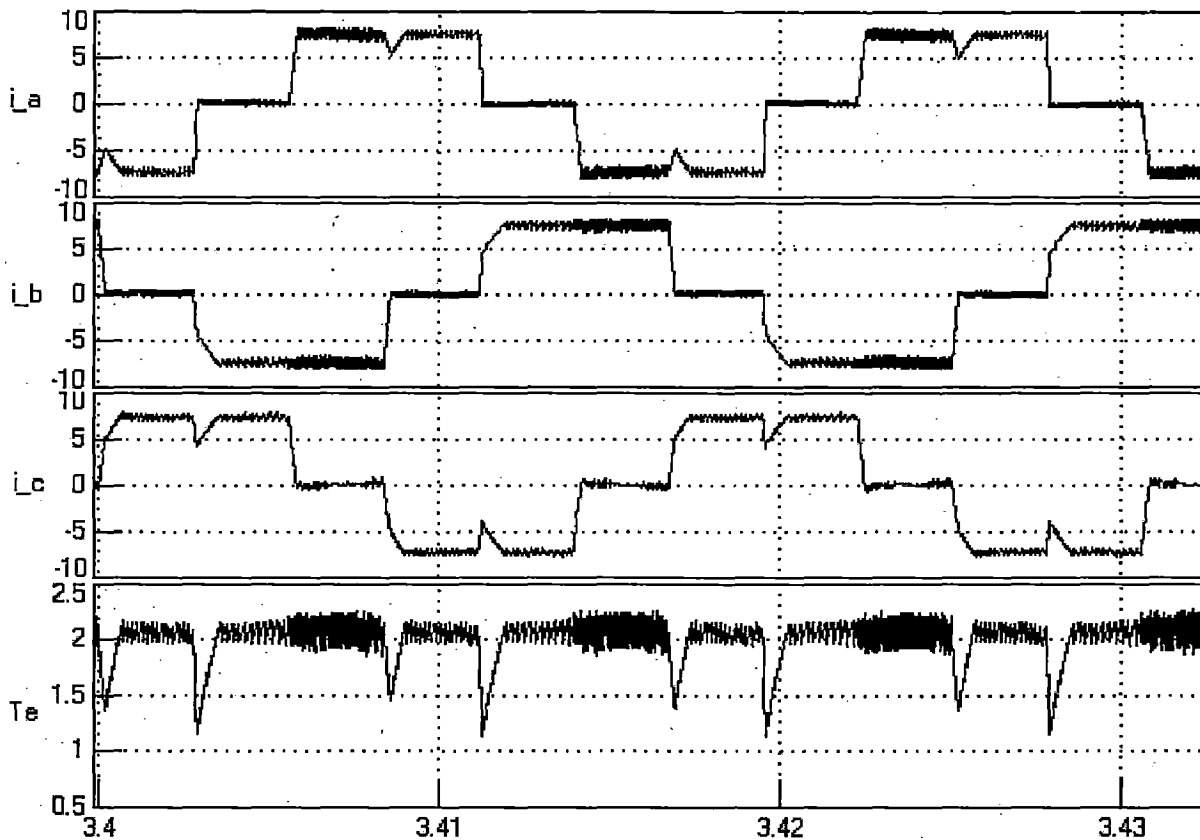


Figure.60. Three phase current responses and torque response of FSTPI-BLDC motor at 1800 rpm and 2N-m load.

The commutation torque ripple reduction technique presented here, can be extended to all modes of operation of the motor i.e. regeneration and reverse motoring. Using this technique causes more ripple torque in transient condition. So, we can develop a method where, normal FSTP method is useful for transient operation while this new technique useful for steady state operation and this becomes a hybrid technique. The Figure.61 shows the three phase current responses and torque response of machine at 1800 rpm of the machine at full load (2N-m).

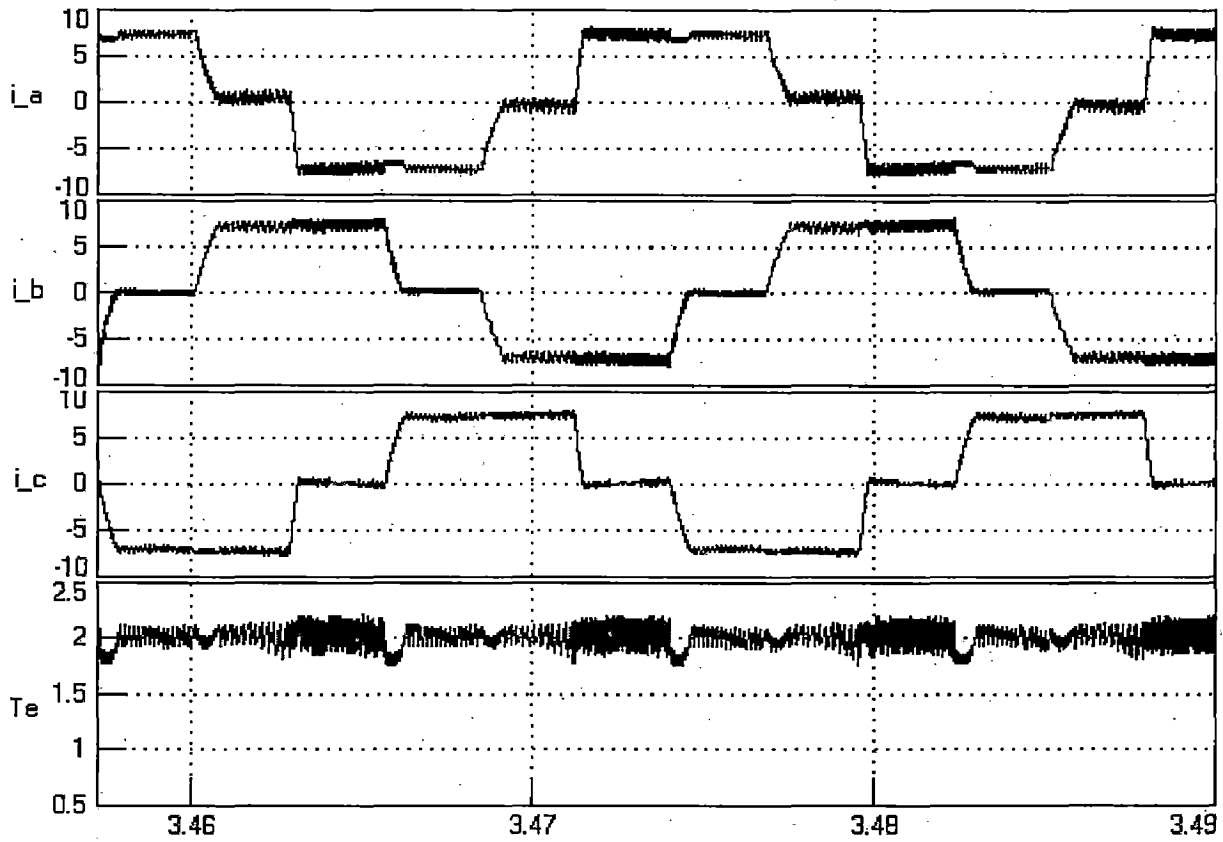


Figure.61. Three phase current responses and torque response of FSTPI-BLDC motor at 1800 rpm and 2N-m load using novel commutation torque ripple reduction technique

CHAPTER 6

CONCLUSION AND FUTURE SCOPE

A four-switch inverter fed Brushless DC motor drive simulation model is developed in MATLAB-Simulink using simulink and power system block set (PSB) toolboxes and the drive response is simulated under different operating conditions such as starting, speed reversal and load perturbation. A comparative study of different speed controller's namely proportional integral (PI) controller, sliding mode controller, fuzzy logic (FL) controller has also been presented for the BLDCM drive system. Since the four switch inverter model evolve from six switch inverter, for a comparative study, six switch inverter fed BLDC motor drive is also developed and performance is compared with its four switch counterpart. Six switch and four switch inverter topologies exhibit their own merits and demerits. This comparative study of different speed controllers for variable speed operation has also shown respective merits and demerits of the individual speed controllers. Since, major drawback of four switch topology is more commutation torque ripples in torque response, which is the result of ripples in the current. A novel way for commutation torque ripple reduction technique is presented in this work. Simulation results show that there is great improvement in the current there by torque response which is equally comparable with six switch inverter torque response. Presented technique overcomes the limitation imposed due to commutation torque ripple. For starting speed response, four switch topology is somewhat inferior to six switch counterpart, while four switch topology has many advantages. Capacitors used in the one of the leg of four switch inverter poses many problems, and commutation torque ripple problem is addressed in this work. Other problems are analyzed and performance of four switch inverter fed drive with different capacitor values is evaluated. Decrease in capacitor value gives poor performance of the drive. A capacitor value has to be taken so that drive gives better performance and less cost.

Comparative study of drive with different speed controllers is performed. If the requirement is that of simplicity and ease of application, the PI speed controller is a good choice. But the PI controller suffers with the disadvantage of occurrence of overshoots and undershoots. If the application prime requirement is not to have any overshoot in starting response, then, sliding mode controller is suitable choice. But sliding mode controller based drive dynamic response is poor and it has some steady state error and minor chattering in speed in steady state. Fuzzy logic controller provides a better dynamic response with little

overshoot and undershoot but better than PI controller. Fuzzy controller introduces steady state error more than the PI controller does and less than the sliding mode controller. Based on application requirement of the motor, speed controller can be chosen.

Presently a wide research is going on in sensor less operation of the four switch inverter fed drives so as to decrease the overall cost of the drive without losing any performance of the drive. Practical implementation of the proposed new way of commutation torque ripple reduction technique and extending the same technique for four quadrant operation are possible areas of future research work. As a way to reduce the overall cost of the drive, there is other way to reduce the cost to this four switch technique and it is: variable input voltage fed thyristorized four switch inverter from the step down chopper and thyristorized inverter feeding the BLDC motor. This is the new area of research work and it has to be implemented in hardware to prove the cost reduction. As the performance of four switch inverter fed drive topologies inferior in dynamic range of motor operation, and there is possibility to improve the performance and this makes the four switch drive suitable option to implement for many applications. When a six switch inverter fed BLDC motor faces a switch failure problem or two switch failure in one leg of inverter, then, it can be converted to four switch inverter and operation will similar to four switch inverter fed drive. So, switch failure analysis for six switch inverter fed drives is another important area of research as this will ensure proper functioning of drive and motor.

REFERENCES

- [1] Microchip Technology Inc. AN885, "*Brushless DC (BLDC) motor Fundamentals*".
- [2] Apex micro technology, "*Driving 3-phase Brushless DC Motors*", Application note 45
- [3] Electric drives by Ion Boldea, S.A.Nasar , crc press.
- [4] A.kusko, S.M.pareen, "*Definition of the Brushless DC motor*" IEEE, 1988
- [3] Paul P. Acarnley, John F. Watson, "*Review of Position Sensorless Operation of Brushless Permanent Magnet Machines*" IEEE transaction on Industrial Electronics, vol.53, no.2, April 2006.
- [4] Muhammad h. Rashid, "*power electronics hand book*".
- [5] Cheng-HuChen, Ming-Yang Cheng, "*A New Cost Effective Sensorless Commutation Method for Brushless DC Motors Without Phase Shift Circuit and Neutral Voltage*", IEEE transaction on Power Electronics, vol.22, no.2, March 2007
- [6] Gui-Jia Su, Donald J. Adams, "*Multilevel DC Link Inverter for Brushless Permanent Magnet Motors with Very Low Inductance*", IEEE IAS 2001 Annual Meeting, September 30 – October 5, 2001, Chicago, Illinois USA
- [7] Yen-Shin Lai, Fu-San Shyu, Shian Shau Tseng, "*New Initial Position Detection Technique for Three-Phase Brushless DC Motor Without Position and Current Sensors*" IEEE transactions on Industry applications, vol.39, no.2, March/April 2003.
- [8] Yen-Shin Lai, Fu-San Shyu, Yung-Hsin Chang, "*Novel Loss Reduction Pulse width Modulation Technique for Brushless dc Motor Drives Fed by MOSFET Inverter*", IEEE transactions on Power Electronics, vol.19, no.6, November 2004.

- [9] Byoung-Kuk Lee, Tae-Hyung Kim, and Mehrdad Ehsani, "On the Feasibility of Four-Switch Three-phase BLDC Motor Drives for Low Cost Commercial Applications: Topology and Control", IEEE transactions on Power Electronics, vol.18, no.1, January 2003.
- [10] Yen-Shin Lai, Fu-San Shyu, "Novel Initial Position Detection Technique for Three-phase Brushless DC Motor without Position and Current Sensors", IEEE,2004
- [11] Tae-Hyung Kim, Mehrdad Ehsani, "Sensorless Control of the BLDC Motors From Near-Zero to High Speeds", IEEE transactions on power electronics, vol. 19, no. 6, November 2004
- [12] Paul P.Acarney and John F. Watson, "Review of Position-Sensorless Operation of Brushless Permanent-Magnet Machines" IEEE Transactions on industrial electronics, Vol. 53, No. 2, April 2006
- [13] C.-G. Kim, J.-H. Lee, H.-W. Kim and M.-J. Youn, "Study on maximum torque generation for sensorless Controlled brushless DC motor with trapezoidal back EMF", IEE 2005
- [14] Tae-Hyung Kim , Hyung-Woo Lee, and Mehrdad Ehsani, "State of the Art and Future Trends in Position Sensorless Brushless DC Motor/Generator Drives" IEEE Transaction on Power electronics, April 2005.
- [15] Joon-Ho Lee, Tae-Sung Kim, and Dong-Seok Hyun, "A Study for Improved of Speed Response Characteristic in Four-Switch Three-phase BLDC Motor" The 30th Annual Conference of the IEEE Industrial Electronics Society, November 2 - 6,2004, Busan, Korea
- [16] Cheng-Tsung Lin, Chung-Wen Hung, and Chih-Wen Liu, "Sensorless Control for Four-Switch Three-Phase DC Brushless Motor Drives", IEEE 2006.
- [17] Qiang Ful and Hui Lin, "Sliding Mode Driving Strategy for Four-switch Three-phase Brushless DC Motor", SICE-ICASE International Joint Conference 2006 Oct. 18-21, 2006 in Bexco, Busan, Korea

- [18] Abolfazl Halvaei Niasar, Abolfazl Vahedi, Hassan Moghbelli, "Analysis and Control of Commutation torque ripple in Four-Switch, Three-Phase Brushless DC Motor Drive", IEEE 2006.
- [19] Fu Qiang, LinHui, Zhang Hai-tao, 'Single-current-sensor Sliding Mode Driving Strategy For Four-switch Three-phase Brushless DC Motor' , IEEE 2006
- [22] V.Donescu, D.O.Neacsu, G.Griva, "Design of a Fuzzy Logic Speed Controller for Brushless DC Motor Drives", IEEE 1996.
- [23] Junyong LU, Deliang LIANG, Xiangyang FENG, "Simulation of Linear Brushless DC Motor Speed-controlled System Based on MATLAB SIMULINK".
- [24] Bhim Singh, A H N Reddy, S S Murthy, "Gain Scheduling Control of Permanent Magnet Brushless dc Motor" IE(I) journal-IE
- [25] Dae-Kyong Kim, Kwang-Woon Lee, Byung-II Kwon, "Commutation Torque Ripple Reduction in a Position Sensorless Brushless DC Motor Drive", IEEE TRANSACTIONS ON POWER ELECTRONICS, VOL. 21, NO. 6, NOVEMBER 2006.
- [26] Yen-Shin Lai, Yong-Kai Lin, "Assessment of Pulse-Width Modulation Techniques DC for Brushless Motor Drives", IEEE 2006.
- [27] Joong-Ho Song, Ick Choy, "Commutation Torque Ripple Reduction in Brushless DC Motor Drives Using a Single DC Current Sensor", IEEE TRANSACTIONS ON POWER ELECTRONICS, VOL. 19, NO. 2, MARCH 2004.
- [28] Juan W.Dixon, S.Tepper, L. Moran, "Practical evaluation of different modulation techniques for current controlled voltage source inverters ", IEE Proc.-Electr. Power. Appl. Vol. 143. No. 4, July 1996.
- [29] Juan W. Dixon and Iván A. Leal, "Current Control Strategy for Brushless DC Motors Based on a Common DC Signal ", IEEE TRANSACTIONS ON POWER ELECTRONICS, VOL. 17, NO. 2, MARCH 2002.

[30] Marian P. Kazmierkowski, and Luigi Malesani, "*Current Control Techniques for Three-Phase Voltage-Source PWM Converters: A Survey*", IEEE TRANSACTIONS ON INDUSTRIAL ELECTRONICS, VOL. 45, NO. 5, OCTOBER 1998.

[31] Renato Carlson, Michel Eajoie-Mazenc, and Joao C. dos S. Fagundes, "*Analysis of torque ripple due to phase commutation in brushless dc machines*" IEEE, 1990.

[32] T. Li and G. Slemon, "*Reduction of cogging torque in permanent magnet motors*", IEEE Transactions on Magnetics, vol.EC-2, n-6, Nov. 1988.

[33] R. Carlson, A.A Tavares, J.P. Bastos and M.Lajoie-Mazenc, "*Torque ripple attenuation in permanent magnet synchronous motors*", Conf. Rec. 1989 IEEE IAS Annual Meeting , San Diego-CA, USA, October 1-5 1989, pp. 57-62.

[34] M. Lajoie-Mazenc, B. Nogarede and J.C. Fagundes, "*Analysis of torque ripple in electronically commutated permanent magnet machines and minimization methods*", Conf. Rec. Fourth Int. Conf. on Electrical Machines and Drives, London (GB), September 13-15 1989, pp.85-89.

[35] P. K. Nandam and P. C. Sen, "*Accessible-states-based sliding mode control of a variable speed system*," IEEE Trans. Ind. Applications., vol.31, no.4, pp. 737-743, July/Aug. 1995.

APPENDIX – A

BLDC MOTOR SPECIFICATIONS:

Rated speed (N_{rated}):	1800 rpm
Rated current (I_{rated}):	7.5 ampere
Maximum torque (T_{max}):	6 N-m
Stator resistance (R):	0.95 Ohm
Stator inductance (L):	1.2 mH
Motor constant (k):	0.28 N-m/A
Total inertia (J):	0.05 Kgm ²
Pole pairs :	2
DC bus voltage (V_{dc}):	154 volt